NTNU

Norwegian University of
Science and Technology

Generation system adequacy studies in the presence of wind energy resources

Mads Bjørkeland

Master of Energy and Environmental Engineering
Submission date: February 2018
Supervisor: Vijay Vadlamudi, IEL

Norwegian University of Science and Technology
Department of Electric Power Engineering

Abstract

Variable renewable energy sources like wind power are in exponential growth worldwide. One of the major challenges regarding high penetration of wind energy in the power system is the degradation of generation adequacy due to the intermittent and random nature of wind.

The deterministic approaches applied today to ensure sufficient power system adequacy are ill-fit to handle stochastic generation behaviour. In response, several generation adequacy metrics with probabilistic basis have been developed in literature. Probabilistic methods for generation adequacy assessment are crucial for securing future power system operation and renewable generation integration.

As part of a project to construct a computational framework for power system reliability this thesis focuses on generation adequacy assessment of power systems with the presence of wind power. The applied concepts include generation adequacy metrics (LOLE and EENS)[1] and capacity credits (ELCC, EFC and ECC)[2]. To evaluate the generation adequacy of relevant test systems (Roy Billinton Test System and IEEE-Reliability Test System), MATLAB scripts that compute adequacy metrics and capacity credits have been developed and deployed. To evaluate the reliability effect from wind power generation, a wind farm has been modelled and integrated in the test systems. Evaluations applying several adequacy metrics and capacity credits have been conducted on the test systems including integrated wind power along with relevant sensitivity analyses.

From the thesis work it has become evident that the myriad of generation adequacy metrics, capacity credits and their combinations provide a powerful means of evaluating different aspects of power system reliability, thereby contributing to optimising renewable energy integration. However, the multitude of possibilities and lack of an established methodological approach makes the process of identifying the optimal metric combination a knowledge-intensive task.

[1] Loss-of-Load Expectation (LOLE), Expected Energy Not Served (EENS)

[2] Effective Load Carrying Capabilities (ELCC), Equivalent Firm Capacity (EFC), Equivalent Conventional Capacity (ECC)

Sammendrag

Variable fornybare energikilder som vindkraft er i eksponentiell global vekst. En av de største utfordringene med store andeler vindkraft i kraftsystemet er redusert leveringspålitelighet, som skyldes de tilfeldige og periodiske egenskapene til vind.

Dagens deterministiske metoder for å sikre tilstrekkelig leveringspålitelighet i kraftsystemet håndterer dårlig stokastisk kraftgenerasjon. Dette har ført til at det i litteraturen er utviklet flere pålitelighetskonsepter med probabilistisk grunnlag. Probabilistiske metoder for å evaluere leveringspålitelighet er fundamentale for å sikre fremtidig systemdrift og integrering av fornybar energi.

Som del av et prosjekt for å utvikle en databasert beregningsramme for leveringspålitelighet i kraftsystemer, fokuserer denne oppgaven på evaluering av tilstrekkelig generasjon i kraftsystemer med vindkraft. Anvendte konsepter inkluderer flere beregningsmetoder for leveringspålitelighet (LOLE og EENS)[3] og kapasitetsbidrag (ELCC, EFC og ECC)[4]. For å evaluere leveringspåliteligheten i relevante testsystemer (Roy Billinton Test System and IEEE-Reliability Test System), har en MATLAB kode som beregner leveringspålitelighet og kapasitetsbidraget blitt utviklet og anvendt. For å evaluere kapasitetsbidraget til vindkraft har en vindfarm blitt modellert og integrert i testsystemene. Evalueringer som anvender flere ulike metoder for å beregne leveringspålitelighet og kapasitetsbidrag ble utført for test systemene, i tillegg ble det gjennomført flere relevante sensitivitetsanalyser.

Arbeidet med oppgaven har gjort det klart at mangfoldet av metoder for beregning av leveringspålitelighet, kapasitetsbidrag og deres kombinasjoner bidrar med gode fremgangsmåter for å evaluere ulike aspekter med kraftsystempålitelighet. De overnevnte metodene kan også bidra til integreringen av fornybar energi. Derimot vil mangfoldet av muligheter, sammen med mangelen på en etablert fremgangsmåte, gjøre prosessen med å identifisere de optimale kombinasjonene av metoder for beregning av leveringspålitelighet og kapasitetsbidrag svært krevende.

[3] Loss-of-Load Expectation (LOLE), Expected Energy Not Served (EENS)

[4] Effective Load Carrying Capabilities (ELCC), Equivalent Firm Capacity (EFC), Equivalent Conventional Capacity (ECC)

Preface

This Master's Thesis is the conclusion of my Master of Science degree in Energy and Environmental Engineering with the Department of Electric Power Engineering at the Norwegian University of Science and Technology (NTNU). The thesis deals with concepts from Power System Reliability (PSR) and statistical approaches to wind modelling. The work was performed under the supervision by Associate Professor Vijay Venu Vadlamudi at the Department of Electric Power Engineering, NTNU.

This work builds on a literature review part of a specialisation project undertaken during Autumn 2017. Over the course of the five months this work has been conducted, I have gained a insights into the knowledge of PSR studies in general and generation adequacy in particular. My sincerest gratitude goes to my supervisor, Vijay Venu Vadlamudi without whom this work would never have come to fruition. He has always been available, willing to answer my questions and encouraged me in my endeavours. Also to the several professors at NTNU who have answered my inquiries, and to my fellow students at the office who have provided an excellent working environment, I owe my gratitude. Last but not least, I would like to thank Mari Lauglo and Espen Aronsveen for helping me with the monumental task of proofreading.

Trondheim, 1.2.2018

Mads Bjørkeland

Contents

Abbreviations

ARMA	Auto Recursive Moving Average
CC	Capacity Credit
COPT	Capacity Outage Probability Table
CYPL	Constant Yearly Peak Load
DPL	Daily Peak Load
ECC	Equivalent Conventional Capacity
EENS	Expected Energy Not Served
EEU	Expected Energy Unserved
EFC	Equivalent Firm Capacity
ELCC	Effective Load Carrying Capability
ENTSO-E	European Network of Transmission System Operator
EV	Electrical Vehicle
FCR-D	Frequency Containment Reserves - Disturbance
FCR-N	Frequency Containment Reserves - Normal
FOR	Forced Outage Rating
FRR-A	Frequency Restoration Reserves Automatic
FRR-M	Frequency Restoration Reserves Manual
HL	Hierarchical Level
HPL	Hourly Peak Load
ICT	Information and Communication Technologies
IEEE	Institute of Electrical and Electronics Engineer
LOEE	Loss of Energy Expectation
LOLE	Loss of Load Expectation
LOLP	Loss of Load Probability
MCS	Monte Carlo Simulation
MTBF	Mean Time Between Failure
MTTF	Mean Time To Failure
MTTR	Mean Time To Repair

PLR	Peak Load Reserve
LPT	Load Probability Table
PSR	Power System Reliability
RBTS	Roy Billinton Test System
RTS	Reliability Test System
SOA	System Operation Agreement
TSO	Transmission System Operator
WTG	Wind Turbine Generator

Nomenclature

λ	Expected failure rate
μ	Expected repair rate
m	Mean time to failure = $MTTF = 1/\lambda$
r	Mean time to repair = $MTTR = 1/\mu$
$m+r$	Mean time between failures = $MTBF = \quad 1/f$
f	Cycle frequency = $1/T$
T	Cycle time = $1/f$
x_j	Outage in [MW]
$P(X \geq x_j)$	Cumulative probability of capacity outage $\geq x_j$
$p(X)$	Individual probability of event X
j	Index for outage states
C	Total installed capacity [MW]
P^{new}	Cumulative probability of system including new unit
P^{old}	Cumulative probability of the original system
i	Generation unit states
p_i	Probability of being in state i
g_i	Capacity of unit added to COPT in state i [MW]
$LOLP_t$	The LOLP value in time period t
L_t	System load in time period t [MW]
ΔT	The time increment, e.g. 1 hour for HPL or 1 day for DPL
E_j	Expected energy not served in generation state j [MW]
$EENS_t$	Expected energy not served for time increment t [MW]
$LOLE_{old}$	LOLE of the original system
$LOLE_{new}$	LOLE of the system with additional generation and/or load
L_i	A load condition for the increment i [MW]
ΔL	The additional load that can be served by the new system [MW]
n	Total number of time increments in the evaluation period
C_{old}	Total possible capacity of the original system [MW]

C_{new}	Maximum capacity of the unit added to the system [MW]
L'_i	Scaled load level [MW]
L_i	Base case load level [MW]
L_{max}	Maximum load in the original load series [MW]
L'_{max}	Maximum load in the new load series [MW]
$LOLE_{goal}$	LOLE of the system with additional generation
$LOLE_{current}$	LOLE of the system with the fictitious generator
C_{goal}	Total possible capacity of the original system [MW]
$C_{current}$	Maximum capacity of the fictitious generator [MW]
WS_t	Wind speed in time interval t [m/s]
P_r	Rated output from the WTG [MW]
V_{ci}	Cut-in wind speed [m/s]
V_r	Rated wind speed [m/s]
V_{co}	Cut-out wind speed [m/s]
k	Number of WTGs in the wind farm
s	Number of wind capacity states
q_j	Probability of wind turbine operating in output state c_j
u	The probability of argument occurring
$p_{unit,i}$	Probability of i generating units being available
c_j	Capacity in state j
x_{output}	Output from wind farm [MW]
$HPL_{h,d,w}$	Hourly peak load calculated by hourly, daily and weekly percentages
YPL	Yearly peak load
l_w	Weekly peak load as a percentage of yearly peak load
l_d	Daily peak load as a percentage of weekly peak load
l_h	Hourly peak load as a percentage of daily peak load

List of Figures

List of Tables

Chapter 1

Introduction

1.1 Background

Wind power as a source of electrical energy is growing significantly and will together with solar make up 80% of the installed renewable effect worldwide the next five years [1]. Support from governmental policies and popular consensus regarding awareness of global climate change has increased the demand for clean energy. Economic subsidies and technological maturation has further spurred the growth of wind energy. However, wind's intermittent and random properties cause uncertainties regarding energy generation and poses a large barrier for its further development. Power quality, security of system operation and power system reliability represent some of the main technical issues concerning wind power integration [2].

To assure a reliable and economic electrical power supply the design, planning and operating of the electrical grid has been dominated by various deterministically based criteria and techniques. The $n-1$ criterion and generation capacity with a fixed percentile reserve are examples of these deterministic approaches applied in many power systems to date [3]. The integration of Information and Communication Technologies (ICT), growing renewable energy penetration, distributed generation and increase in load demand variability encourages a more flexible power system. A modern power system would benefit from applying probabilistic methods to operate better under the stochastic conditions caused by these principles.

In power systems where wind energy make up a big portion of the energy mix will, due to the intermittent and stochastic nature of wind, be subject to uncertainties in energy generation. So when installing wind power as new capacity or replacing conventional electrical generators, evaluating the reliability impact from such changes is crucial. Methods for calculating and modelling this reliability contribution has become an important task for power system operators, planners and researchers. Applying the correct methods and techniques will allow further growth in wind power integration and in turn aid solving climate change issues. As stated in second paragraph of the UN's declaration on renewable energy, "The Way Forward on Renewable Energy"[4]: *"Increasing the use of renewable energy is an essential element to achieve sustainable development at national and global level. Renewable energy can provide important new ways to reduce pollution, diversify and secure energy supply and help provide access to energy in support of poverty eradication. Furthermore, the burning of fossil fuels is the biggest source of greenhouse gas emissions and these emissions need to be reduced to mitigate the adverse effects of climate change in order to achieve the ultimate objective of the United Nations Framework Convention on Climate Change to prevent dangerous climate change."*

1.2 Scope

This thesis is a contribution to the project of building a computational framework for power system reliability evaluation at the Department of Electric Power Engineering at NTNU, and is partly an extension of the work performed in [5]. By focusing on the application of reliability metrics to evaluate the capacity credit of wind power generation this thesis aims to state the impact that integration of wind power has on the reliability of a power system.

The probabilistic methods applied are well established from the field of Power System Reliability. The main concepts are Loss-of-Load Probability (LOLP), Loss-of-Load Expectancy (LOLE), Expected Energy Not Served (EENS), Effective Load Carrying Capability (ELCC), Equivalent Firm Capacity (EFC) and Equivalent Conventional Capacity (ECC). The evaluations are limited to the generation level of the power system and only concerns generation adequacy. The main part of the work performed in this thesis is the development of MATLAB scripts that apply the various

power system reliability concepts to quantify the reliability contribution from wind power. This is done by applying the probabilistic methods to established test systems like the Roy Billinton Test System (RBTS)[6] and the IEEE Reliability Test System (RTS) [7].

The main focus of this thesis is on evaluate the produced MATLAB-scripts, comparing them with corresponding results found in literature, performing sensitivity analysis and see if conclusions based on the resulting data concur with established concepts. Therefore, the thesis does not consider obtaining qualitative data input, nor present results from real life power systems or the use of energy from other sources e.g. solar.

1.3 Thesis Contributions

- The thesis builds on a specialisation project regarding generation adequacy assessment of renewable energy sources, undertaken the spring of 2017 at NTNU. The objective is to study and implement the algorithmic approaches to calculate the ELCC and EFC/ECC metrics for power systems with wind-integration.
- The methodology applied in this thesis combines several methods and concepts from the relevant literature available on power reliability studies and wind modelling to reach the aforementioned objective. The attributes and theoretical foundation of these concepts are presented to clarify their usefulness and subtleties.
- MATLAB scripts have been developed to implement the algorithmic approaches to calculate the ELCC and EFC/ECC metrics for small and large test systems including wind turbines. These scripts are released for further use and research at the Department of Electric Power Engineering at NTNU.

1.4 Thesis Structure

Chapter 1 - *Introduction*: Provides the background for the work performed in the thesis, including the scope and contributions of the thesis.

Chapter 2 - *Overview: Wind Power and Generation Adequacy*: Provides a presentation of status quo and development in wind energy both globally and domestically. Also, a presentation of generation adequacy assessment in the Nordic power market is given.

Chapter 3 - *Power System Reliability*: Reliability concepts and other theoretical knowledge necessary to compute the ELCC and EFC/ECC capacity credits are presented. Also, the wind energy and turbine modelling concepts required to evaluate wind power reliability are elaborated.

Chapter 4 - *Methodological Approach*: The methodology of evaluating ELCC and EFC/ECC metrics is presented. Simple examples are given to illustrate the approaches for different metrics.

Chapter 5 - *Case Study: Applying the ELCC and EFC/ECC methodology to Test Systems*: Presents a short demonstration of the methodological approach on test systems. Results of the application of the scripts are shown along with commentary on the observations from the results. Lastly, several sensitivity analysis are conducted to further strengthen the basis for discussion.

Chapter 6 - *Conclusion and Future Work*: Presents a summary of results from Chapter 5, leading to discussion and some concluding remarks on the work done in the thesis. Lastly, limitations of the thesis and suggestions for future work are presented.

Chapter 2

Overview of International Wind Power and Generation Adequacy in the Nordics

This chapter presents an overview of the current situation in wind power both on a global scale and in Norway. Installation rates, governmental policies and overall amount of wind power are elaborated. Also, the Nordic markets approach to assure generation adequacy is presented. These themes are covered to further demonstrate the motivation behind this thesis.

2.1 Increase in Wind Power

2.1.1 Global Wind Power

The issue of climate change has seen the world community coming together and state explicit goals for lowering the emission of CO_2 and other greenhouse gases. Increasing renewable energy and decommissioning conventional energy is paramount in achieving the goal of keeping the average temperature increase below two degrees Celsius, as stated in the Paris Agreement. Paramount to achieve the goals put forward by the Paris Agreement to stay below an average rise in temperature of two degrees Celsius, is increasing the worlds renewable energy as more polluting alternatives are decommissioned.

Global wind power penetration in power systems has increased considerably the last years

and wind energy together with solar energy play key roles in the surge of clean energy. However, investments have fallen after the record year of 2015, when the global installed wind effect exceeded the 60 GW mark for the first time [8]. The three main contributors to the growth in 2016[1] were China, USA and India. China with the indisputably highest installed wind capacity of 23 370 MW, USA second installing 8 203 MW and Germany being the biggest contributor in Europe with 5 443 MW installed wind capacity [8].

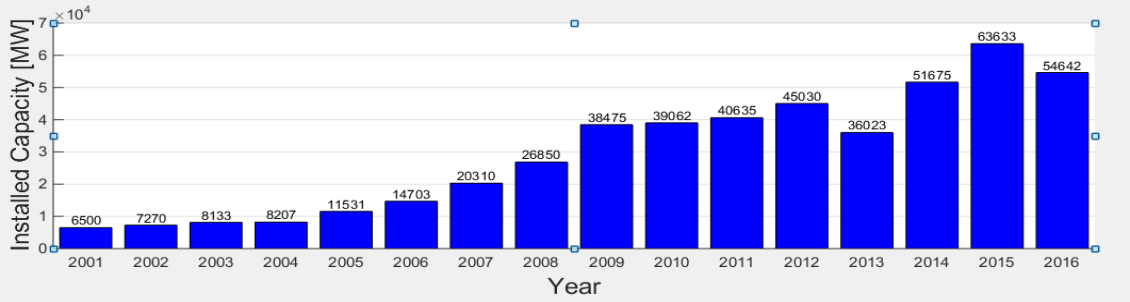

(a) Annual installed wind capacity worldwide 2001-2016

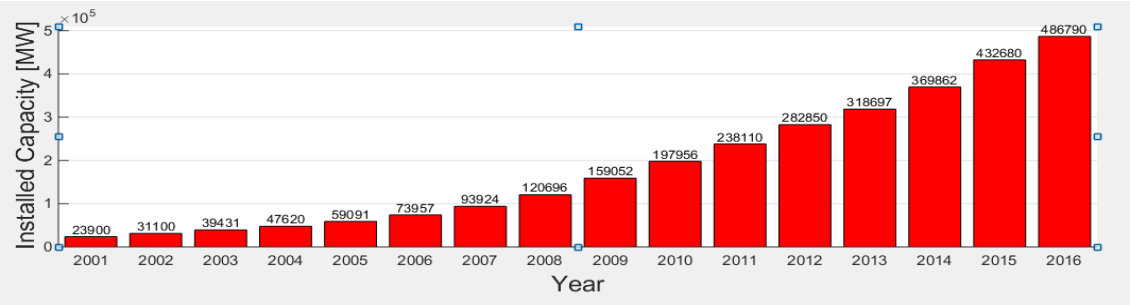

(b) Annual cumulative wind capacity worldwide 2001-2016

Figure 2.1: Annual installed and cumulative wind power capacity [8]

Figure 2.1a shows the global installed wind generation capacity. Apart from dips in 2013 and 2016, a steady increase in wind power development is evident. Figure 2.1b shows the global cumulative installed effect. It can be observed that in 15 years the effect contribution from wind has grown significantly from 23.9 GW in 2001 to 4 867.8 GW in 2016, an increase of more than twenty times.

[1]The annual Global Wind Council report for 2017 is not available as of February 2018.

2.1.2 Wind Energy in Norway

Norway, one of the countries in the world with the highest percentage of its electrical energy being generated by renewable sources, still has a poorly developed wind energy sector. This is mainly due to the large hydro power capacity and being part of the highly integrated Nordic market, which covers most of the energy demand with a high reliability [8]. In accordance with international consensus, the Norwegian government has put forward several policies for increasing renewable electricity production and overall lowering emissions in the country. Norway has, as of January 1. 2018, statutory emission goals for 2030 and 2050 when emissions are to be reduced with 40% and 80-95% compared to the reference year 1990 [9]. The generation mix for Norwegian electricity in 2016 and its percentage of total production can be seen in Table 2.1.

Table 2.1: Generation mix for Norwegian electricity in 2016 [10]

	2016 [GWh]	Percentage [%]
Hydro	143 417	96.3
Thermal	3 456	2.3
Wind	2 116	1.4
Total Production	148 989	100.0

Norwegian wind energy is on the rise, 2015 saw the installation of 16 MW of onshore wind power bringing the total capacity to 873 MW, as can be seen in Figure 2.2. However, the largest impact is yet to come from projects started in 2016. The Fosen wind power project with its 1 000.8 MW of planned capacity will, when operational by 2021, almost double the installed wind power and become the largest onshore wind farm in Europe. Other smaller projects like Hamnefjell and Raskiftet are also expected to increase the wind capacity to 1 400 MW by early 2018 [11]. In all 1 240 MW of wind capacity is being built and concessions are given to an additional 4 210 MW [12]. Figure 2.2 shows the cumulative installed effect in Norway from 2006 to 2016.

There are more governmental policies to encourage more renewable energy. One is a joint green electricity certificate market with Sweden, where the two countries aim to increase their renewable energy production by 28.4 TWh. This is planned to mainly be achieved by installing new wind and hydro power. Another is a bipartisan agreement to include a strategy for commer-

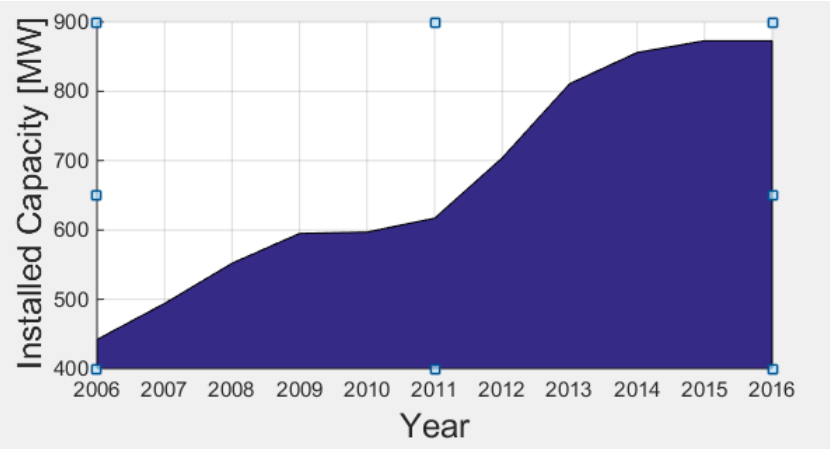

Figure 2.2: Cumulative installed effect in Norway 2006 to 2016 [13]

cial development of floating wind turbines in the governmental budget for 2018. These policies along with the statutory climate goals and further technological maturing are expected to increase Norway's renewable generation with 20 TWh by 2030, where 15 TWh is expected to come from wind energy [14].

Norway has a tremendous potential for wind energy, especially offshore as shown in Figure 2.3. If this potential is to be fulfilled new methods with a probabilistic basis that take into account the power system adequacy aspect should be developed and implemented.

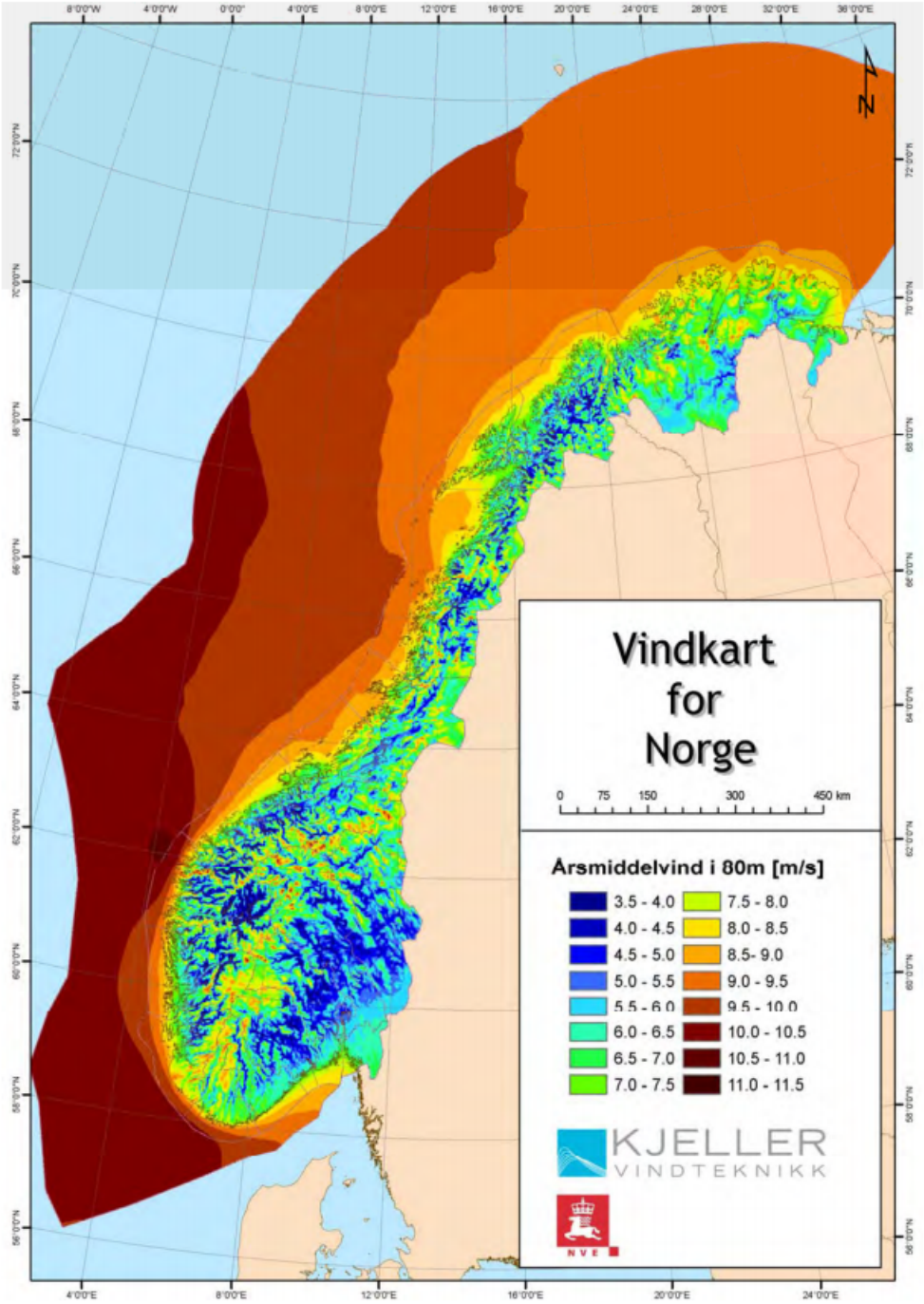

Figure 2.3: Map of the wind power potential in Norway [15]

2.2 Generation Adequacy in the Nordic Power Market

Providing a satisfying level of generation adequacy has historically been achieved using deterministic approaches. The Nordic power market countries, see Figure 2.4, follow the ENTSO-E three main aspects for generation adequacy characterisation [16].

- Peak load: Do we have sufficient capacity (including demand response) to handle peak load situations?
- Flexibility: Is the capacity (including demand) sufficiently flexible to handle variations in load and balance the system in real-time?
- Energy back-up: Do we have sufficient energy back-up capacity to serve demand during prolonged periods of low wind and solar generation?

Handling peak load situations is a matter of having sufficient capacity installed in the system. It goes without saying having insufficient capacity to meet load demand, will lead to load curtailment in a isolated system. So countries not able to produce sufficient energy to meet their load demand can import energy from other countries, provided they are part of an integrated market. Several are dependent on importing from neighbouring countries.

Generation flexibility is directly connected to generation response time, and is an increasingly important factor in the modern power systems where EVs and distributed power generation create a greater load magnitude and variability [18].

Backup energy is provided by generators that can provide capacity to the system should the need occur. Today most net operators apply the $n-1$ criteria to dimension the needed backup generation capacity. The $n-1$ criteria means that if any one component in the system should fail the system will still be able to provide the needed generation and transport it to the load point. Using this criteria, the backup should be able to deliver the same amount as the largest generation unit in the system should it fall out, known as the loss-of-largest generation principle [17].

Figure 2.4: The Nordic Power Market [17]

Generation used for backup and flexibility purposes is purchased by the system grid operator much in the same fashion as generation purchased to meet load demand. In the Nordic countries this market is called the reserve capacity market and is divided in three strategical areas depending on their response and operation time as shown in Table 2.2.

Frequency Containment Reserves (FCR): operating reserves for balancing the system within the normal frequency band from 49.90 Hz to 50.10 Hz, (FCR-N) and in the case of disturbances (FCR-D). According to the existing Nordic System Operating Agreement (SOA) the reserves for FCR-N should be at least 600 MW divided in the control area within the synchronous system.

Frequency Restoration Reserves (FRR): operating reserves necessary for restoring the frequency back to 50.00 Hz. These can be either activated manually (FRR-M) or automatically (FRR-A).

Should the market be unable to meet the load demand in time a strategic Peak Load Reserve (PLR) is activated. As of today, only the Swedish and Finnish TSO's have PLRs with respectively 1500 MW and 365 MW capacity consisting of generation units and demand response [17].

Table 2.2: Strategical reserve market levels[19]

	Activation procedure	Response time	Market Solution
Primary Reserves	Automated feedback control based on frequency	Zero	FCR-N and FCR-D: markets for capacity to primary reserves. Daily and Weekly markets with hourly or load block resolution.
Secondary Reserves	Units are controlled by TSO	Max 210 sec.	FRR-A: Market design under development for the Nordic synchronous area.
Tertiary Reserves	Units are manually activated	Max 15 min.	FFR-M: Hourly market for energy, separate markets for ramping up and ramping down of generator and load.

Today's reserve capacity and adequacy assessments are based on deterministic measures and calculations. A future generation adequacy assessment method is under development for the Nordic System. This method aims to incorporate many of the probabilistic methods and techniques discussed later in this thesis like LOLE, EENS, Hourly Peak Load (HPL) model and briefly mentioned Monte Carlo Simulations (MCS). Implementation of the new method can reduce the needed reserve energy in scenarios with low risk probability, better integrate renewable energy and improve grid operation, resulting in a more reliable, economic and less polluting power system [17].

Thus, quantification of generation adequacy with probabilistic basis, in the presence of renewable energy integration in power systems is a timely and relevant research topic. The thesis work deals with the study of select few probabilistic algorithmic approaches (e.g. ELCC, EFC and ECC) that examine the adequacy of renewable (wind) energy integrated power systems.

Chapter 3

Power System Reliability

Power system reliability is a wide field of study that encompasses several under disciplines. This chapter specifies the area of PSR that is the focus of this thesis, namely generation adequacy. The theoretical principles of the applied adequacy metrics LOLE and EENS are presented alongside the capacity credits ELCC, EFC and ECC. Also, as the renewable energy source evaluated in this thesis is wind, the concepts for modelling wind energy are elaborated.

3.1 Hierarchical Levels

To specify the segment of interest, PSR studies categorise the power system levels based on the system's functional zones. The three different zones; HL-I, HL-II and HL-III levels as demonstrated in Figure 3.1.

HL-I refers to the generation system and its abilities to deliver sufficient energy to satisfy the system demand. HL-II refers to the composite system, i.e. generation and transmission systems, and its ability to generate and deliver sufficient energy to system load points. HL-III refers to all three levels, generation, transmission and distribution and the systems ability to generate and deliver the energy demand to individual consumers. HL-III studies are rarely performed due to the sheer scale of the system. This thesis only evaluates generation adequacy and thus only the HL-I is relevant [20].

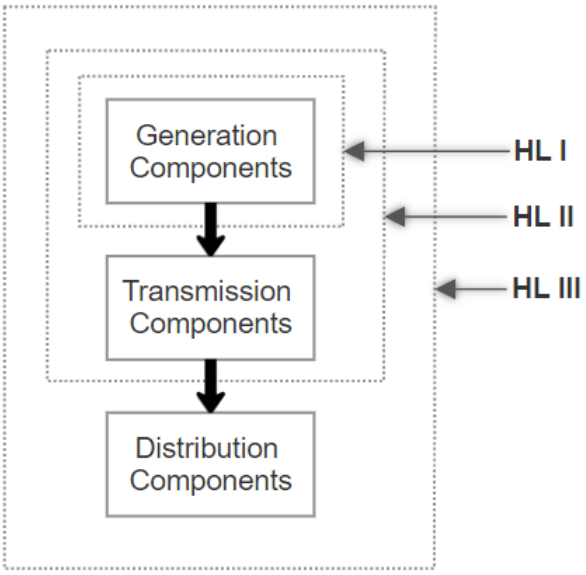

Figure 3.1: Hierarchical Levels in the power system

3.2 Generation Adequacy

PSR studies are normally categorised in two sections: *System Adequacy* and *System Security*. System adequacy is related to the existence of sufficient generation facilities to cover the consumer demand. As the system facilities are static conditions, this dictates that also generation adequacy is a combination of static conditions. System security is related to the system's ability to maintain its level of energy quality in the occurrence of contingencies. As this deals with changes, system security is a combination of dynamic conditions [3, 20].

3.2.1 Generation Adequacy Concepts

Generation adequacy indices can be calculated using either deterministic or probabilistic methods. The increase in renewable energy sources and more flexible load demand has gradually led to the preference shifting from deterministic- to probabilistic methods. Probabilistic methods are then again divided in two main fields, analytical and simulation [21, 22]. This division is visualised in Figure 3.2.

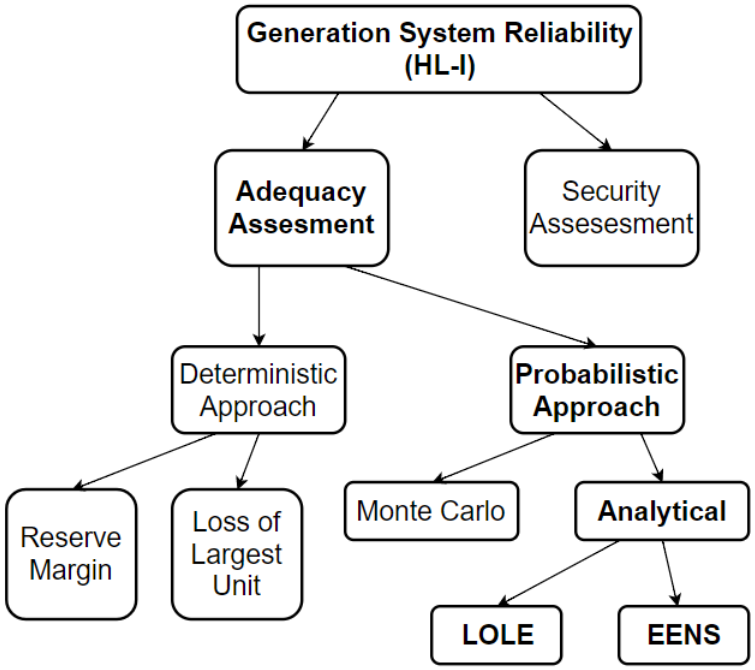

Figure 3.2: Flowchart of some of the methodologies used in generation system reliability

Analytical methods apply mathematical models to represent the system, and the reliability indices are obtained through direct numerical calculation. This gives a short calculation time and has relatively small demands to computational power [23]. However, for the mathematical model to give a good representation of an increasingly complex system, an increasing number of assumptions are required to simplify the problem and acquire the analytical model of the system. A big amount of assumptions will have a disadvantageous effect on the accuracy and realism of the evaluation. Also, analytical methods are incapable of incorporating the load/generation correlation. For non-storable resources like wind and solar this correlation between availability and load level is of high interest.

Simulation techniques like MCS can simulate the different processes and behaviour of the system down to random occurrences like element repair, dependent events, and generation/load correlation. The extensive modelling of components requires a vast amount of data for each component and big computational resources. These two requirements are the main reason for the analytical methods historically dominating position. The increase in computational power

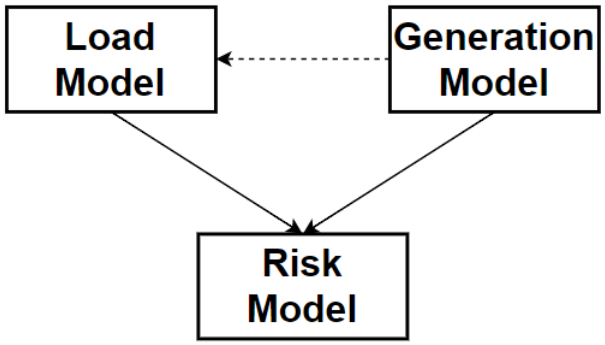

Figure 3.3: Concept in HL-I evaluation

and better component information has seen an increase in simulation techniques popularity [22]. Most simulation techniques build on the same foundation used in analytical methods, but with modifications for data collecting and sampling [24]. This thesis will not apply simulation techniques but strive to provide a qualitative presentation of an analytically based methodology.

3.3 Loss-of-Load Based Indices

The process of assessing the generation adequacy of a system is fundamentally the same for any technique. A load- and generation model are convolved to form the system risk model, the principle of which is demonstrated in Figure 3.3. Several methods can be applied to acquire the load- and generator models, but the ones applied in this thesis are presented in the following section along with generation adequacy metrics and capacity credits.

3.3.1 Load Model

The load model is a representation of the system load demand and its variation in time. Obtaining the load by simulating each components behaviour would be a very tedious and near impossible endeavour, therefore the most common way of obtaining the load model is through historical data with values of the total system load and its variations. This information can then

be directly applied to create chronological models with peak loads or load probability models. The most common is the chronological representation with peak loads. The peak loads can be chosen for different time resolutions or reformed to seasonal models to preserve some wind power and load correlation.

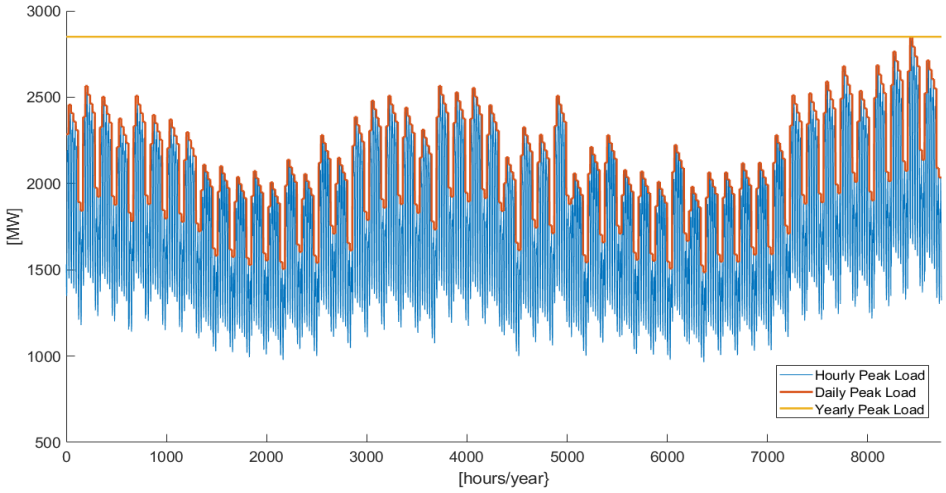

(a) The load variation during one year

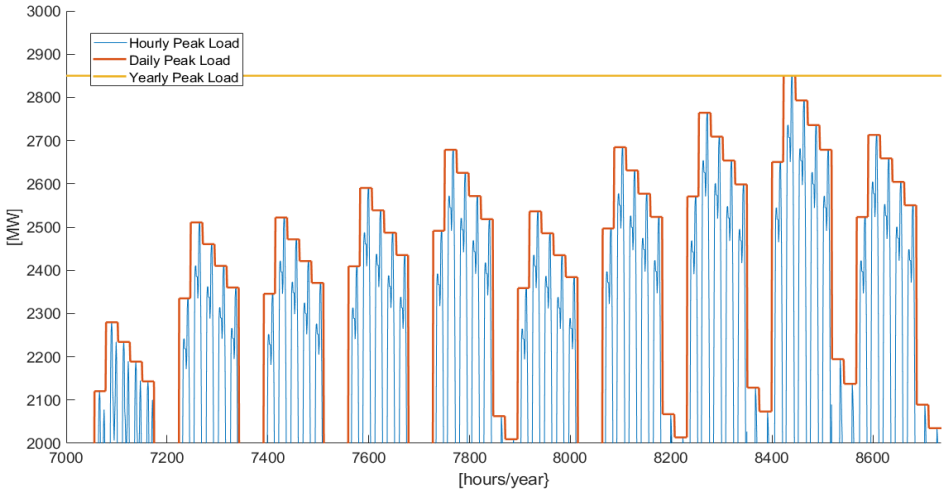

(b) The load variations zoomed in

Figure 3.4: The different load resolutions

Constant Yearly Peak Load Model

Constant Yearly Peak Load (CYPL) represents the entire year as one load increment equal to the annual peak load. As the maximum load is accounted for the entire year this model will yield

pessimistic results when assessing the system generation adequacy. Computational operations are kept to a minimum as only one load level is considered [3].

Daily Peak Load Model

Daily Peak Load (DPL) represents the entire year as 364 load increments with a load equal to the daily peak load. One year only consists of 364 days as PSR studies use a calendar based on 52 weeks. The maximum load for each day is modelled to last for the entire day. As this is not very realistic it gives slightly pessimistic values, but is much more accurate than the CYPL model. Having 364 load levels instead of one increases the number of calculations and thus a longer computational time.

Hourly Peak Load Model

Hourly Peak Load (HPL) represents the entire year as 8736 load increments with a load equal to the hourly peak load. As with DPL, PSR studies use a year of 364 days a year which equals 8736 hours. The maximum load for each hour is modelled to last for the entire hour. This gives very realistic values, especially when compared to the CYPL-model. The drawback is the same as for DPL, more load levels equals more calculations and further increases the computational time [3].

Load Probability Table

The Load Probability Table (LPT) applies the same load increment resolutions as mentioned earlier, but the values are rearranged according to magnitude and thus loses its chronological information. The table is used to obtain a probability model for the load by summing the number of data points with equal load magnitude and dividing the sum by the number of load increments. As an example, if we use daily values and the load is equal to 100 MW for 20 days a year the probability of the load being 100 MW equals, $20\text{days} \div 364\text{days} = 0.0549$.

3.3.2 Generation Model

Fundamental for representing the reliability of components is the Forced Outage Rate, (FOR) [3]. FOR describes the unplanned outages that occur in a component and is not an official unit in reliability studies as it is comprised of two time values known as Mean Time To Failure (MTTF) and Mean Time To Repair (MTTR). How they are calculated is shown in Equations (3.1) and (3.2).

$$\text{Unavailability} = U = \frac{\lambda}{\lambda+\mu} = \frac{r}{r+m} = \frac{r}{T} = \frac{f}{\mu} = \frac{\sum[\text{down time}]}{\sum[\text{down time}] + \sum[\text{up time}]} \tag{3.1}$$

$$\text{Availability} = A = \frac{\mu}{\lambda+\mu} = \frac{m}{r+m} = \frac{m}{T} = \frac{f}{\lambda} = \frac{\sum[\text{up time}]}{\sum[\text{down time}] + \sum[\text{up time}]} \tag{3.2}$$

$where$:	λ	=	expected failure rate
	μ	=	expected repair rate
	m	=	mean time to failure = $MTTF = 1/\lambda$
	r	=	mean time to repair = $MTTR = 1/\mu$
	$m+r$	=	mean time between failures = $MTBF = 1/f$
	f	=	cycle frequency = $1/T$
	T	=	cycle time = $1/f$

These methods for modelling the availability and the unavailability are associated with a two-state model, as shown in Figure 3.5. Expanding this model to include more states with rated generator outages, known as derated states, can be done in the same manner. Each de-

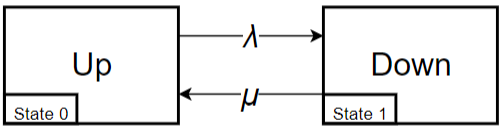

Figure 3.5: Two-state model for generating unit

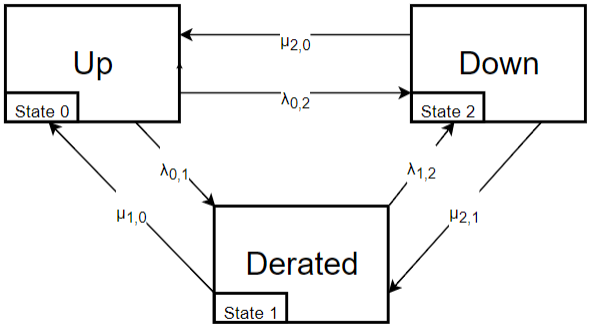

Figure 3.6: Three state model for generating unit

rated state is assigned a probability value equal to the probability for the generator to be in a specific output state. A simple multi-state model is shown in Figure 3.6 represented by one derated state along with the fully operational- and non-operational states. The state transmission probabilities of a generator can be computed from suiting reliability models, e.g., Markov modelling of the generator [25]. An alternative is to estimate the probabilities from field data, e.g. historical availability.

Capacity Outage Probability Table

The most common generation model representation in PSR is referred to as a Capacity Outage Probability Table (COPT). This is, as the name describes, an array of system capacity outage levels and their associated probabilities based on the generator's FOR. The COPT is built by calculating the probability of all the outage states and their combinations as done in [26] or by using the recursive algorithm to sequentially add the units to the COPT [3, 27]. The concept of the COPT and its calculation is illustrated in the following example.

The example system consists of two 10 MW generators and one 20 MW generator which have the same FOR of 2%, as shown in Table 3.1. The total capacity of the system is 40 MW.

Table 3.1: Generator data

Number of generators	Capacity [MW]	FOR
2	10	0.02
1	20	0.02

The COPT contains each possible capacity outage state represented by a given amount of outage x_j in MW, with its corresponding cumulative probability $P(X \geq x_j)$ of having an outage equal to or greater than x_j. The cumulative probability can be found by applying Equation (3.3) where the individual probabilities $p(X)$ are summed for all outage states from x_j to C, where C represents the total installed capacity in the system.

$$P(X \geq x_j) = \sum_{X=x_j}^{C} p(X) \tag{3.3}$$

Each outage state in the COPT represents a multiplicative combination of the generator's availabilities that put the system in configurations with a certain outage state. The individual probabilities might also be comprised of the sum of several system configurations yielding the same amount of capacity outage.

The COPT is constructed by adding the generators one by one, convolving each outage state of the unit with the outage states already in the COPT. This is done by calculating all possible generator outages and generator outage combinations and summing their individual probabilities, but as this gets exceedingly complex when dealing with several generators the recursive algorithm is utilised. This also allows for direct calculation of the cumulative probability without having to calculate and sum all the individual probabilities for each state. Assuming at least one unit is already added to the COPT, the recursive algorithm, presented in Equation (3.4) adds a multi-state unit to the COPT. It then updates the cumulative probabilities of all the other states

for each added state. As for certain values the arguments for the cumulative probability might become zero or negative, this is handled by the definition in Equation (3.5). For further elaboration on the construction of COPT the reader is referred to [3, 27].

$$P^{new}(X \geq x_j) = \sum_{i=1}^{n} p_i \cdot P^{old}(X \geq x_j - g_i) \tag{3.4}$$

$$P^{old}(X \geq x_j) = 1 \; for \begin{cases} x_j & \leq 0 \\ x_j - g_i & \leq 0 \end{cases} \tag{3.5}$$

$where:$

P^{new}	=	Cumulative probability of system including new unit
P^{old}	=	Cumulative probability of system excluding new unit
j	=	COPT outage states
i	=	Generation unit state
x_j	=	Amount of outage in state j
p_i	=	Probability of unit being in state i
g_i	=	Capacity of unit added to COPT in state i
n	=	Total generator states

For each time a new unit is added to the COPT, the algorithm updates all previous outage states and their cumulative probabilities as well as adding new ones, thus creating a new COPT that includes the added unit. The cumulative probabilities $P^{old}(X \geq x_j)$, are found in the COPT from before the addition of the current unit. As $(x_j - g_i)$ might return values between two outage states from the previous COPT the cumulative probability arguments are not possible to look up in the current COPT. Since the probability distribution deals with cumulative probabilities, the next state larger than $(x_j - g_i)$ is used.

Table 3.2 shows the COPT acquired from the simple system in Table 3.1 by applying the methods presented above.

Table 3.2: COPT for example system

State j	Capacity Outage x_j [MW]	Individual Probability $p(X = x_j)$	Cumulative Probability $P(X \geq x_j)$
1	0	0.941192	1
2	10	0.038416	0.058808
3	20	0.019600	0.020392
4	30	0.000784	0.000792
5	40	0.000008	0.000008

3.3.3 Generation Adequacy Indices

The dominating probabilistic indices in generation adequacy studies are the LOLP and LOLE [3]. Both metrics are closely related and in some special cases the LOLE can be derived from LOLP and vice-versa. Both rely on a generation model and load model to provide a system risk model. The generation model commonly used is the COPT while the load models can consider various peak-load models and different time intervals to benefit computational time and/or accuracy.

The LOLE and LOLP metrics have the disadvantage of equally weighing all load supply shortcomings and do not consider their severity e.g. a loss of 100 MW in comparison with a loss of 1 MW are treated equally [3]. To account for the severity of an outage the EENS[1] index can be used. EENS is an expansion on LOLE to include the magnitude of the lost capacity, in the event of unsupplied load demand. This thesis applies both the combination of LOLE/LOLP and EENS in generation adequacy assessment simulations.

LOLP

LOLP is a probabilistic metric that returns the probability of a loss-of-load occurrence in the system for a given time period. By combining the COPT and the load model to investigate a

[1] EENS is referred to by many names, such as Expected Energy Unserved (EEU), Expected Unserved Energy (EUE) or Loss of Energy Expectation (LOEE)

given time period, the probability for the generation capacity not being able to meet the load demand is calculated. Shortage in supply can be due to a generator outage, the load exceeding the installed system capacity or poor wind conditions in systems with renewable penetration. Equation (3.6) shows how the calculation is performed [3].

$$LOLP_t = P(X > C - L_t) \tag{3.6}$$

$where$: $LOLP_t$ = The LOLP value in time period t

L_t = System load in time period t

C = Total installed generation capacity in the system not on scheduled outage

$P(X > x)$ = Cumulative probability from the COPT table

As an example of a LOLP calculation, consider a CYPL of 25 MW and using the COPT from Table 3.2 describing a system with 40 MW of capacity. Equation (3.6) will result in, $LOLP = P(X > C - L) = P(X > 40 - 25) = P(X > 15) = 0.02039$ i.e. the probability of a loss-of-load situation is 0.02039. This probability can also be interpreted as the amount of time when there is a loss-of-load situation in the considered time period. For the example with a LOLP of 0.02039 years/year, a conversion to days, or hours per year can be made by multiplying with the appropriate quantity. Converting the LOLP to hours/year for the given examples, 0.02039 years/year $\cdot$ 8736 hours/year = 178.127 hours/year. This only applies when a single load increment is considered e.g. using one load increment for the entire year, like with CYPL.

LOLE

The LOLE is a probabilistic metric quantifying the number of times a loss-of-load situation occurs in the overall time period. It can be imagined as a sum of LOLP, although this is only true in some cases. LOLE is a metric with the unit of time, but is not to be interpreted as the amount of time a system will be in black-out. Power systems have several tools to avoid black-outs e.g.

reserve generators, interconnecting cables and load shedding [28]. LOLE only describes when the capacity installed in a system is not able to deliver the system load demand, and the TSO must use some of the aforementioned tools.

LOLE is often wrongfully referred to as LOLP or the terms are used interchangeably. The confusion likely stems from the fact that LOLP is an imperative part of the LOLE calculations and that the LOLP can be re-calculated from the LOLE by dividing the LOLE by the number of time increments in the entire time period.

Usually the LOLE is calculated on an annual basis, using either *days/year* or *hours/year*. The procedure for calculation is demonstrated by Equations (3.7) and (3.8).

$$LOLE = \sum_{t=1}^{364} P(X > C - L_t)\Delta T \left[\frac{days}{year}\right] \tag{3.7}$$

$$LOLE = \sum_{t=1}^{8736} P(X > C - L_t)\Delta T \left[\frac{hours}{year}\right] \tag{3.8}$$

$where:$ ΔT = The time increment, e.g. 1 hour for HPL or 1 day for DPL

L_t = System load in time period t [MW]

C = Total installed generation capacity in the system not on scheduled outage

$P(X > x)$ = Is the cumulative probability from the COPT table

As mentioned in the previous section, LOLP is part of the calculation of LOLE and can be recognised as $P(X > C - L_t)$. Thus Equations (3.7) and (3.8) can be rewritten as Equations (3.9) and (3.10)

$$LOLE = \sum_{t=1}^{365} LOLP_t \Delta T \left[\frac{days}{year} \right] \tag{3.9}$$

$$LOLE = \sum_{t=1}^{8736} LOLP_t \Delta T \left[\frac{hours}{year} \right] \tag{3.10}$$

In adequacy planning studies a commonly used LOLE standard value is "1 day in 10 years" or a LOLE of 0.1 days/year. The standard dates back to the 1950s when G. Calabrese and Watchorn based it on systems they deemed to have a satisfying reliability level [29]. This standard has been widely integrated in industrial standards for planning adequate reserve margins for a reliable system. As more system planning simulations move from a DPL-model to a HPL-model, the LOLE standard of 0.1 day/year is often converted to 2.4 hours/year. This is not correct as a LOLE calculated with a HPL-model will differ from one with a DPL-model, except from the unrealistic case where peak load lasts for 24 full hours. Some countries have defined HPL-model standards for the LOLE, where they allow an LOLE of the values presented in Table 3.3.

Table 3.3: Countries with defined HPL-model LOLE standards [30]

Country	LOLE [hours/year]
Belgium	3
France	3
Great Britain	3
Ireland	8
The Netherlands	4

EENS

As mentioned before the LOLP/LOLE metrics are criticised as a system reliability measure, due to its lack of information concerning the outage severity and only the probability that a loss-of-load situation occurs. It is natural that a 100 MW outage should be weighted more than a 1 MW outage. The EENS is an expansion on the LOLE that includes the size of the capacity shortcoming and most often has the unit of MWh/year.

The calculation of the probabilistic EENS for a time period can be divided in three stages. First, the probabilistic expectation of energy not served for a given generation capacity outage and load, E_j is calculated as shown in Equation (3.11). Then, the probabilistic expectation of energy not served for the system at a specific time increment, $EENS_t$, is calculated by summing all instances where there is a capacity deficiency, as shown in Equation (3.12). Finally, to obtain the $EENS$ for a system over the entire time period, the sum over all time increments in the time period is calculated, e.g. an HPL-model over the period of a year, as shown in Equation (3.13).

$$E_j = \left[x_j - (C - L_t)\right] \cdot p(X = x_j) \qquad \left[MWh\right] \tag{3.11}$$

$$EENS_t = \sum_{x_j = C - L_t}^{C} \left[x_j - (C - L_t)\right] \cdot p(X = x_j) \qquad \left[MWh\right] \tag{3.12}$$

$$EENS = \sum_{t=1}^{8736} \sum_{x_j = C - L_t}^{C} \left[x_j - (C - L_t)\right] \cdot p(X = x_j) \qquad \left[MWh/year\right] \tag{3.13}$$

$where$:

	x_j	=	the generation capacity outage in state j
	L_t	=	System load in time period t [MW]
	C	=	Total installed generation capacity in the system not on scheduled outage
	$p(X = x)$	=	The individual probability of being in state x_j

As an example of EENS calculation, consider the same example system as in Section 3.3.3 with a CYPL of 25 MW and using an expansion of the COPT from Table 3.2 describing a system with 40 MW generation capacity, shown in Table 3.4. It is evident that three outage states cause a generation capacity deficit and the $EENS_t$ for this time period is given as the sum of the E_j values for the outage states, $EENS_t = 0.098 + 0.01176 + 0.0002 = 0.10996$. Assuming a HPL-model is used

the units will be MWh/hour. As the calculations normally are done for a year using 8736 hours[2] the EENS for this system over the time period of a year is $0.10996 \times 8736 = 960.94$ MWh/year. Note this way of calculation only holds true as this example applies a CYPL-model and thus has no change in load.

A normalised version of EENS, EUE, is used as reliability standard by the Australian Energy

Table 3.4: Extended COPT for example calculation of EENS

State j	Capacity Outage x_j [MW]	Individual Probability $p(X = x_j)$	Cumulative Probability $P(X \leq x_j)$	Capacity Deficit $[x_j - (C - L_t)]$	E_j
1	0	0.941192	1	0	0
2	10	0.038416	0.058808	0	0
3	20	0.01960	0.020392	5	$5 \times 0.01960 = 0.0980$
4	30	0.000784	0.0000792	15	$15 \times 0.000784 = 0.01176$
5	40	0.000008	0.000008	25	$25 \times 0.000008 = 0.0002$

Marker Commission's Reliability Panel. It is constructed by dividing the EENS by the total annual energy consumption and is currently set in Australia at 0.002% [30]. Otherwise EENS based standards are much less used than LOLE based ones.

3.4 Capacity Credit

When planning a new power system, or expanding an existing one, having enough generation capacity to reliably meet the load demand is crucial. LOLE and EENS can be used to evaluate the system reliability and the reliability effect from new generator on the system. Interpreting the metrics into quantities of practical applications other than just an evaluation of the system reliability level is difficult and has led to the development of the Capacity Credit (CC) concepts.

CCs applies LOLE or EENS to evaluate how much generating capacity is replaced by variable renewables while maintaining the reliability level. One such CC, and arguably the most recognised, is the Effective Load Carrying Capability (ELCC). Other CCs are Equivalent Firm Capacity

[2]As earlier described, the calendar used in reliability calculations defines one year as 8736 hours because it is based on 52 weeks and 364 days.

(EFC) and Equivalent Conventional Capacity (ECC). All three CCs share the feature of quantifying the added capacity in terms of MWs as the reliability level remains at the same level after the addition of generation and load.

3.4.1 Effective Load Carrying Capability

ELCC was initially presented by Garver in 1966 [31] as a tool for generation expansion planning to evaluate the increase in possible load demand, and it has later been established as a robust metric for evaluating the reliability contribution of renewable energy sources, especially wind power [21, 32, 33]. ELCC is flexible as it can apply various load- and generation models in addition to reliability metrics like LOLE or EENS for system evaluation. ELCC is classically presented using the LOLE metric and will also be done so in this section, although as previously stated it can be swapped for the EENS metric. The ELCC calculation approach is presented in Equations (3.14) and (3.15).

$$LOLE_{old} = LOLE_{new} \tag{3.14}$$

$$\sum_{i=1}^{n} P_i\left(X_{old} > C_{old} - L_i\right) = \sum_{i=1}^{n} P_i\left(X_{new} > (C_{old} + C_{gen}) - (L_i + \Delta L)\right) \tag{3.15}$$

$where$:

	$LOLE_{old}$	=	LOLE of the original system
	$LOLE_{new}$	=	LOLE of the new system with additional generation and/or load
	L_i	=	Load condition for the time duration i [MW]
	ΔL	=	Additional load that can be served by the new system [MW]
	n	=	Total number of time increments in the evaluation period
	C_{old}	=	Total possible generation capacity for the original system
	C_{gen}	=	Maximum capacity of the generation unit added to the system
	$P_i(X_{old} > x)$	=	Cumulative probability obtained from the original COPT
	$P_i(X_{new} > x)$	=	Cumulative probability obtained from the new COPT

The equations are evaluated with an iterative increasing ΔL and calculation of $LOLE_{new}$ until the LOLE of the new system equals that of the original system. When both LOLE values are equal, the corresponding ΔL represents the additional load that can be met at the same reliability level when adding a generator with a capacity of C_{new} to the system. The ELCC for that specific generator added to that specific system is quantified as the ΔL. The value of ELCC has in this case the unit of MW, but another common unit is as a percentage of the generator's capacity, as shown in Equation (3.16).

$$ELCC = \frac{\Delta L}{C_{gen}} \times 100\% \tag{3.16}$$

The iterative approach on how to calculate ELCC as presented by Equations (3.14) and (3.15) gives exact solutions and will be the method of choice for this thesis. The algorithmic approach to obtain the ELCC is presented in three steps, and exemplified by utilising the same example system as in Section 3.3.3 with a CYPL of 25 MW and a generating capacity of 40 MW. The added generator has a FOR of 4%, capacity of 10 MW and two operating states, the outage data for the generator is presented in Table 3.5. The desired reliability level is set to 0.4 days/year as it is fairly close to that of the original system and gives a good illustrative result of an ELCC equal to 7.69 MW or using Equation (3.16), 76.9%.

Table 3.5: Data for the additional generator

State j	Outage [MW]	Ind.prob P(X=x)
1	0	0.96
2	10	0.04

1. The LOLE for the original system is plotted by iteratively increasing the load. As the load can vary within the evaluated time interval only the peak load is increased. The other load points L'_i are scaled according to Equation (3.17). See Figure 3.7a.

2. Generation is added to the original system and the COPT for the new system is obtained. The Process from Step 1 is repeated using the now updated COPT and a new value is plotted for the same load/time series as in Step 1. See Figure 3.7b.

3. The ELCC is calculated in MWs from the horizontal distance between the two curves at the desired reliability, measured by the chosen reliability metric on the y-axis, in this case LOLE. The reliability level can be defined by a standard like 0.1 days/year or more commonly compared with the reliability level in the original system. See Figure 3.7c.

$$L'_i = L_i \frac{L'_{max}}{L_{max}} \tag{3.17}$$

$where$:

	L'_i	=	Scaled load level [MW]
	L_i	=	Base case load level
	L_{max}	=	Maximum load in the original load series [MW]
	L'_{max}	=	Maximum load in the new load series [MW]

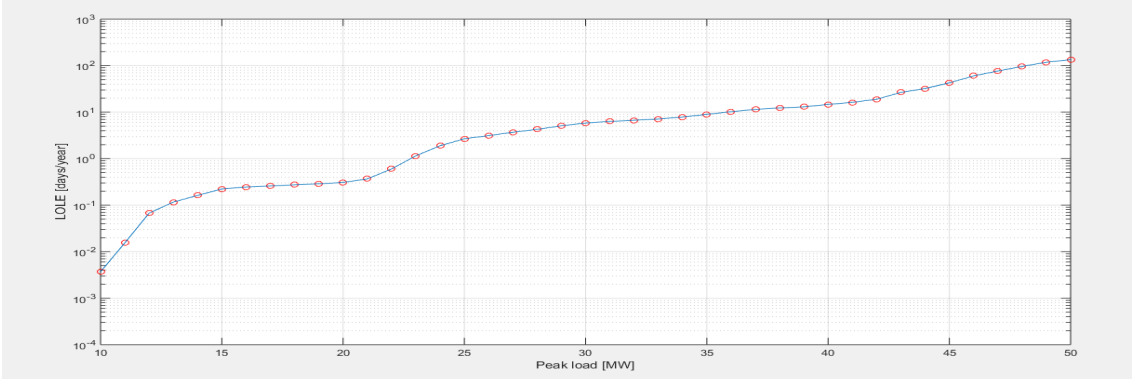

(a) Step 1: LOLE plot of original system with increasing top load

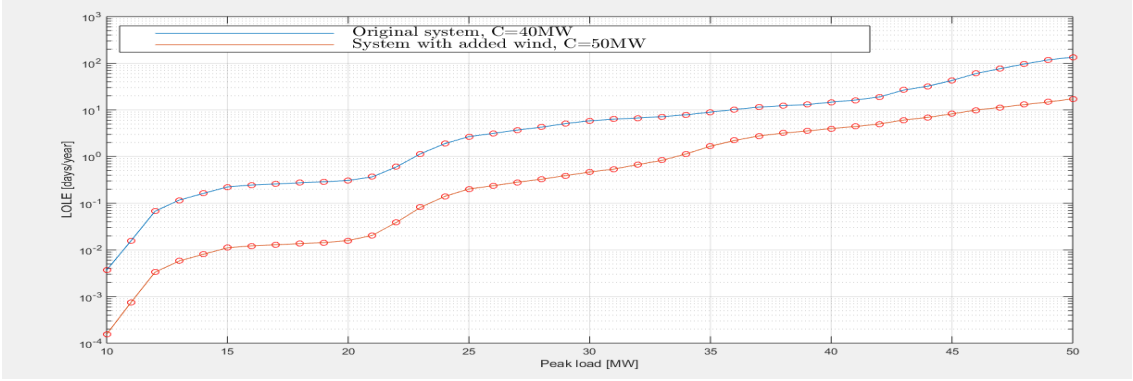

(b) Step 2: LOLE plot of system with additional generation and increasing top load

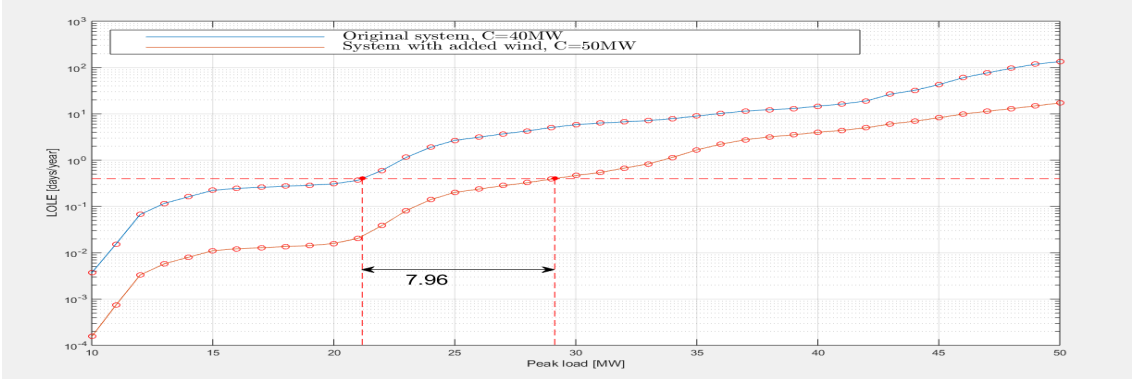

(c) Step 3: The intersection between the desired reliability level and the LOLE curves

Figure 3.7: Steps for calculating LOLE

3.4.2 Equivalent Firm Capacity and Equivalent Conventional Capacity

EFC and ECC are very similar in the way they are calculated. Both use a reliability metric, like LOLE or EENS to evaluate a system with the additional renewable generator that is to be evaluated. Then the renewable generator is replaced by a fictitious generator with known availability. The fictitious generator's capacity is iteratively increased until the same reliability level as for the original system is achieved. The CC of the added generator is then set to same value as the capacity of the fictitious generator when reliability levels were equal. The difference between EFC and ECC is that the added generator is an ideal 100% reliable generator for EFC, whereas the added fictitious generator is a realistic conventional generator with a specified unavailability for ECC [34, 35, 36].

$$LOLE_{goal} = LOLE_{current} \tag{3.18}$$

$$\sum_{i=1}^{n} P_i\left(X_{goal} > C_{goal} - L_i\right) = \sum_{i=1}^{n} P_i\left(X_{current} > (C_{goal} + C_{gen}) - L_i\right) \tag{3.19}$$

$where$:

	$LOLE_{goal}$	=	LOLE of the system with additional generation
	$LOLE_{current}$	=	LOLE of the system with the fictitious generator
	L_i	=	Load condition for the time duration i [MW]
	n	=	Total number of time increments in the evaluation period
	C_{goal}	=	Total possible generating capacity for the original system [MW]
	$C_{current}$	=	Maximum generating capacity of the fictitious unit [MW]
	$P_i(X_{goal} > x)$	=	The cumulative probability obtained from the original COPT
	$P_i(X_{current} > x)$	=	The cumulative probability obtained from the new COPT

The algorithmic approach to evaluate EFC and ECC using the LOLE metric for a system is presented in three steps.

1. The $LOLE_{goal}$ of a system with the additional generation is calculated.

2. The added generator is then removed from the system and a fictitious generator with either a 100% availability (EFC) or a generator with a more realistic availability (ECC) is added.

3. The capacity of the generator is iteratively increased and the new $LOLE_{current}$ of the system i calculated until the $LOLE_{current}$ of the system with the fictitious equals the $LOLE_{goal}$ of the system with the generator to be evaluated. The EFC/ECC is the capacity of the generator, C_{gen} when the systems have the same $LOLE$ value.

As EFC and ECC are so similar only an example of ECC calculation is shown in Figure 3.8. Consider the same example system as in Section 3.3.3 with a capacity of 40 MW using a DPL-model. A generator of 10 MW and a FOR of 4% is added. The LOLE calculated from this system is 0.4665 days/year and is shown as the dotted horizontal line. The fictitious conventional generator has a FOR of 3%, its starting capacity is 8 MW and the iterative increase in capacity is set to 0.25 MW. The increasing capacity increases the reliability of the system and reduces the LOLE as shown by the blue line. The intersection between the LOLE curve and the horizontal dotted LOLE line describes the ECC value of the additional generator, in this case 9.0139 MW. As this simple example basically only compares two conventional generators with slightly different availability, it has little practical value. The method is much more useful when finding ECC of non-conventional generator like wind or solar power, as they have several generating capacity states.

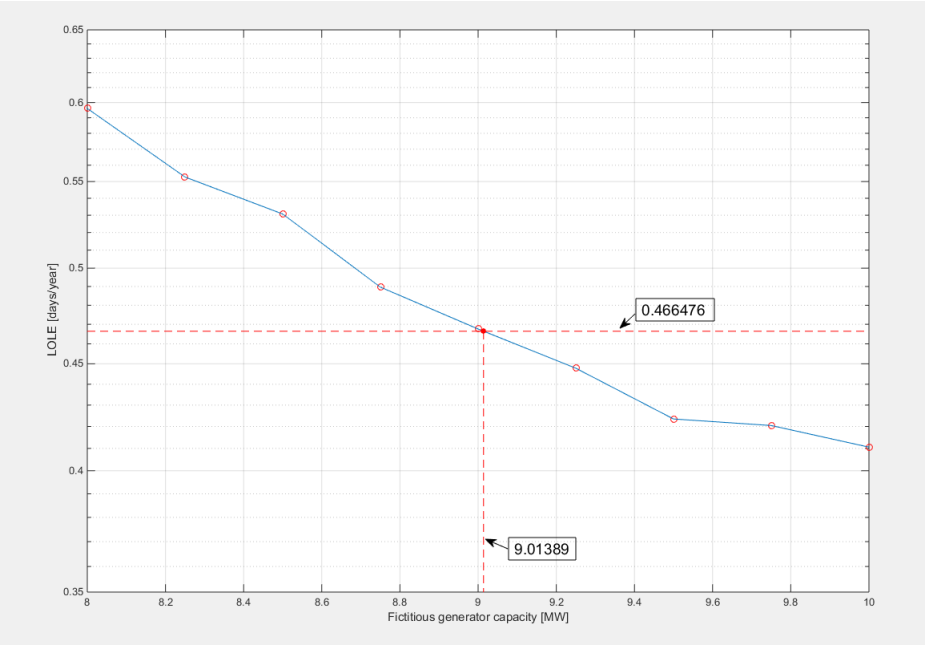

Figure 3.8: Example of ECC calculation

3.5 Wind Generation Modelling

Extensive research has been performed to develop mathematical models and methods to evaluate reliability in power systems containing wind energy [26, 32, 35, 37]. The approaches are similar for most of the studies and follow the same steps. Each step can be viewed as a building block laying the foundation for the next step. Several choices can be made as to which models or methods are applied in each step, which further affects the possibilities and results for the following step. The first step concerns how to model the wind, the second concerns wind generator modelling and the third concerns how the wind generators are combined to form a wind farm model.

3.5.1 Wind Modelling

When developing wind as an energy source, one of the first steps is to survey the available wind resources, which in turn dictates the wind farms location and generating capacity [38]. The most common way to model wind is the hourly wind speed series. The wind speed for a certain height above ground are presented in hours over the course of one time period. The reason for using wind speed is its direct correlation with the amount of energy produced by the turbines at

different rotor speeds. This correlation known as the power curve varies between turbine models and is a major factor in deciding on the type and number of wind turbines to be installed [39].

The hourly wind speed model can be obtained directly from historical data by directly applying measured wind speeds from one year of observation. As wind is a highly fluctuating and random variable, the values over the course of one year will, apart from seasonal trends, have little probability of occurring in the same sequence in the future and thus has poor predictive abilities. Utilising measured data from several years and their average values, gives a model with much better predictive accuracy. Other statistical methods and simulation techniques like the Auto Recursive Moving Average model (ARMA) [40] can also be deployed, but will not be covered in this thesis.

3.5.2 Generator Modelling

Power Curve

The output of a Wind Turbine Generator (WTG) is highly dependent on the local wind regime as well as the performance of the rotor and the efficiency of the generator. As mentioned earlier the correlation between wind speed and turbine output are referred to as the power curve. Figure 3.9 shows the power curve of a Vestas V90-2MW turbine, the same turbine model used for calculations in this thesis. The Vestas turbine is chosen as it is the most numerous turbine worldwide, with over 20 000 installed units [41]. For this turbine the wind speed where the turbine starts to produce power, known as the cut-in speed, is 4 m/s. The rated wind speed at which it produces rated output is 15 m/s. The speed where the rotor is stopped to avoid mechanical harm, known as the cut-out speed, is 25 m/s. The output, and thus also, power curve in Figure 3.9 is obtained from the hourly wind speeds using Equation (3.20).

$$P(WS_t) = \begin{cases} 0 & 0 \leq WS_t < V_{ci} \\ (A + B \cdot WS_t + C \cdot WS_t^2) \cdot P_r & V_{ci} \leq WS_t < V_r \\ P_r & V_r \leq WS_t < V_{co} \\ 0 & WS_t \geq V_{co} \end{cases} \tag{3.20}$$

$where:$ $P(WS_t)$ = WTG output with the wind speed in time interval t [MW]

WS_t = Wind speed in time interval t [m/s]

P_r = Rated output from the WTG [MW]

V_{ci} = Cut-in wind speed [m/s]

V_r = Rated wind speed [m/s]

V_{co} = Cut-out wind speed [m/s]

The constants A, B and C can be found as functions of V_{ci}, V_r and V_{co} as shown in Equation (3.21) [42].

$$A = \frac{1}{(V_{ci} - V_r)^2} \left\{ V_{ci}(V_{ci} + V_r) - 4V_{ci}V_r \left[\frac{V_{ci} + V_r}{2V_r} \right]^3 \right\}$$

$$B = \frac{1}{(V_{ci} - V_r)^2} \left\{ 4(V_{ci} + V_r) \left[\frac{V_{ci} + V_r}{2V_r} \right]^3 - (3V_{ci} + V_r) \right\} \tag{3.21}$$

$$C = \frac{1}{(V_{ci} - V_r)^2} \left\{ 2 - 4 \left[\frac{V_{ci} + V_r}{2V_r} \right]^3 \right\}$$

Two-State and Multi-State Representation

The WTG output curve obtained from combining the power curve and the wind speed data consists of chronological hourly represented output levels. These values form the basis of how to model a conventional generator with probabilistic output levels equivalent to the WTG. By

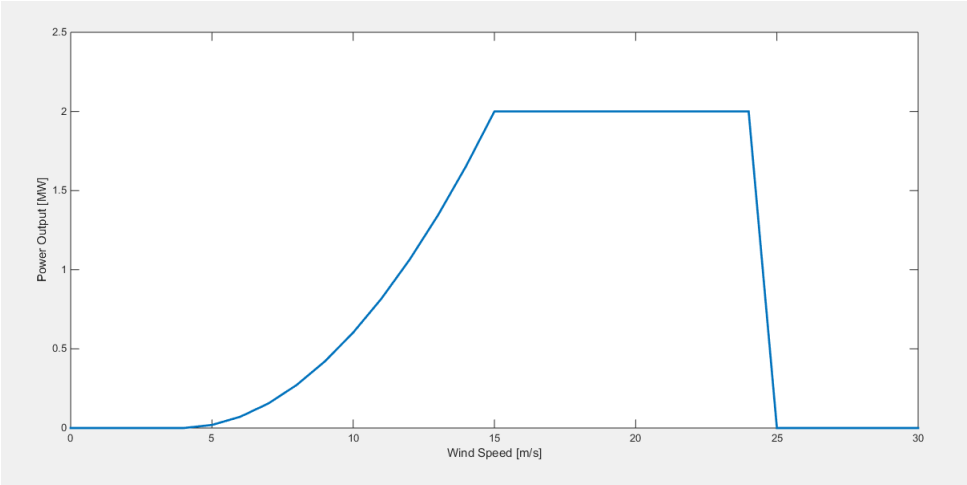

Figure 3.9: The power curve for a Vestas V90-2MW wind turbine

summing the number of times the output level has the same values and dividing it by the total number of increments the probability for each output level is obtained [26]. As the possible output levels from the WTG are very numerous, it is not advantageous from a computational perspective to continue using all state occurrences. A simplification is done by choosing the number of feasible states for the wind turbine and using state rounding to reduce the number of states [42]. This can be done either pre- or post- WTG output calculation.

In Section 3.3.2 conventional generators are represented by two-state or multi-state models. A two-state model consists of the fully operational, rated output, and fully non-functional, zero output. It will give a very pessimistic representation of a WTG where a big amount of energy is produced under rated output. Since WTGs have a natural high occurrence of output levels below rated output, a multi-state representation seems most fit and will be applied throughout the thesis.

Here follows an example of how to model a multi-state representation of a WTG with three output levels and using the very simplified and highly unrealistic wind measurements in Table 3.6. The low number of observations is only for the ease of calculation. The same principles applies if the measurements are performed only once a month or once an hour for a year. The table shows the month of measurement, the measured wind speed and the output from the wind turbine when applying Equation (3.20).

Table 3.6: Monthly wind measurements

Month	Wind Speed [m/s]	Output [MW]
January	30	0
February	30	0
March	20	2
April	0	0
May	12	1
June	12	1
July	0	0
August	0	0
September	12	1
October	20	2
November	20	2
December	30	0

Table 3.7: Multi-state representation of WTG

State	Output [MW]	Probability
1	0	0.5 = q_0
2	1	0.25 = q_1
3	2	0.25 = q_2

To model the multi-state generator, all the occurrences of different output values are summed and divided by the total amount of observations. An output of 2 MW occurs three times and the total amount of observations are twelve. This gives $3 \div 12 = 0.25$ as the probability of the WTG delivering 2 MW of power, or 25%. The same operations for the rest of the values result in a WTG with the output levels and probabilities shown in Table 3.7.

3.5.3 Wind Farm Modelling

As each individual WTG has a relative small generation capacity several WTGs are combined into large wind farms. In a wind farm, the individual WTG has an output dominantly related to wind speed. As the same wind regime accounts for the production for all WTGs, their output cannot be modelled as independent variables. To arrive at the cumulative distribution function for the entire wind farm the individual WTGs output probability distributions are convoluted. Also, the mechanical failure rate of each individual WTG must be included in the modelling. In [42] a method for convoluting the wind model, WTG data and the number of turbines to form an equivalent conventional generator representing the wind farm is presented. This approach is represented by Equation (3.22) that returns the outage states for the entire wind farm and their associated cumulative probability. For further explanation the reader is referred to [42].

$$\sum_{i=0}^{k} \left(\sum_{j=0}^{s} q_j \, u \left(\frac{x_{output}}{i} - c_j \right) \right) \cdot p_{unit,i} \tag{3.22}$$

$where:$

k = Number of wind turbines in the wind farms

s = Number of wind generator's capacity states

q_j = Probability of wind turbine operating in output state c_j

u = Probability of argument occurring

x_{output} = Output from wind farm [MW]

i = Available wind power units

c_j = Generation capacity in state j

$p_{unit,i}$ = Probability of i units being available

Here follows an example of how to model a wind farm consisting of two turbines as one equivalent generator taking into consideration the mechanical outage of the turbines. To do this, q_i values found in Table 3.7 describing a multi-state WTGs and a mechanical forced outage of 3% are used. The mechanical availability is found by constructing Table 3.8 using established probability calculations. Then Equation (3.22) calculates the total capacity output of the wind farm.

Table 3.8: Mechanical availability of two WTGs

State	Available Turbines	Calculation	Probability
0	0	0.03^2	$p_0 = 0.0009$
1	1	$2 \cdot (0.97 \cdot 0.03)$	$p_1 = 0.0583$
2	2	$(0.97)^2$	$p_2 = 0.9409$

Output equals 0 MW, x=0:

This output occurs when both WTGs are unavailable, or there is zero output from the WTG and both or one WTG is available (wind speeds being too low or too high).

$$\text{For zero WTG} \quad (i=0), \qquad u\left(\frac{0}{0}-c_j\right)=1, \text{ for all j}$$

$$\text{prob} = p_0q_0 + p_0q_1 + p_0q_2$$

$$\text{For one WTG} \quad (i=1), \qquad u\left(\frac{0}{1}-c_j\right)=\begin{cases}1, & \text{for } j=0\\ 0, & \text{otherwise}\end{cases}$$

$$\text{prob} = p_1q_0$$

$$\text{For two WTG} \quad (i=2), \qquad u\left(\frac{0}{2}-c_j\right)=\begin{cases}1, & \text{for } j=0\\ 0, & \text{otherwise}\end{cases}$$

$$\text{prob} = p_2q_0$$

$$\text{Summing } F_x(0) = p_0q_0 + p_0q_1 + p_0q_2 + p_1q_0 + p_2q_0 = 0.5005$$

Output equals 1 MW, x=1:

This output occurs when one WTG is available and has an output of 1 MW.

$$\text{For zero WTG} \quad (i=0), \qquad u\left(\frac{1}{0}-c_j\right)=1, \text{ for all j}$$

$$\text{prob} = p_0q_0 + p_0q_1 + p_0q_2$$

$$\text{For one WTG} \quad (i=1), \qquad \left(\sum_{j=0}^{s} q_j\, u\left(\frac{1}{1}-c_j\right)\right)\cdot p_1$$

$$\text{prob} = p_1q_0 + p_1q_1$$

$$\text{For two WTG} \quad (i=2), \qquad \left(\sum_{j=0}^{s} q_j\, u\left(\frac{1}{2}-c_j\right)\right)\cdot p_2$$

$$\text{prob} = p_2q_0$$

$$\text{Summing } F_x(0) = p_0q_0 + p_0q_1 + p_0q_2 + p_1q_0 + p_1q_1 + p_2q_0 = 0.5150$$

Output equals 2 MW, x=2:

This output occurs when one WTG is available and has an output of 2 MW, or both are available and have an output of 1 MW each.

For zero WTG $(i = 0)$, $u\left(\frac{2}{0} - c_j\right) = 1$, for all j

$$\text{prob} = p_0 q_0 + p_0 q_1 + p_0 q_2$$

For one WTG $(i = 1)$, $\left(\sum_{j=0}^{s} q_j \, u\left(\frac{2}{1} - c_j\right)\right) \cdot p_1$

$$\text{prob} = p_1 q_0 + p_1 q_1 + p_1 q_2$$

For two WTG $(i = 2)$, $\left(\sum_{j=0}^{s} q_j \, u\left(\frac{2}{2} - c_j\right)\right) \cdot p_2$

$$\text{prob} = p_2 q_0 + p_2 q_1$$

Summing $F_x(0) = p_0 q_0 + p_0 q_1 + p_0 q_2 + p_1 q_0 + p_1 q_1 + p_1 q_2 + p_2 q_0 + p_2 q_1 = 0.7648$

Output equals 4 MW, x=4:

This output occurs when both WTGs are available and produce 2 MW each.

For zero WTG $(i = 0)$, $u\left(\frac{4}{0} - c_j\right) = 1$, for all j

$$\text{prob} = p_0 q_0 + p_0 q_1 + p_0 q_2$$

For one WTG $(i = 1)$, $\left(\sum_{j=0}^{s} q_j \, u\left(\frac{4}{1} - c_j\right)\right) \cdot p_1$

$$\text{prob} = p_1 q_0 + p_1 q_1 + p_1 q_2$$

For two WTG $(i = 2)$, $\left(\sum_{j=0}^{s} q_j \, u\left(\frac{4}{2} - c_j\right)\right) \cdot p_2$

$$\text{prob} = p_2 q_0 + p_2 q_1 + p_2 q_2$$

Summing $F_x(0) = p_0 q_0 + p_0 q_1 + p_0 q_2 + p_1 q_0 + p_1 q_1 + p_1 q_2 + p_2 q_0 + p_2 q_1 + p_2 q_2 = 1$

These calculations result in the wind farm's output states and their cumulative and individual probabilities shown in Table 3.9. Note that this example only calculates valid states. An output of 3 MW was not calculated, as it is not possible to obtain with two turbines with outputs of 0 MW, 1 MW or 2 MW. For more effective calculations the valid states were calculated beforehand using the number of turbines and the individual turbine outputs. Also, note the equation returns outputs not outages. What notation is used varies in literature and this thesis does not make changes to equations or methods developed by others, but rather switches output with outage, as this is fairly easy.

Table 3.9: Equivalent multi-state representation of wind farm

State	Output [MW]	Cumulative Probability	Individual Probability
1	0	0.5005	0.5005
2	1	0.515	0.0146
3	2	0.7648	0.2498
4	4	1	0.2352

Chapter 4

Methodological Approach

To present and evaluate algorithmic approaches for assessing the generation adequacy impact of a wind farm added to a power system, ELCC, EFC and ECC are chosen as the guiding adequacy metrics for this process, as supported by [32] and [26]. These are calculated by modelling a wind farm as an equivalent multi-state generator as done in Section 3.5 and adding it to established test systems RBTS [6] and IEEE-RTS [7]. Several other established power system adequacy methodologies, presented in Chapter 3 are also embedded in the approach. The approach used to obtain the ELCC, EFC and ECC results, follows the algorithmic steps presented below. All procedures used have been presented in earlier chapters and are referenced, or are part of the MATLAB scripts.

4.1 ELCC Using LOLE Metrics

1. Calculate the LOLE values of the system without the additional generation provided by the wind farm throughout the chosen time period.
   (a) Obtain the COPT for the original system.
   (b) For time increment t:
      i. Obtain the LOLE value using the COPT and load level in that time increment
      ii. Repeat step i) for all time increments.

2. Obtain the LOLE values of the system with the additional generation provided by the wind farm throughout the chosen time period.

   (a) Model the wind farm as an equivalent generator using the method described in Section 3.5.

   (b) Add the new generator to obtain $COPT_{new}$

   (c) For time increment t:

      i. Obtain the $LOLE_{new}$ value using the $COPT_{new}$ and load level in that time increment

      ii. Repeat step i) for all time increments.

3. Plot the peak load vs. $LOLE$ and peak load vs. $LOLE_{new}$ curves for the system.

   (a) By scaling the peak load create new time/load series.

   (b) Repeat step 1) and 2) for each new time/load series and plot the peak load vs LOLE and peak load vs $LOLE_{new}$ for each instance.

4. Obtain the ELCC for the chosen reliability level. This level can be predetermined using a reliability standard, e.g. LOLE of 0.1 days/year (or EENS) or by using the LOLE value of the base system with original time/load series.

   (a) The ELCC value is defined as the horizontal distance between the intersections of the top load vs LOLE and top load vs $LOLE_{new}$ and the chosen reliability level. This value represents the additional load that the system with the wind farm can supply at the chosen reliability level. The ELCC obtained serves as the effective load carrying capabilities of the wind farm.

4.1.1 Simple Example For ELCC Calculation Using LOLE

To exemplify the algorithmic approach for the ELCC value using LOLE, a small wind farm is added to a small generation system. The system consists of three generators with a total of 40 MW installed effect as shown in Table 4.4. A DPL-model is used for the load with a 20 MW peak load. The wind farm consists of two turbines with an individual capacity of 2 MW and FOR of

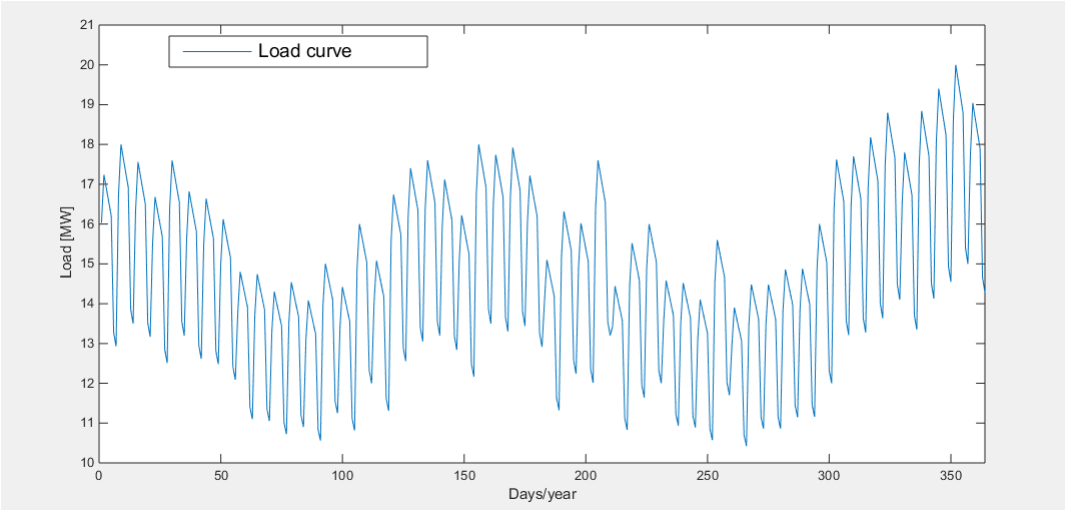

Figure 4.1: Annual load variation for DPL-model

3%, as presented in Table 4.2. The power output probability for one wind turbine is presented in Table 4.3. Note that these values are unrealistically high, but provide good values for calculation and illustrative purposes.

Table 4.1: Generator data

Number of generators	Capacity [MW]	FOR
2	10	0.02
1	20	0.02

Table 4.2: Turbine data output

Turbines	Capacity [MW]	FOR
2	2	0.03

Table 4.3: Output probability for one wind turbine

State	Turbine Output	State Probability
1	0	0.25
2	1	0.25
3	2	0.5

Table 4.4: Example system data

Step 1:

(a): The base system is the same as in Section 3.3.2, and the procedure and resulting COPT will therefore be the same. Table 3.2 shows the different states and their corresponding cumulative probability value.

(b): The DPL-model contains 364 load levels calculated to a $LOLE_{old}$ of 0.3079 days/year. This LOLE value is relatively large when compared to the standard of 0.1 days/year which demonstrates that this system has a low reliability.

Step 2:

(a): The wind and WTG data are used to model the output states of a single wind turbine and their probabilities. Then several of those wind turbines are combined to form a model of an entire wind farm. This procedure is performed as in Section 3.5. The resulting multi-state representation is shown in Table 3.9.

(b): To obtain the $COPT_{new}$ for the new system, the equivalent multi-state generator is added to the base case system and the $COPT_{new}$ is calculated as in step 1.(a). Table 4.5 shows the updated and larger $COPT_{new}$ for the system including the wind farm.

Step 3:

Plotting the LOLE lines for both the original system and the system with added generation, is done by scaling the load/time series and calculating the LOLE for each set of values. The LOLE lines are represented by the two curves in in Figure 4.2.

Table 4.5: $COPT_{new}$ for the simple system

State	Capacity Outage [MW]	Cumulative Probability	Individual Probability
1	0	1	0.338935004
2	2	0.661064996	0.131237460
3	4	0.529827536	0.471019536
4	10	0.058808000	0.013834082
5	12	0.044973918	0.005356631
6	14	0.039617287	0.019225287
7	20	0.020392000	0.007058205
8	22	0.013333795	0.002732975
9	24	0.010600820	0.009808820
10	30	0.000792000	0.000282328
11	32	0.000509672	0.000109319
12	34	0.000400353	0.000392353
13	40	0.000000008	0.000002880
14	42	0.000005120	0.000001115
15	44	0.000004003	0.000004003

Step 4:

The small number of generators in the example system exposes it to a high risk of not meeting the load demand and thus obtaining a low system reliability. Figure 4.2 illustrates the curves for peak load vs $LOLE_{old}$ and peak load vs $LOLE_{new}$ together with the chosen reliability level and their intersection point. The difference between the intersection points give an ELCC of 1.07 MW, or 26.75% of the installed effect.

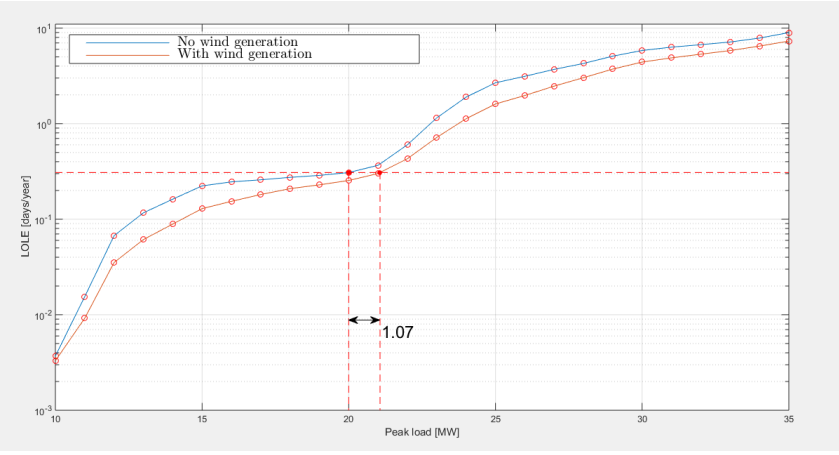

Figure 4.2: Peak load vs $LOLE_{old}$ and peak load vs $LOLE_{new}$ curves

4.2 ELCC Using EENS Metrics

Calculating ELCC with EENS is done almost identically as with LOLE. The procedure for EENS follows the same steps as for LOLE, but replaces the reliability level calculations done for LOLE with EENS and chooses a reliability level based on MWh instead of a time interval.

4.2.1 Simple Example For ELCC Calculation Using EENS

The example utilises the same system as in Section 4.1.1. The generator from the system is described in Table 4.4. Data for the wind farm with two turbines is given in Table 4.2 and the individual turbine output in Table 4.3.

Step 1:

(a): The base system used is the same as in Section 3.3.2 the COPT will therefore be the same. Table 3.2 shows the different states and their corresponding cumulative probability value.

(b): The DPL-model gives 364 data points that for the base case is summed to a $EENS_{old}$ of 1.414 MWh/year.

Step 2:

(a): The wind and WTG data are used to model the output states of a single wind turbine and their probabilities. Then several of those wind turbines are combined to form a model of an entire wind farm. This procedure is performed as in Section 3.5. The resulting multi-state representation is shown in Table 3.9.

(b): To obtain the $COPT_{new}$ for the new system, the equivalent multi-state generator is added to the base case system and the $COPT_{new}$ is calculated as in step 1.(a). Table 4.5 shows the updated and larger $COPT_{new}$ for the system including the wind farm.

Step 3:

Plotting the EENS lines for the original system and the system with added generation is done by scaling the load/time series. This is represented by the two curves in Figure 4.3.

Step 4:

Figure 4.3 shows the peak load vs $EENS_{old}$ and the peak load vs $EENS_{new}$ curves together with the chosen reliability level and their intersection point. The difference between the intersection points give an ELCC of 1.78 MW, or 44.50% of the installed effect.

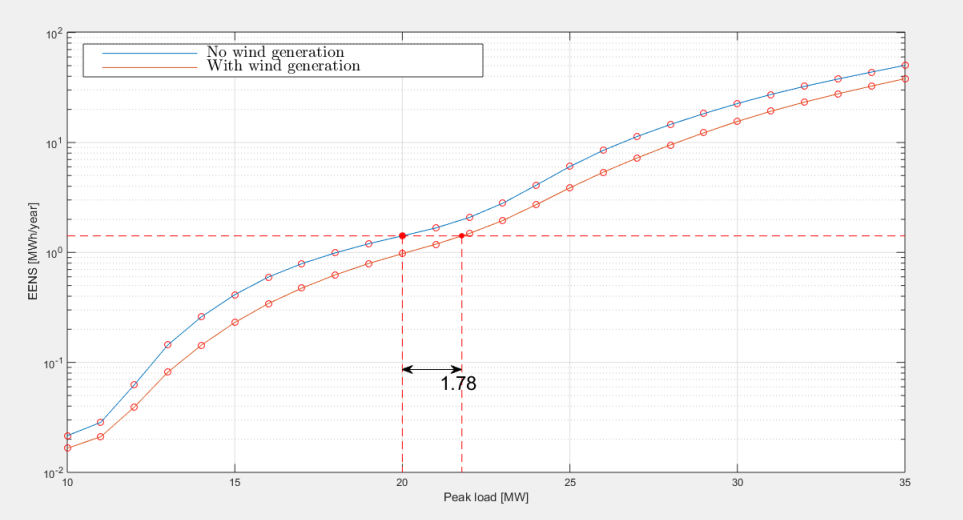

Figure 4.3: ELCC calculation example using EENS

4.3 EFC and ECC Using LOLE Metrics

As the computational procedures for EFC and ECC are similar, only ECC will be provided with an example in this section.

1. Obtain the LOLE values of the system with the additional generation provided by the wind farm for the chosen time period.

   (a) Model the wind farm as an equivalent generator using the method described in Section 3.5.

(b) Add the new generator to obtain $COPT_{new}$

(c) For time increment t

i. Obtain the $LOLE_{new}$ value using the $COPT_{new}$ and load level in that time increment

ii. Repeat step i) for all time increments.

2. Replace the wind farm equivalent generator with a conventional generator that has a known availability.

(a) Remove the additional generation provided by the wind farm.

(b) Add a fictional generator with availability representing a conventional generator with known availability or an ideal generator.

3. Obtain the LOLE value of the system with the fictional generator.

(a) With the new generator obtain $COPT_{current}$

(b) For time increment t

i. Obtain the $LOLE_{current}$ value using the $COPT_{current}$ and load level in the current time increment

ii. Repeat step i) for all time increments.

4. Plot the $LOLE$ vs. capacity curve for the system with the fictitious generator.

(a) For a reasonable interval iteratively increase the capacity of the fictitious generator.

(b) For each increase in capacity repeat step 3.

5. Obtain the EFC/ECC for the chosen reliability level.

(a) The EFC/ECC is defined as the capacity value of the fictitious generator at the intersection point of the $LOLE_{current}$ curve and the $LOLE_{goal}$ value.

4.3.1 Simple Example for ECC Calculation Using the LOLE Metric

The example utilises the same system as in Section 4.1.1. The generator from the system is described in Table 4.4. Data for the wind farm with two turbines is given in Table 4.2 and the individual turbine output in Table 4.3.

Step 1:

(a): The wind and WTG data are used to model the output states of a single wind turbine and their probabilities. Then several of those wind turbines are combined to form a model of an entire wind farm. This procedure is done as in Section 3.5. The resulting multi-state representation is shown in Table 3.9.

(b): To obtain the $COPT_{current}$ for the new system the equivalent multi-state generator is added to the base-case system and the $COPT_{current}$ is calculated as in Section 3.3.2. Table 4.5 shows the $COPT_{current}$ for the system including the wind farm.

(c): The DPL-model gives 364 data points, which for the case with the added wind farm is summed to a $LOLE_{goal}$ of 0.2543 days/year.

Step 2:

The wind farm equivalent generator is removed from the calculation, and the fictitious generator is added.

Step 3:

The initial capacity of the conventional generator is set to 0.25 MW. Following Equation (3.19) this yields a $LOLE_{current}$ of 0.2889 days/year.

Step 4:

For this example, the capacity interval is chosen from 0.25 MW to 5 MW with incremental increase of 0.25 MW. The $LOLE_{current}$ vs. capacity curve is shown in Figure 4.4.

Step 5:

Figure 4.4 shows the plotted curve for $LOLE_{current}$ together with the horizontal dotted line representing the $LOLE_{goal}$. At the intersection point the vertical dotted line represents the ECC value, C_{gen}. The ECC in this example is 2.202 MW or 55.05%.

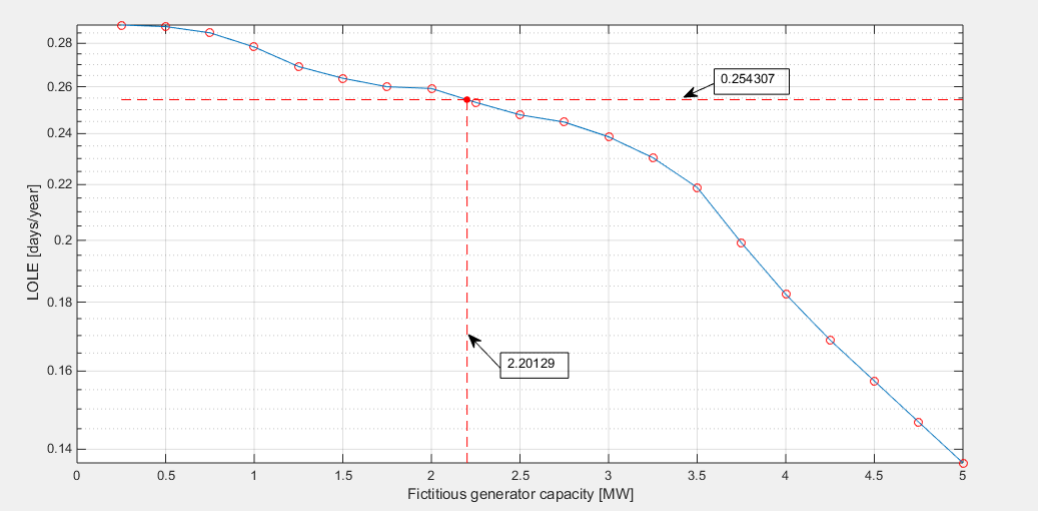

Figure 4.4: ECC calculation example using LOLE

Chapter 5

Case Study: Application of ELCC and EFC/ECC Methodologies on Test Systems

To analyse the various approaches for obtaining the capacity credits, the computer codes developed for this thesis are applied to the Roy Billinton Test System (RBTS) and the IEEE Reliability Test System (RTS). The main results from the analysis are from the more manageable RBTS, due to computational resource restrictions. The larger and more complex IEEE-RTS is also included in the results, but later discussion is conducted with emphasis on the RBTS results.

5.1 Wind Speed Data

The observed wind speed data from Ørland in Norway is obtained from The Norwegian Meteorological Institute [43]. Hourly speed data is chosen from January 1. 2011 to January 1. 2016. In the few hours where no data is available, presumably due to equipment malfunction, the wind speed is set to the average of the previous and next hour. Hourly resolution is necessary to apply various models in the adequacy calculations. The wind model is obtained by calculating the average value for each hour from the five years of data.

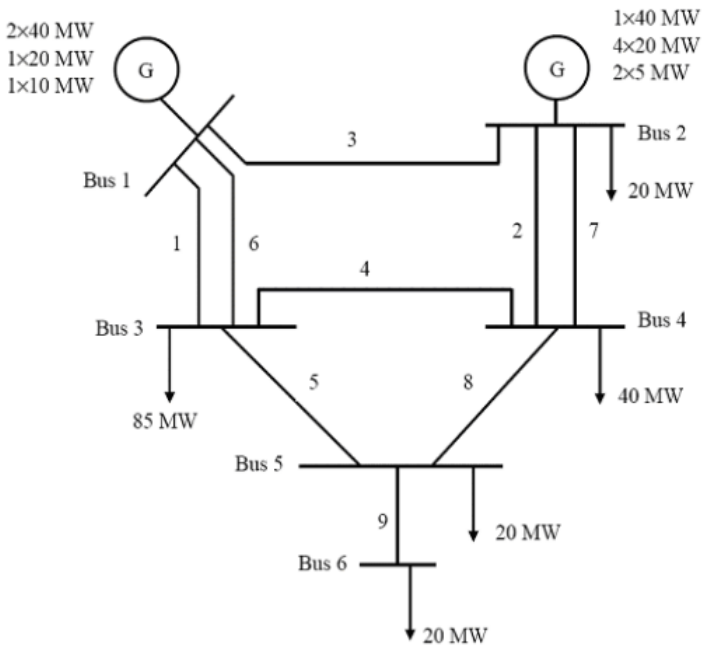

Figure 5.1: Single line diagram for the RBTS [6]

5.2 RBTS

The Roy Billinton Test System (RBTS) is a small composite system developed for the reliability education programs conducted by the Power Systems Research Group at the University of Saskatchewan, Canada. It contains basic system data for performing reliability analysis on the generation (HL-I) and composite (HL-II) system levels. As stated in [6]: *"The main object in designing a reliability test system for educational purposes is to make it sufficiently small to permit the conduct of a large number of reliability studies with reasonable solution time but sufficiently detailed to reflect the actual complexities involved in a practical reliability analysis."*

The size and required computational resources of the RBTS makes it the test system of choice for the analysis performed in this thesis. The RBTS consists of 6 buses, 9 transmission lines, a generation capacity of 240 MW and a peak load of 185 MW. Further it contains data for outage and impedances for transmission lines, fuel-, operating- as well as capital costs for generators and cost of interruption. As the studies in this thesis only invokes data for generation adequacy analysis, only load and generation data are of interest.

5.2.1 Generation Data

The generation in RBTS consists of 11 generators ranging from a capacity of 5 MW to 40 MW. The generator data is presented in Table 5.2a, alongside the number of each unit type and their FOR.

(a) Generation data for RBTS

Unit size MW	Number of units	Forced outage rate
5	2	0.010
10	1	0.020
20	4	0.015
20	1	0.025
40	1	0.020
40	2	0.030

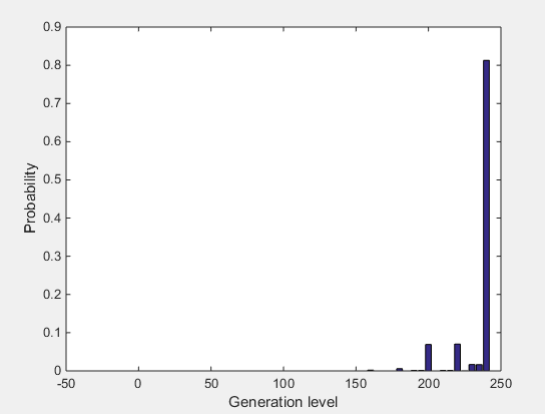

(b) Generation probability for RBTS

Figure 5.2: Data for RBTS generation

The generating system's COPT is obtained using the method explained in Section 3.3.2. It is shown with system outages and their corresponding cumulative probability in Appendix B.1, but a shorter version is presented in Table 5.1 for illustrative purposes.

Table 5.1: COPT for the RBTS

State	Capacity Outage [MW]	Individual Probability	Cumulative Probability
1	0	1	0,812859614
2	5	0.187140386	0.016421406
3	10	0.170718979	0.016671908
4	15	0.154047071	0.000335131
5	20	0.153711941	0.070358538
6	25	0.083353403	0.00142135
7	30	0.081932052	0.001443033
8	35	0.08048902	2.90072E-05
9	40	0.080460012	0.069269729
10	45	0.011190284	0.001399385
11	50	0.009790898	0.001420733
12	55	0.008370166	2.85589E-05
13	60	0.008341607	0.005828452
14	65	0.002513155	0.000117744
15	70	0.002395412	0.00011954
.	.	.	.
.	.	.	.
.	.	.	.
.	.	.	.
45	220	2.28E-14	2.18951E-14
46	225	9.00E-16	4.42047E-16
47	230	4.58E-16	4.48791E-16
48	235	9.07E-18	9.02138E-18
49	240	4.56E-20	4.55625E-20

5.2.2 Load Data

The RBTS contains load information on various resolutions. The CYPL is given as 185 MW. Smaller time resolutions are given as a percentage of larger resolutions. The weekly load level is a percentage of the yearly load, the daily load is a percentage of the weekly load and the hourly load is a percentage of the daily load. An hourly representation will therefore have 8736 values and a daily representation will have 364 values.

The different load models are illustrated in Figure 3.4a and a zoomed in version in Figure 3.4b to better illustrate the differences in load peak. To calculate the HPL for a specific week, w, specific day, d and a specific hour, h, one multiplies the YPL with the associated percentile

values l, as shown in Equation (5.1).

$$HPL_{h,d,w} = YPL \times l_w \times l_d \times l_h \tag{5.1}$$

$where$: $HPL_{h,d,w}$ = Hourly Peak Load calculated by hourly, daily and weekly percentages [MW]

YPL = Yearly peak load [MW]

l_w = Weekly peak load as a percentage of yearly peak load

l_d = Daily peak load as a percentage of weekly peak load

l_h = Hourly peak load as a percentage of daily peak load

5.3 IEEE-RTS

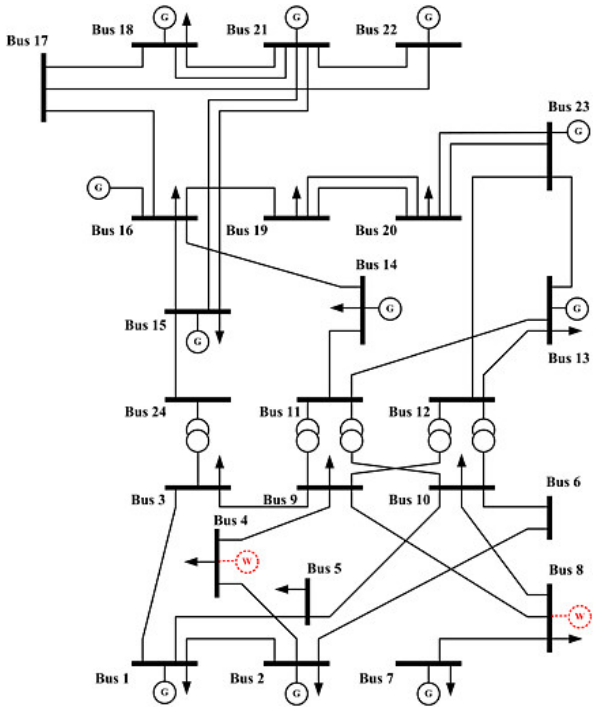

Figure 5.3: Single line diagram for the IEEE-RTS [7]

The first IEEE Reliability Test System was developed in 1979 and later expanded and refined in 1986. The basis for the system has been *to satisfy the need for a standardised data base to test*

and compare results from different power system reliability evaluation methodologies [7]. The system has a significantly larger generation fleet, compared to the RBTS, with installed capacity of 3405 MW. The load profile has the same variation as the RBTS using the same percentile weekly-, daily- and hourly- values, but the top load is 2850 MW.

5.3.1 Generation Data

The generator data for the RTS is presented in Table 5.4a and the capacity availability is shown in Figure 5.4b.

(a) Generation data for RTS

Unit size MW	Number of units	Forced outage rate
12	5	0.02
20	4	0.10
50	6	0.01
76	4	0.02
100	3	0.04
155	4	0.04
197	3	0.05
350	1	0.08
400	2	0.12

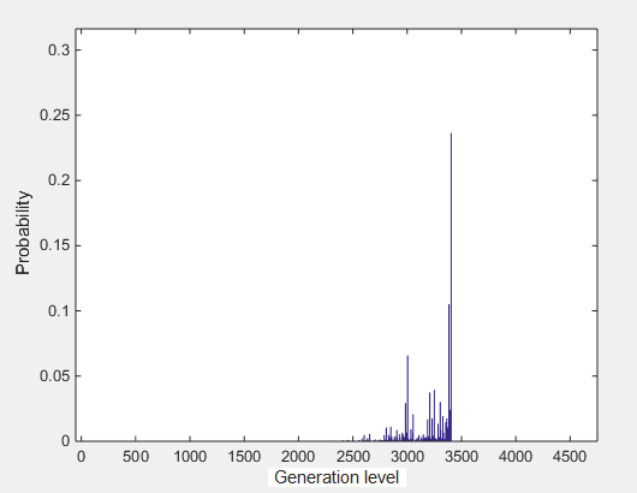

(b) Generation probability for the IEEE RTS

Figure 5.4: Data for RTS generation

5.4 Results From Case Study

This section presents the results obtained when applying the developed MATLAB codes to the test systems. ELCC results for both RBTS and IEEE-RTS are shown for LOLE and EENS based calculations. As the calculations of EFC and ECC are very similar only EFC is shown using LOLE and EENS metrics. The multi-state wind farm representation approach presented in Section 3.3.2 is used for both RBTS and RTS results.

The purpose of the case study is to apply scripts developed for this thesis using the ELCC and ECC methods to assess the capacity credit of a wind farm in both the RBTS and the RTS. Also, the various effects that occur when changing certain model variables is investigated in the sensitivity analysis section.

Table 5.2a shows how the code developed for this thesis performs compared to benchmark results from literature [37, 44], including results for both the HPL- and the CYPL-model. The small difference in results from the script and the benchmarks, represented by ϵ, proves that the scripts are functioning satisfyingly.

(a) Script values compared with benchmark values using the HPL-model

	LOLE [hours/year]			EENS [MWh/year]		
System	Benchmark	Script	ϵ [%]	Bench	Script	ϵ [%]
RBTS	1.091900	1.091700	0.018320	9.861300	9.862892	0.016142
RTS	9.368810	9.419200	0.537848	1181.95000	1176.372477	0.408275

(b) Script values compared with benchmark values using the CYPL-model

	LOLE [hours/year]			EENS [MWh/year]		
System	Benchmark	Script	ϵ [%]	Bench	Script	ϵ [%]
RBTS	73.072800	73.382400	0.423687	823.255500	821.184	0.2516229
RTS	N/A	834.561331	N/A	128 364.000	128 364.163	0.000127

Table 5.2: LOLE and EENS values from script compared to benchmark values from [37, 44]

5.4.1 RBTS

This section contains the results for the RBTS system. The wind farm that is added to the system consists of 10 individual wind turbines with a capacity of 2 MW and FOR of 3%, giving the wind farm a total capacity of 20 MW. The modelling of the wind farm is performed as in Section 3.5 using ten different derated states and wind speed data from [43].

CYPL

The RBTS has a LOLE value of 0.0084 years/year when subject to the CYPL-model. When this is chosen as the reliability level for the system it yields an $ELCC_{LOLE}$ of 8.88 MW, which equals 44.4% of the installed capacity. This is somewhat high compared to results found in literature, where a wind generator with wind resources comparative to those used in this thesis normally performs in the range of 20-40% [21]. CYPL supposedly yields the most pessimistic results of the load models, as it deploys the worst-case load scenario throughout the entire year. The results in Figure 5.5a therefore shows remarkably positive results. One of the issues concerning the CYPL-model, is that it limits the possible LOLE-levels to essentially the same levels as found in the COPT. This is evident in the characteristic step-wise increase in the LOLE curves for CYPL-models. The step effect gives results that vary greatly depending on the set reliability level, and thus might yield big changes in ELCC for small changes in reliability level, as demonstrated later in the sensitivity analysis by Figure 5.19.

Figure 5.5b has less of a step-wise increase than its LOLE-based counterpart. This is due to the inclusion of generation capacities when constructing the COPT, thus providing more possible EENS-levels than what is the case for the LOLE-index. For this scenario the $ELCC_{EENS}$ of 8.33 MW also provides a high ELCC value for the wind farm with a capacity credit of 41.65%.

The same tendencies as mentioned for the ELCC plots can be observed in the ECC results in Figure 5.5. The LOLE has a very step-wise decrease and the EENS is smoother, although with evident steps. Both ECC_{LOLE} and ECC_{EENS} have similar results due to an advantageous reliability level in the system being evaluated.

The ELCC-plot for RBTS in Figure 5.7 shows the result of calculating the ELCC using the DPL-model, but with the hourly peak equal to the CYPL. Comparing Figure 5.7 with Figure 5.5a illustrates that an LOLE calculated with a CYPL-model is equal to an LOLE calculated with a HPL-model where all hourly peak loads are equal to the CYPL. Note the y-axis where the $LOLE_{CYPL}$ of 0.00834 years/year from Figure 5.5a is convertible with the $LOLE_{HPL}$ of 73.382 hours/year by multiplying with the factor of 8736 hourly peaks/year. This only holds true when the LOLE is a scaling of LOLP and all the hourly loads are equal to the CYPL.

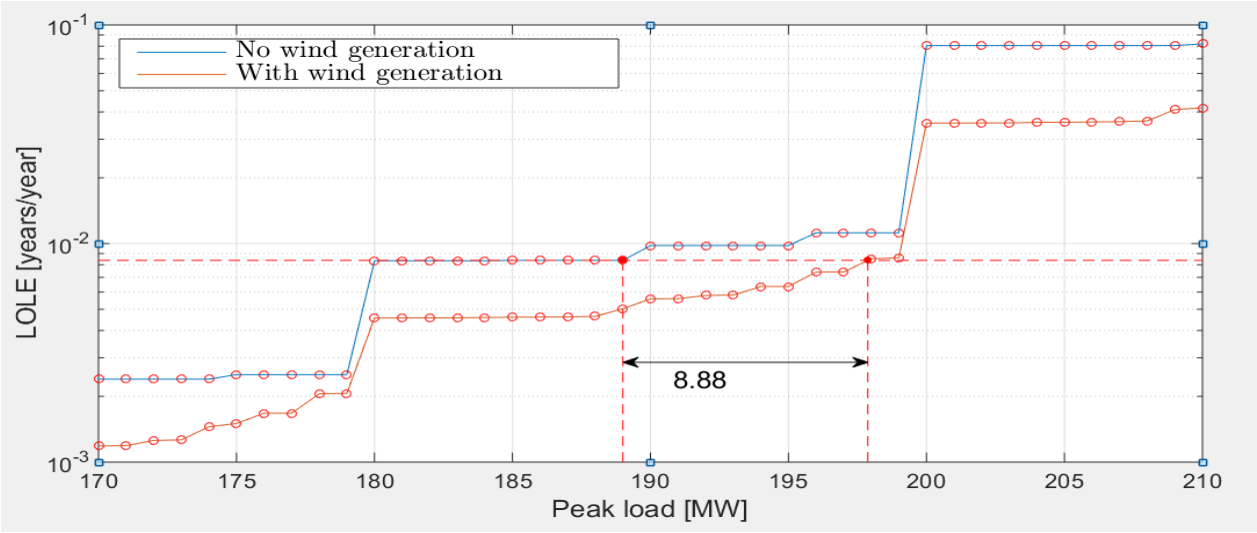

(a) $ELCC_{LOLE}$ plot with constant yearly peak load

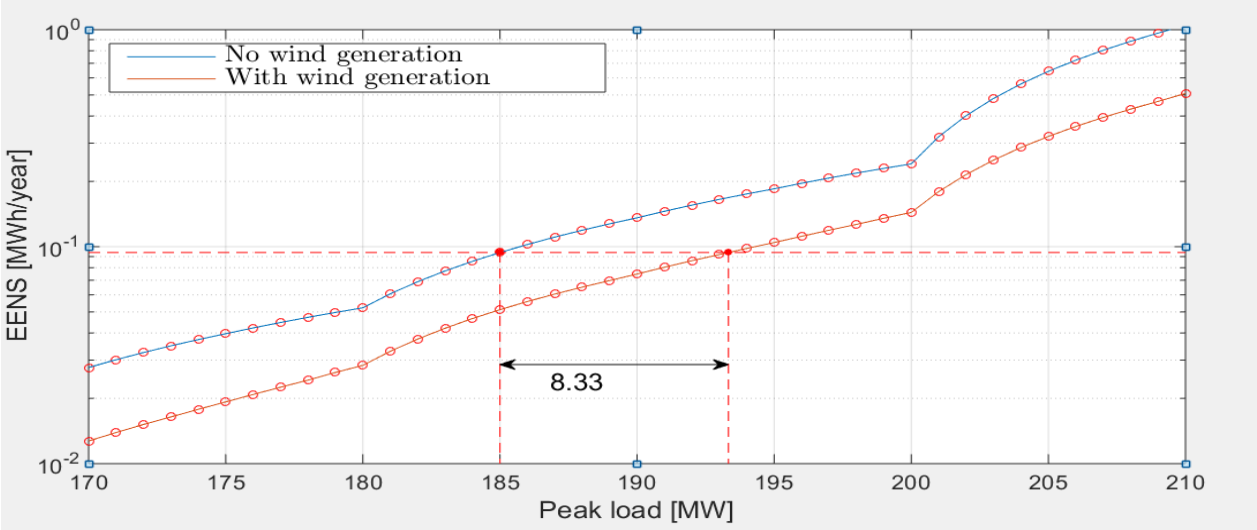

(b) $ELCC_{EENS}$ plot with constant yearly peak load (y-axis scaled with 8736)

Figure 5.5: $ELCC_{LOLE}$ (a) and $ELCC_{EENS}$ (b) plot for the RBTS system using the CYPL-model

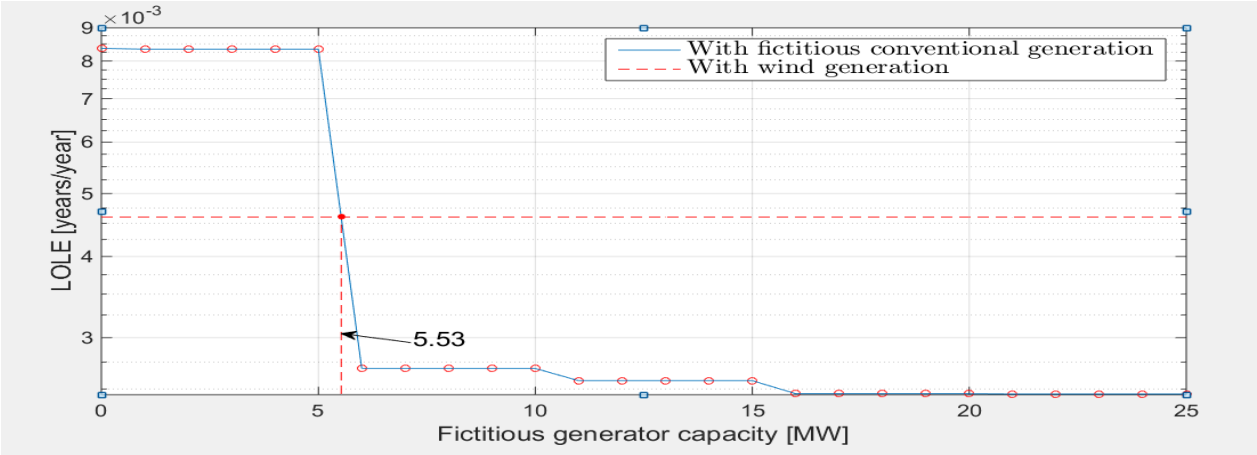

(a) ECC_{LOLE} plot with constant yearly peak load

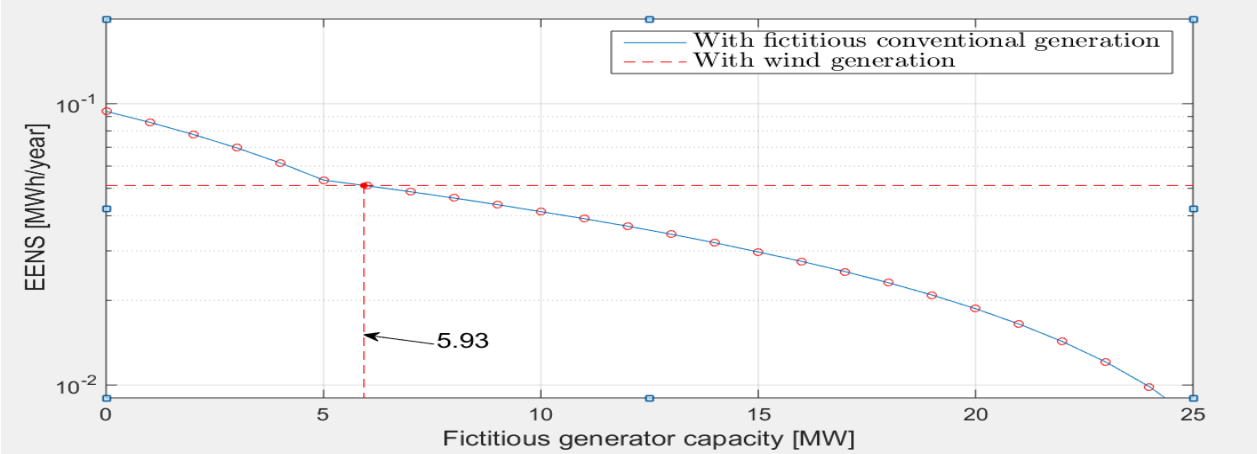

(b) ECC_{EENS} plot with constant yearly peak load (y-axis scaled with 8736)

Figure 5.6: ECC_{LOLE} (a) and ECC_{EENS} (b) plot for the RBTS system using the CYPL-model

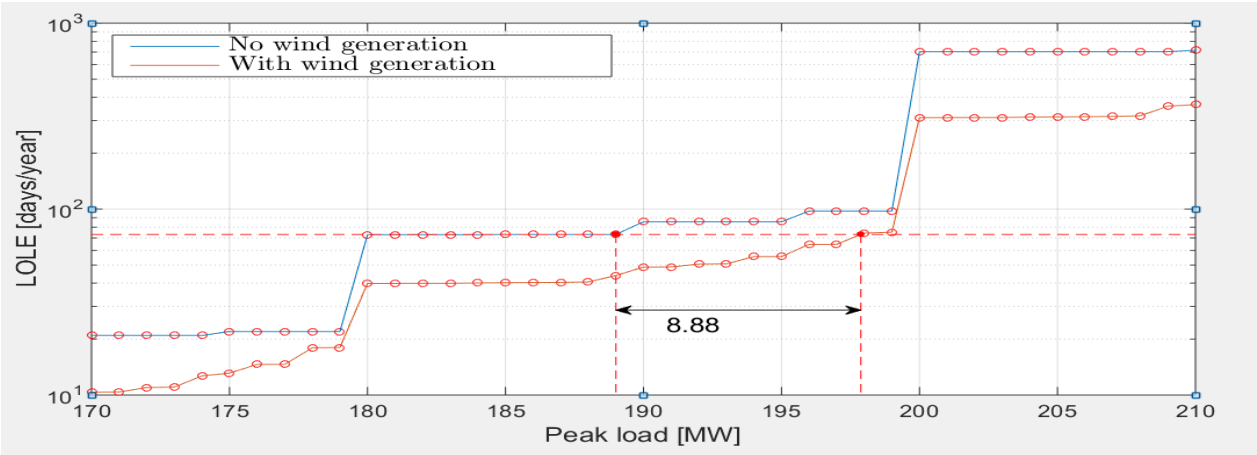

Figure 5.7: $ELCC_{LOLE}$ plot for HPL-model with hourly peak loads equal to the yearly peak load

DPL

Figure 5.8 shows the ELCC results when the DPL-model is used. The increase in possible LOLE-levels demonstrates a less step-wise increase, however a step-wise trend can still be observed for the $ELCC_{LOLE}$ in Figure 5.8a. The reliability levels for the $ELCC_{LOLE}$ and $ELCC_{EENS}$ calculations are set to 0.10697 days/year and 1.41024 MWh/year as this is the LOLE and EENS of the base system using the DPL load model. The resulting ELCC values, $ELCC_{LOLE}$ of 7.85 MW and $ELCC_{EENS}$ of 7.57 MW, are a reduction from the values obtained from the CYPL-model. As mentioned earlier this contra-intuitive reduction in ELCC is a result of the number of possible LOLE and EENS levels and the set reliability level. This phenomenon will be further elaborated in the sensitivity analysis.

Figure 5.9 illustrates the ECC_{LOLE} and ECC_{EENS}. Compared to the ELCC levels it can be noted that the step-wise decrease is still evident for the LOLE based metrics, also the difference between the ELCC and ECC metrics is decreasing. By comparing the ECC levels it can be observed that the difference between the LOLE and EENS calculated metrics equal to those calculated for ELCC.

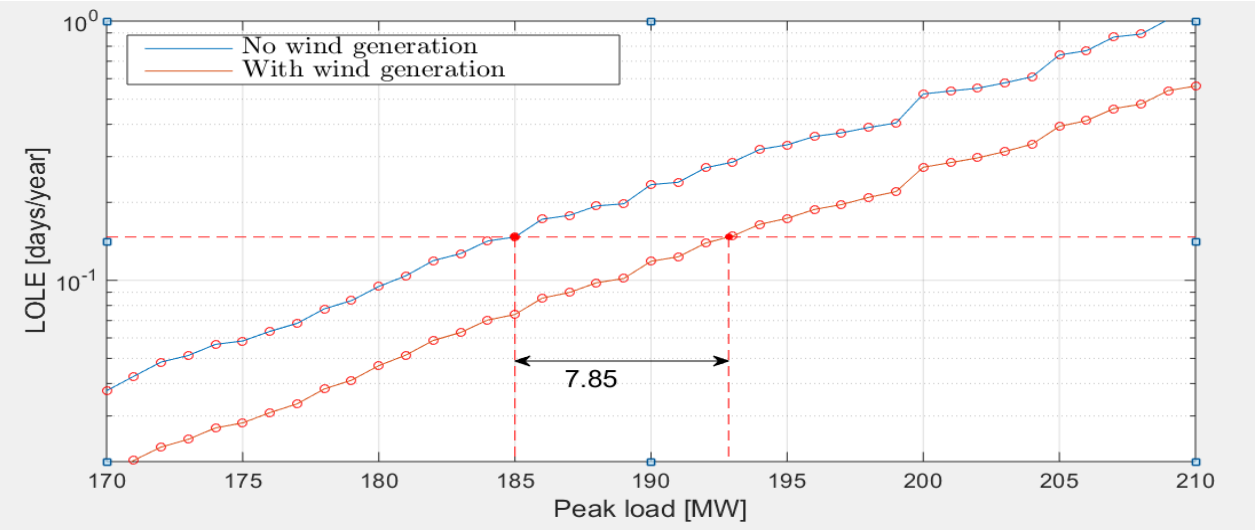

(a) $ELCC_{LOLE}$ plot with daily peak load

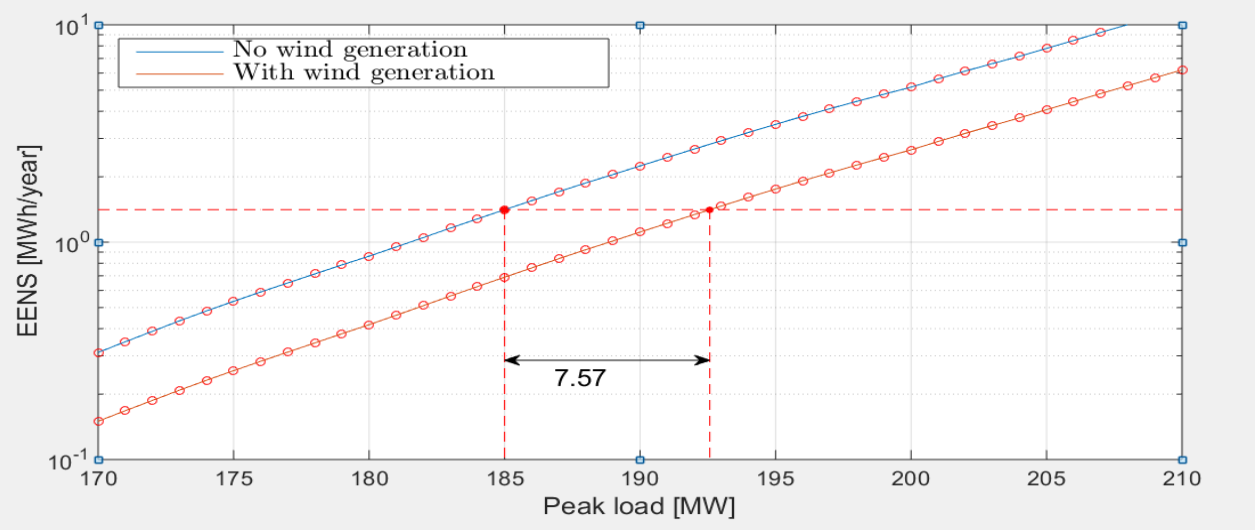

(b) $ELCC_{EENS}$ plot with daily peak load(y-axis scaled with 364)

Figure 5.8: $ELCC_{LOLE}$(a) and $ELCC_{EENS}$(b) plot for the RBTS system using the DPL-model

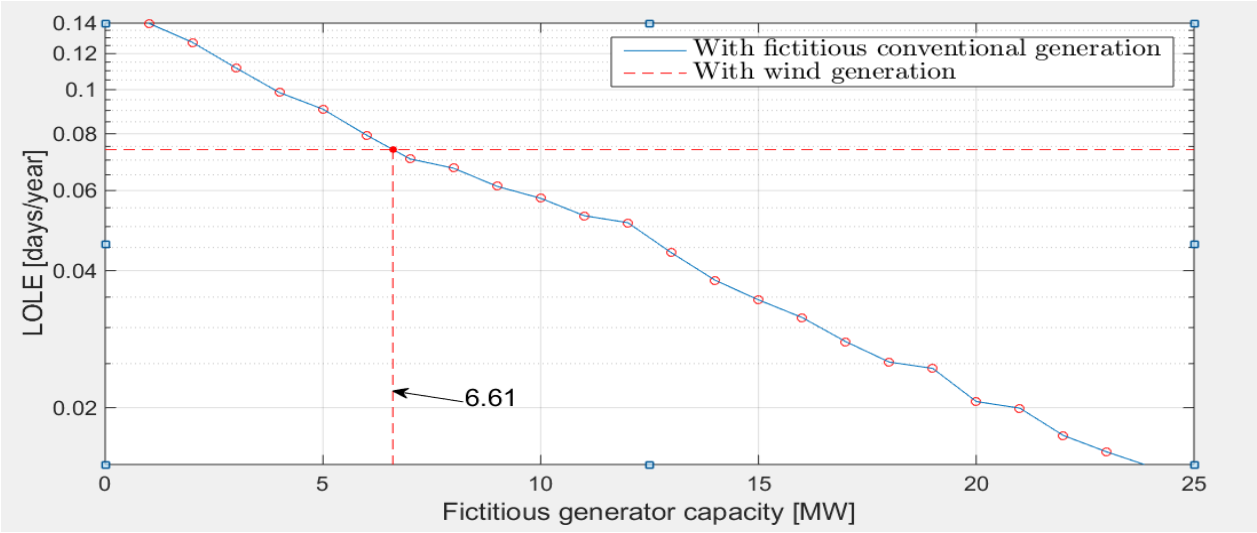

(a) ECC_{LOLE} plot with daily peak load

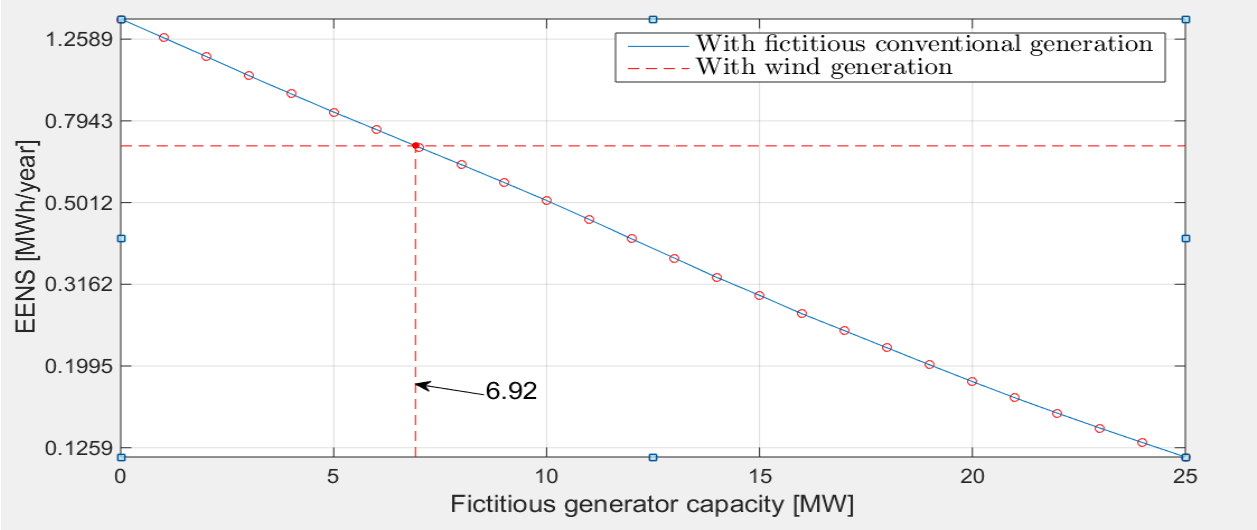

(b) ECC_{EENS} plot with daily peak load (y-axis scaled with 364)

Figure 5.9: ECC_{LOLE}(a) and ECC_{EENS}(b) plot for the RBTS system using the DPL-model

HPL

Figure 5.10 shows the results for $ELCC_{LOLE}$ and $ELCC_{EENS}$ for the RBTS system using the HPL-model. Compared to the results obtained using the DPL model, the step-wise increase is hard to observe in Figure 5.10a and Figure 5.10b has no observable steps and appears to be two parallel linear lines. The reliability of the base case yields a LOLE of 1.09 hours/year and EENS of 9.861 MWh/year when applying the HPL load model. These reliability levels yield a $ELCC_{LOLE}$ of 8.07 MW and a $ELCC_{EENS}$ of 7.62 MW. There is little difference between the values obtained with the DPL- and HPL-model, which might indicate that DPL provides sufficiently accurate values for this example.

The results for ECC_{LOLE} in Figure 5.11a and ECC_{EENS} in Figure 5.11b support the observations for the ELCC results and show a stabilised value compared to the DPL model.

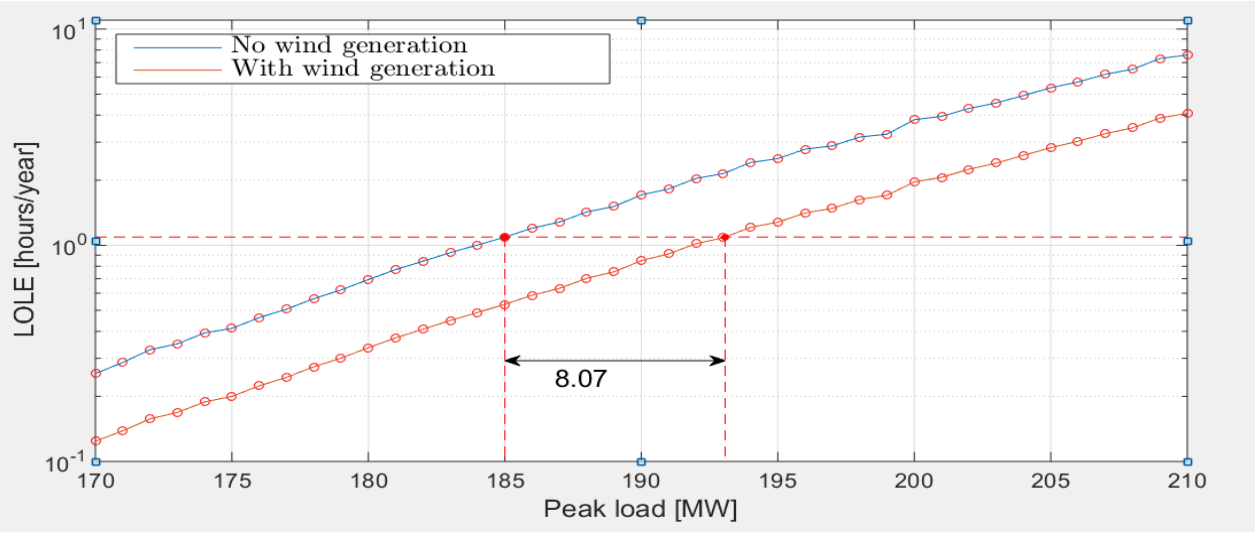

(a) $ELCC_{LOLE}$ plot with hourly peak load

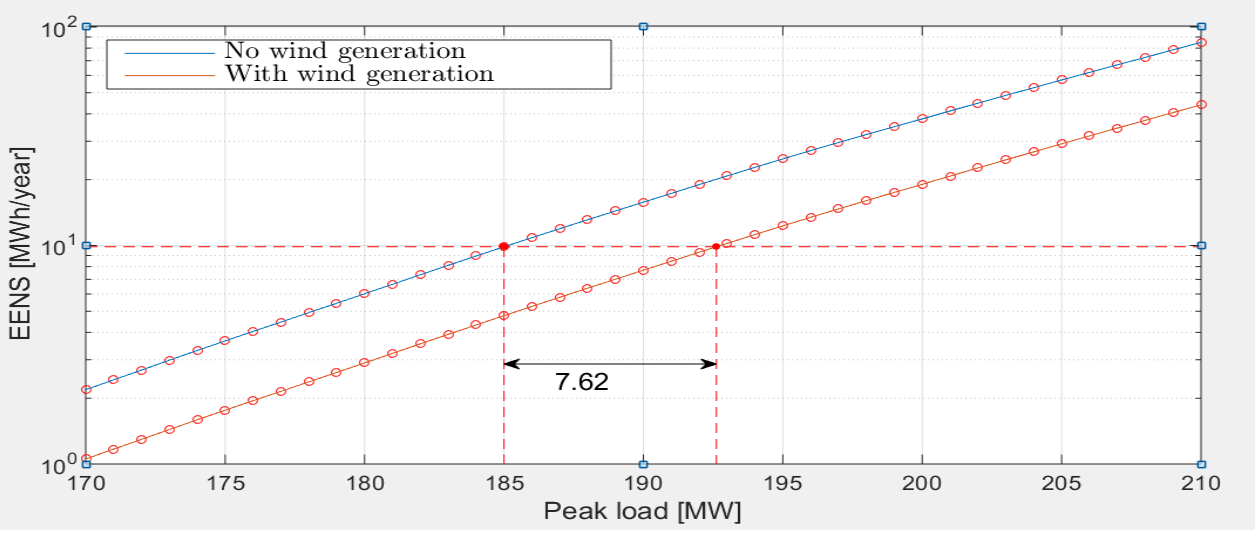

(b) $ELCC_{EENS}$ plot with hourly peak load

Figure 5.10: $ELCC_{LOLE}$(a) and $ELCC_{EENS}$(b) plot for the RBTS system using the HPL-model

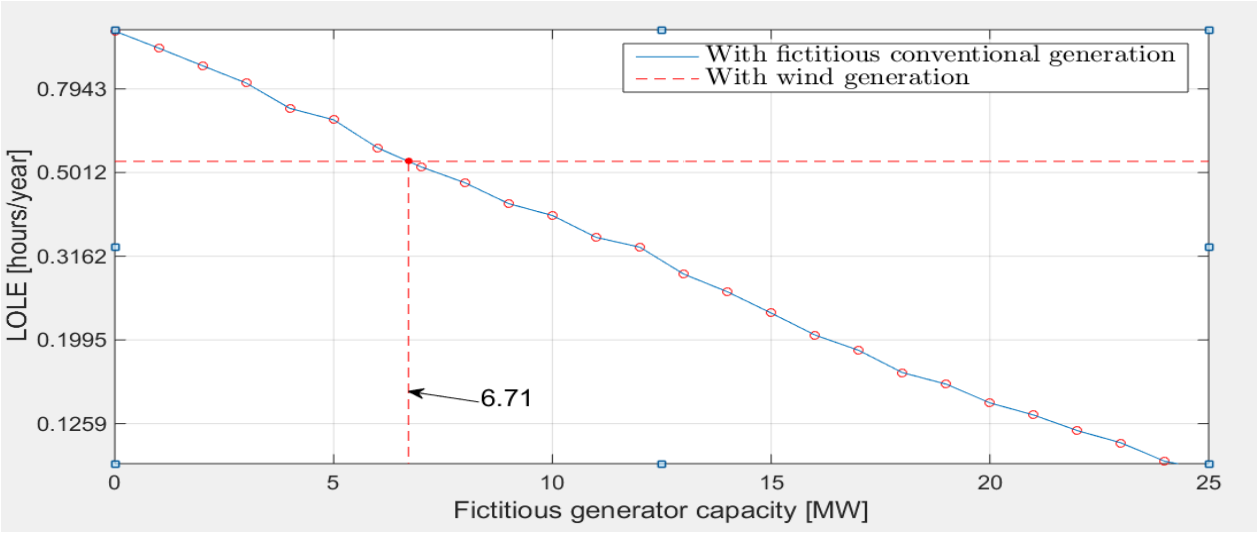

(a) ECC_{LOLE} plot with hourly peak load

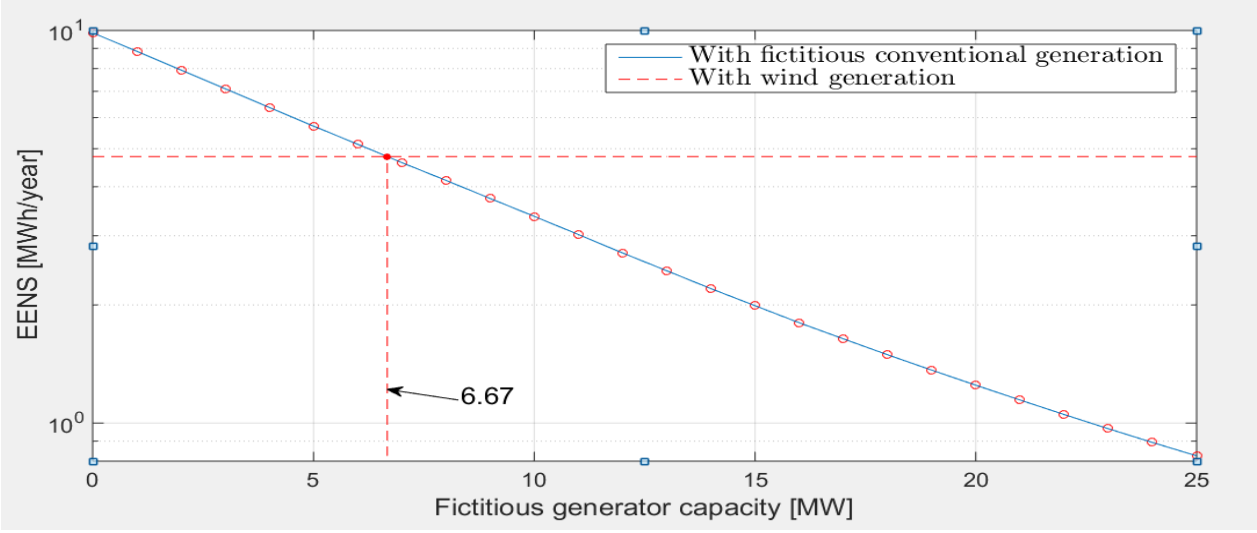

(b) ECC_{EENS} plot with hourly peak load

Figure 5.11: ECC_{LOLE}(a) and ECC_{EENS}(b) plot for the RBTS system using the HPL-model

5.4.2 IEEE-RTS

This section contains the results for the IEEE-RTS system. The wind farm added to the system consists of 10 individual wind turbines with a capacity of 2 MW and FOR of 3%, giving the wind farm a total capacity of 20 MW. The modelling of the wind farm is performed as in Section 3.5 using ten possible derated states.

CYPL

Figure 5.12 shows the result for $ELCC_{LOLE}$ and $ELCC_{EENS}$ for the RTS system using the CYPL-model. Compared to the CYPL-model for the RBTS system the step-wise increase is less evident. Especially for the $ELCC_{EENS}$ which has a nearly linear increase. These smoother lines occur due to the larger generation fleet in the system that allows for more LOLE and EENS levels. Still the $ELCC_{LOLE}$ is subject to a very evident step-wise increase. The resulting $ELCC_{LOLE}$ of 17.58 MW (87.9% of the installed capacity) and $ELCC_{EENS}$ of 9.49 MW (47.45% of the installed capacity). The $ELCC_{LOLE}$ follows the same trend as for the RBTS with evident step-wise increase that might lead to very polarising results depending on the reliability level.

The ECC_{LOLE} and ECC_{EENS} shown in Figure 5.13 provide even more polarising results and strengthens the impression that the CYPL-model is not accurate enough when evaluating generation adequacy.

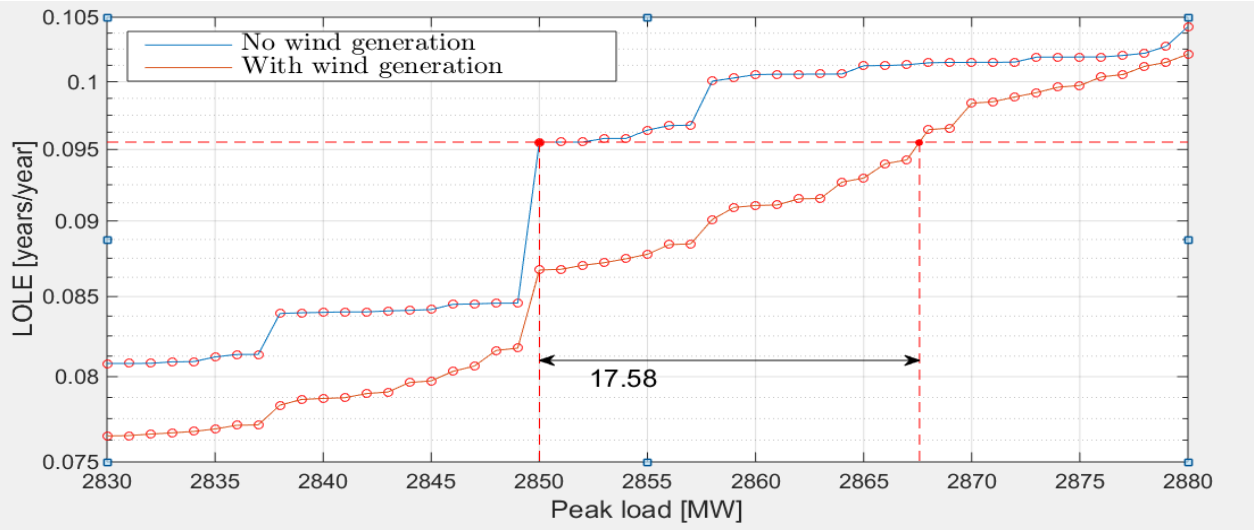

(a) $ELCC_{LOLE}$ plot with constant yearly peak load

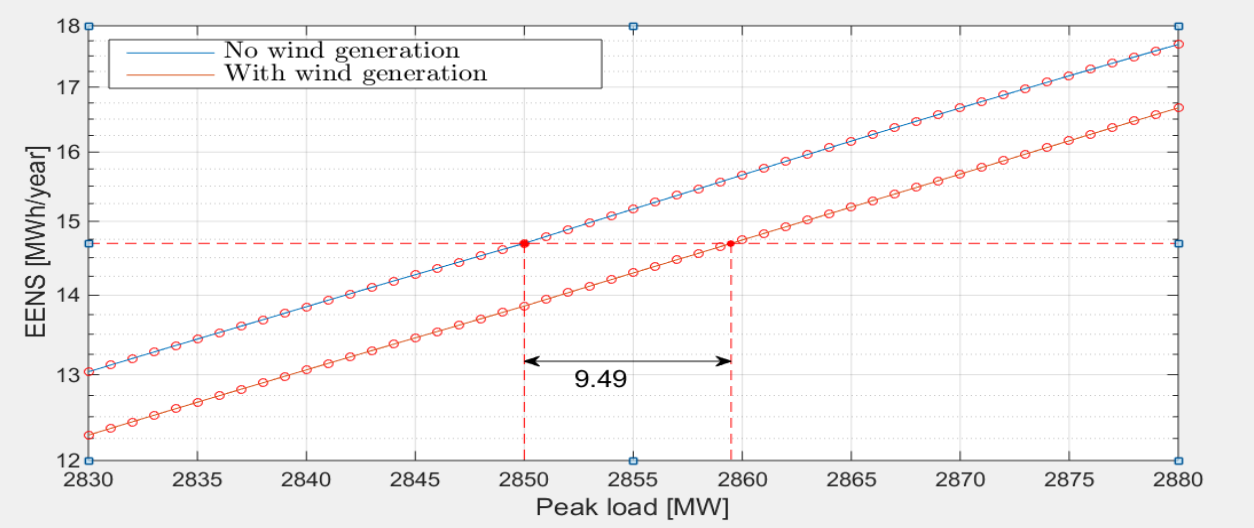

(b) $ELCC_{EENS}$ plot with constant yearly peak load (y-axis scaled with 8736)

Figure 5.12: $ELCC_{LOLE}$(a) and $ELCC_{EENS}$(b) plot for the RTS system using the CYPL-model

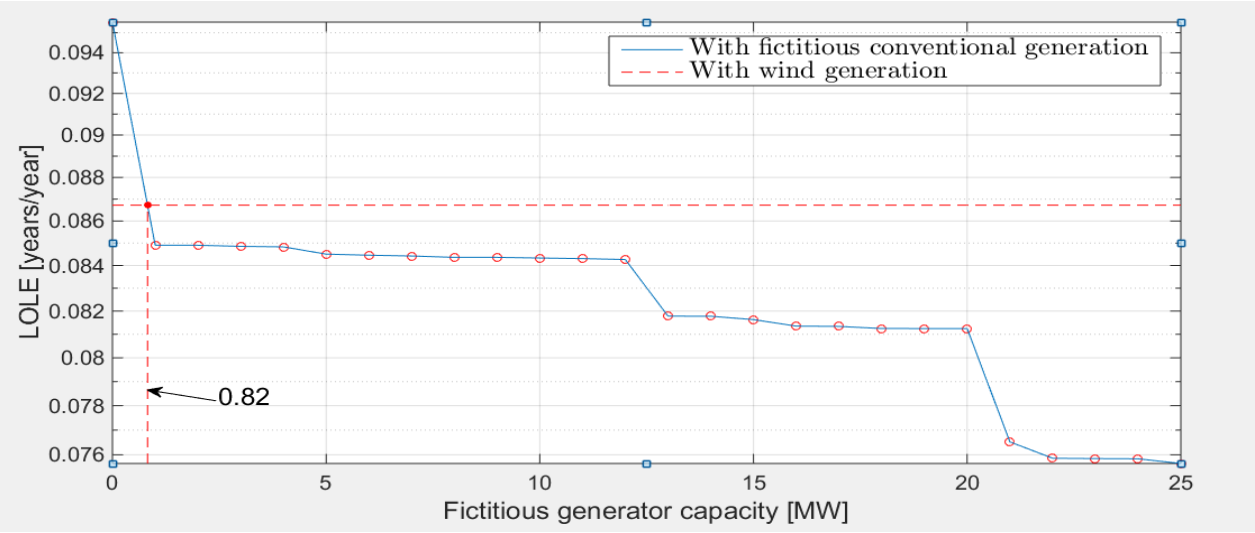

(a) ECC_{LOLE} plot with constant yearly peak load

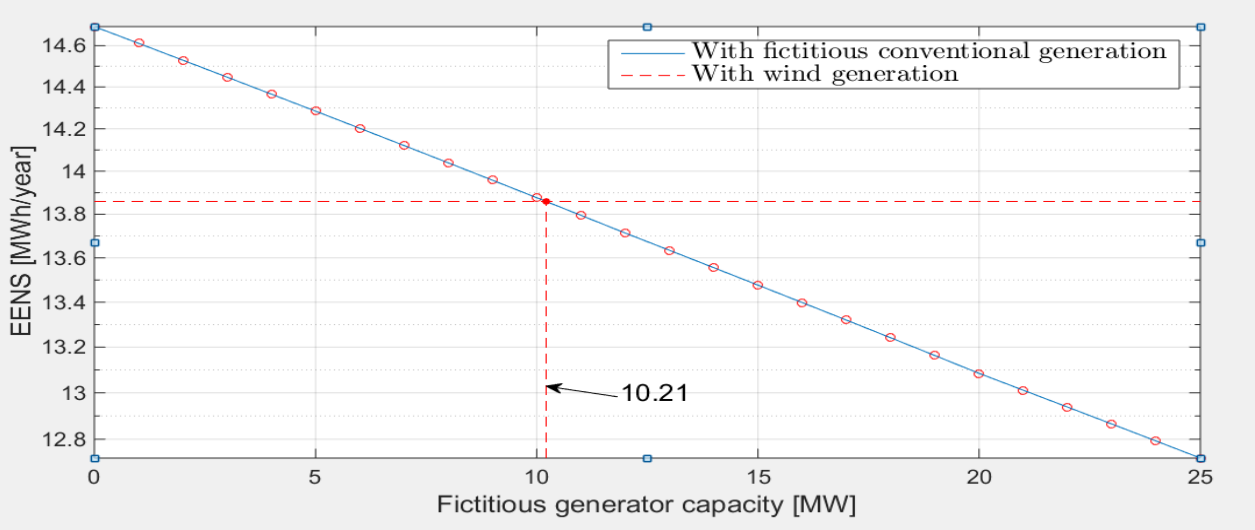

(b) ECC_{EENS} plot with constant yearly peak load (y-axis scaled with 8736)

Figure 5.13: ECC_{LOLE}(a) and ECC_{EENS}(b) plot for the RTS system using the CYPL-model

DPL

Figure 5.14 shows the result for $ELCC_{LOLE}$ and $ELCC_{EENS}$ for the RTS system using the DPL-model. Compared to the CYPL-model for the RTS system the step-wise increase is less evident, still the $ELCC_{LOLE}$ is subject to evident step-wise increase. The resulting $ELCC_{LOLE}$ of 11.14 MW (55.7% of the wind farm capacity) and $ELCC_{EENS}$ of 10.57 MW (52.85% of the wind farm capacity). The $ELCC_{LOLE}$ follows the same trend as for the RBTS with less step-wise increase than for the CYPL-model.

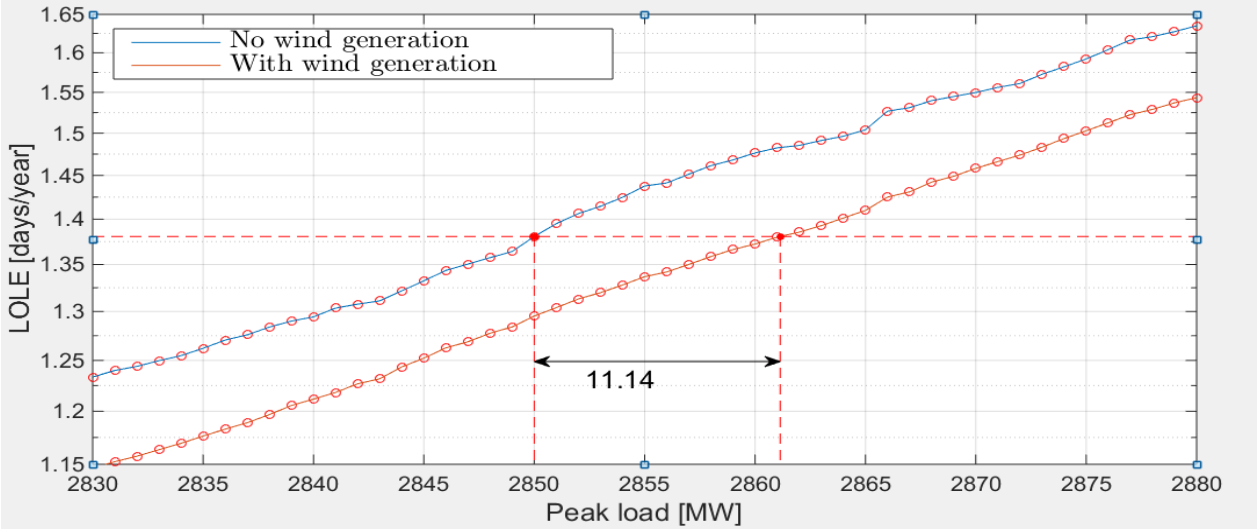

(a) $ELCC_{LOLE}$ plot with daily peak load

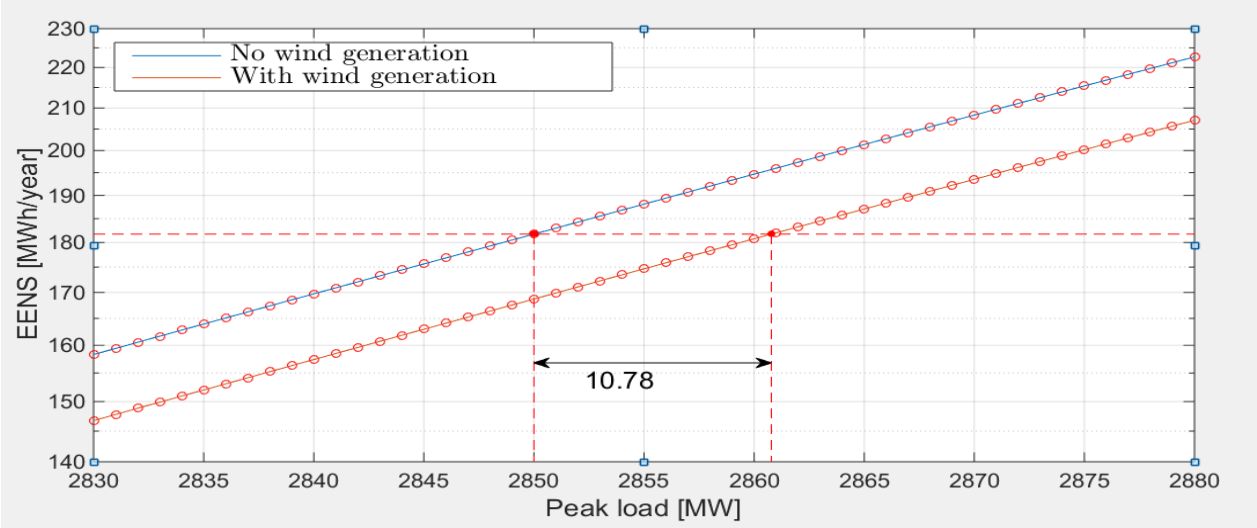

(b) $ELCC_{EENS}$ plot with daily peak load (y-axis scaled with 364)

Figure 5.14: $ELCC_{LOLE}$(a) and $ELCC_{EENS}$(b) plot for the RTS system using the DPL-model

The ECC_{LOLE} and ECC_{EENS} in Figure 5.15 show less difference in results compared to the ones for CYPL-model and the LOLE calculated value follows the trend as for the RBTS with a lower value for the ELCC and ECC.

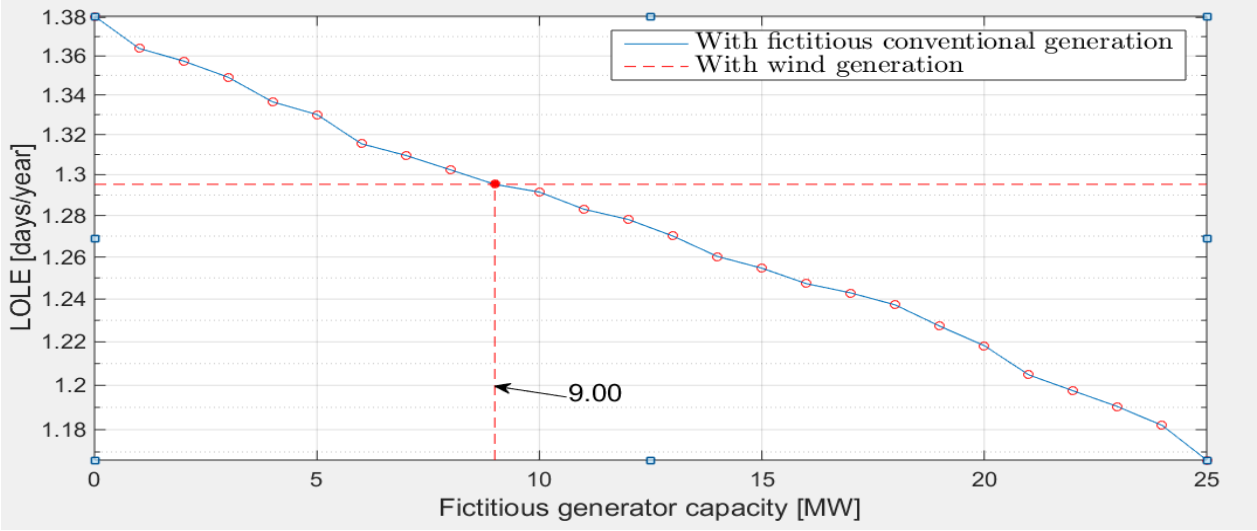

(a) ECC_{LOLE} plot with daily peak load

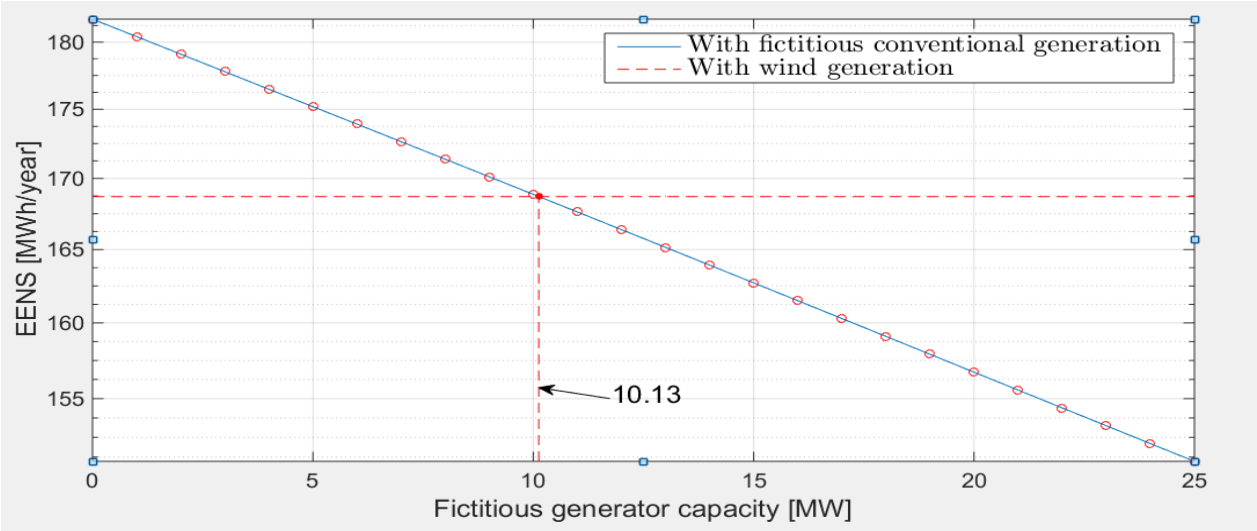

(b) ECC_{EENS} plot with daily peak load (y-axis scaled with 364)

Figure 5.15: ECC_{LOLE}(a) and ECC_{EENS}(b) plot for the RTS system using the DPL-model

HPL

Figure 5.16 shows the result for $ELCC_{LOLE}$ and $ELCC_{EENS}$ for the RTS system using the HPL-model. Compared with the CYPL-model for the RTS system the step-wise increase is hardly

evident. The increase for $ELCC_{LOLE}$ is close to linear and $ELCC_{EENS}$ is seemingly linear with two lines parallel. The many possible capacity and load levels provide a big number of possible LOLE and EENS levels. This results in $ELCC_{LOLE}$ of 10.18 MW, 40.35% and $ELCC_{EENS}$ of 11.09 MW, 55.45%.

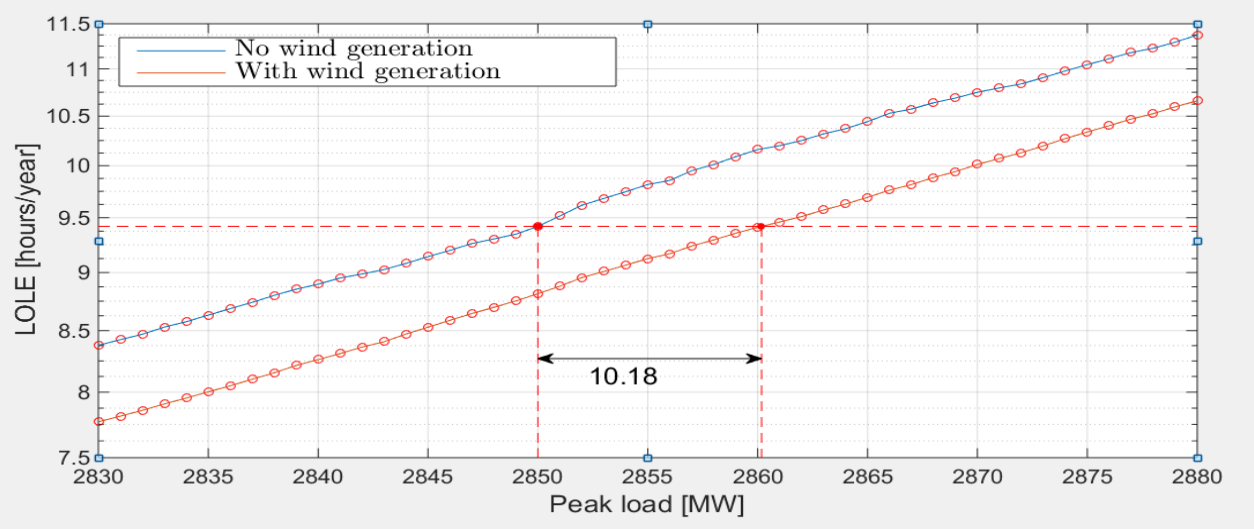

(a) $ELCC_{LOLE}$ plot with hourly peak load

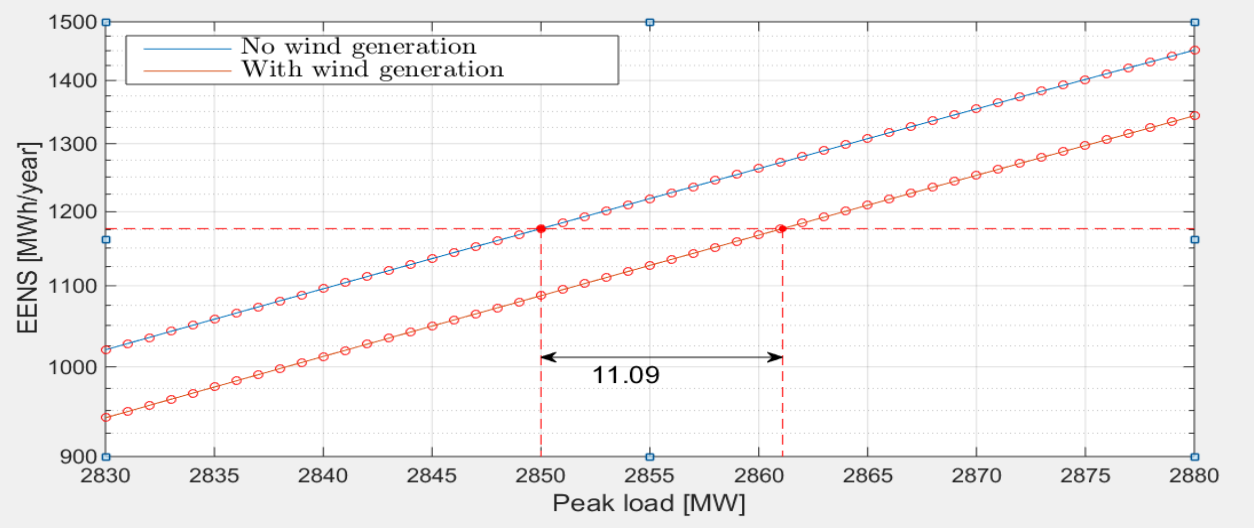

(b) $ELCC_{EENS}$ plot with hourly peak load

Figure 5.16: $ELCC_{LOLE}$(a) and $ELCC_{EENS}$(b) plot for the RTS system using the HPL-model

The ECC_{LOLE} and ECC_{EENS} in Figure 5.17 show the same trend as for the ELCC calculations with only a slight non-linear line for the ECC_{LOLE}.

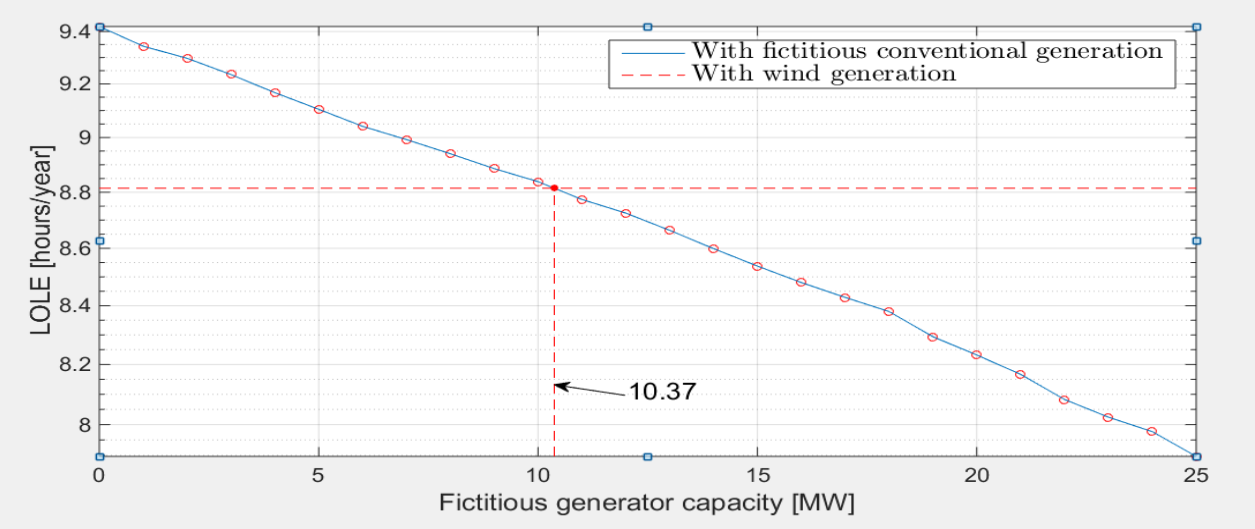

(a) ECC_{LOLE} plot with hourly peak load

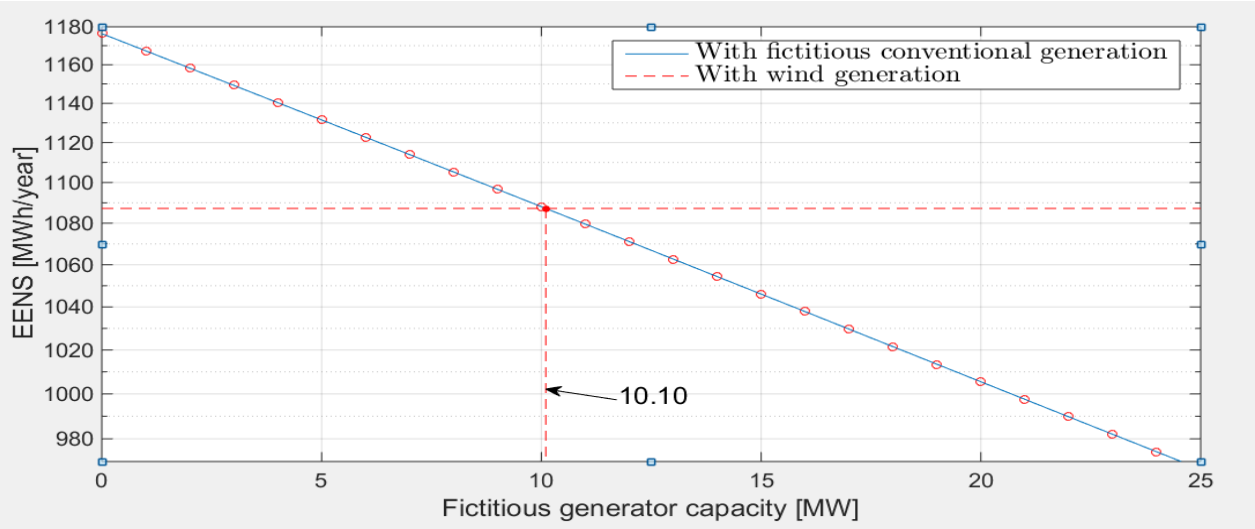

(b) ECC_{EENS} plot with hourly peak load

Figure 5.17: ECC_{LOLE}(a) and ECC_{EENS}(b) plot for the RTS system using the HPL-model

5.5 Sensitivity Analysis

To strengthen and expand the foundation for discussion, several sensitivity analyses are performed in this section. Different variables and concepts are investigated and subject to thorough simulation.

5.5.1 ELCC for Different Reliability Levels

The preliminary results from the RBTS for different load models showed a trend where the ELCC decreased as the load resolution decreased. According to literature however, this relation is supposedly the opposite of what is observed. To investigate this, the $ELCC_{LOLE}$ is calculated for the same system with the same installed wind farm as in Section 5.2, but with different and fixed reliability levels presented in Table 5.3. The values are based on $LOLE_{HPL}$ values and scaled to fit the other CYPL-model by dividing by the amount of data points, i.e. $\frac{3\text{ hours/year}}{24\text{ hours/day}} = 0.125$ days/year. The following $ELCC_{LOLE}$ results show that the CYPL-model does not yield consequently pessimistic values as one would assume, but vary from high to low. Figure 5.18 illustrates how this occurs using the reliability levels of 2 hours/year and 3 hours/year.

Table 5.3: Different load models with their corresponding reliability level and $ELCC_{LOLE}$ result

HPL [hours/year]		CYPL [years/year]	
Reliability level	$ELCC_{LOLE}$ [MW]	Reliability level	$ELCC_{LOLE}$ [MW]
1	5.932318	0.000114	8.957114
2	7.108893	0.000229	9.094500
3	6.357626	0.000343	0.161268
4	6.532929	0.000458	0.191716
5	6.245287	0.000572	0.215123
10	6.451346	0.001145	0.288208
20	6.304690	0.002289	9.948075

Figure 5.19 illustrates the polarising results obtained using the CYPL-model versus the less varying results using the HPL-model with the same reliability level. It is evident the step-wise character of the CYPL-model gives an erratic and unrealistic ELCC or ECC assessment. The cases evaluated show a trend where the peak load vs. LOLE curves for the systems become smoother

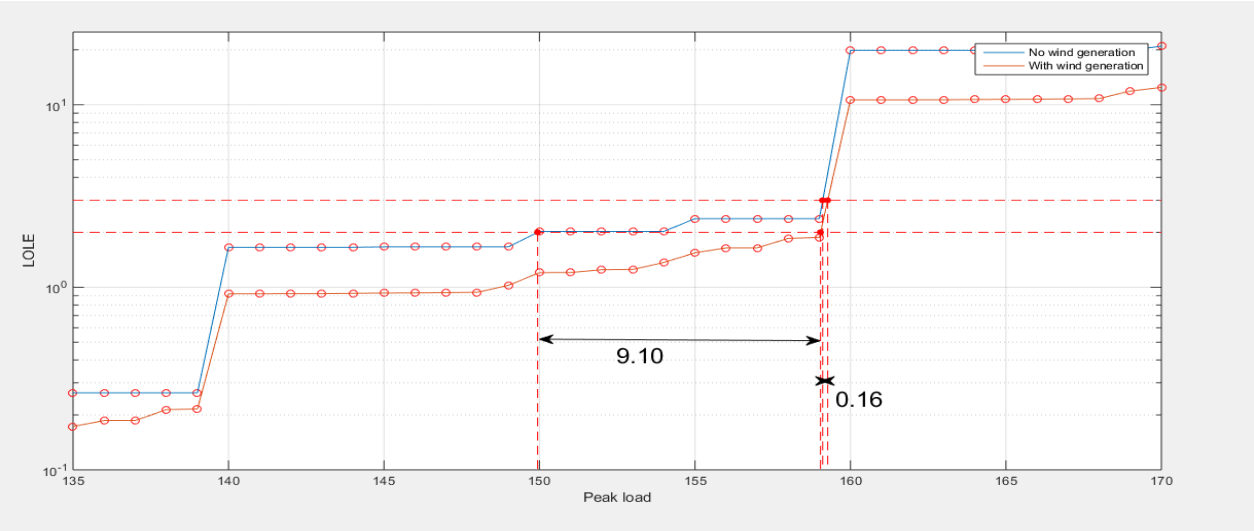

Figure 5.18: The $ELCC_{LOLE}$ value for two reliability values using the CYPL-model

and more parallel with increasing generation fleet and several possible load points. If it is known the base model yields peak load vs. LOLE curves that are close to linear and parallel, the load increments can be larger without reducing the accuracy and in the process reducing the computation time. This demonstrates the advantages of why it is preferable to use models that give smooth and close to linear peak load vs. LOLE and peak load vs. EENS curves.

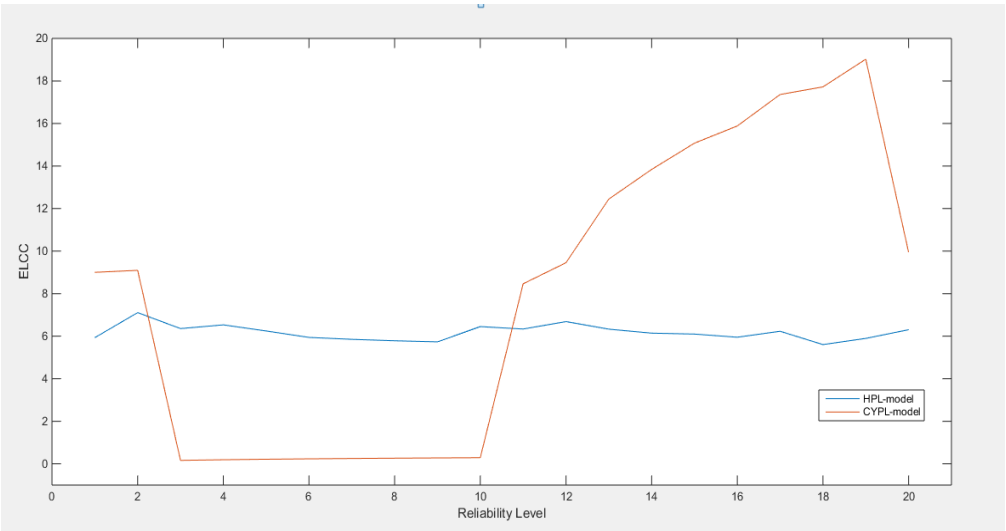

Figure 5.19: The change in ELCC with increasing reliability level

5.5.2 ELCC for Different Amounts of Derated States

In the main result section the equivalent multi state generator representation of the wind farm consisted of ten different outage states with corresponding probabilities. The amount of states has a direct impact on computational time, but to observe the impact on the calculated ELCC values the $ELCC_{LOLE}$ is calculated for various amounts of states using the RBTS and the same load and wind farm as earlier. The additional capacity gained by increasing the number of derated states for the wind generation model is illustrated using the power curve in Figure 5.20. The biggest square represents the capacity when only two states are used. The additional squares represent the capacity when using five states. Figure 5.21 presents the $ELCC_{LOLE}$ value when modelling the wind farm as an equivalent generator with the amount of possible states from 2 up to 50.

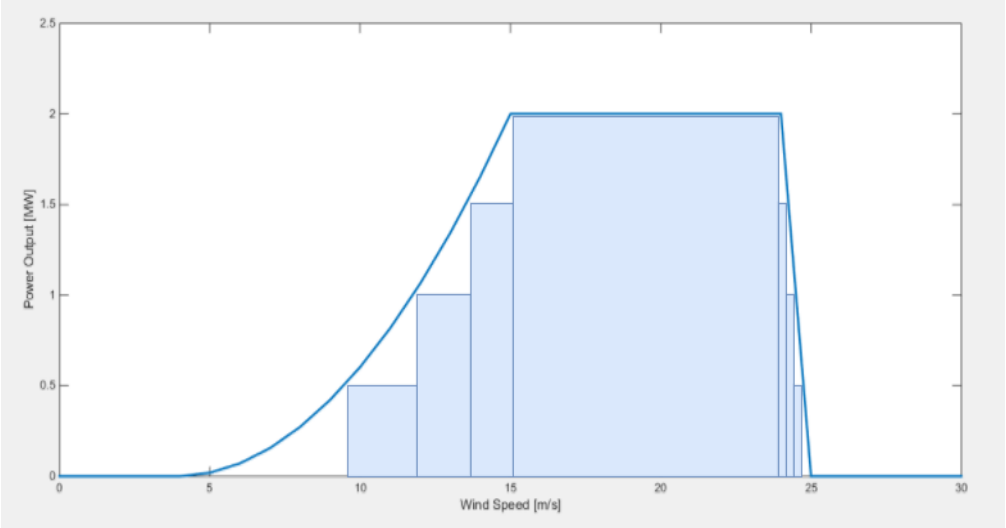

Figure 5.20: The additional capacity gained by increasing the amount of derated states

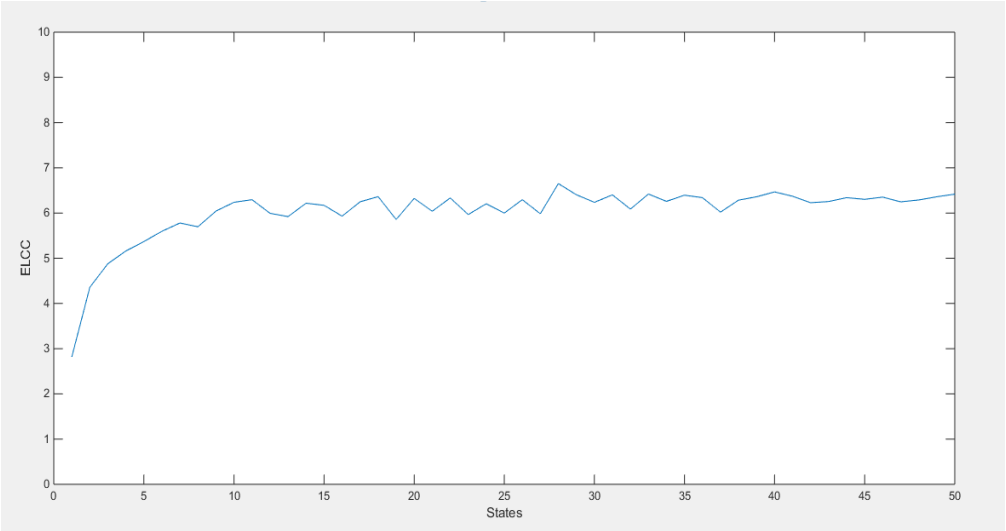

Figure 5.21: The change in ELCC with increasing amount of states

As the results from Figure 5.21 show, the $ELCC_{LOLE}$ increases greatly from two states to multiple states. The results flatten out and oscillate around the same value after around 10 states. As an increasing amount of states also increases the needed computational time, the lowest amount of states where the values are stabilised is optimal. This appears to be around the point of ten states and is used for the calculations. This coincides with the findings in [26].

5.5.3 ELCC Saturation

When planning a wind farm, key issues are deciding on a location with good wind resources and the generation capacity of the wind farm. From a reliability point of view, bigger does not necessarily mean better. Intuitively the larger the capacity of the wind farm the larger the impact on the system reliability, this is true, but only to a certain point. The intermittent and random nature of wind is itself a source of uncertainty and this uncertainty affects the reliability impact of the farm. This inherent uncertainty in energy production from wind generators, comes to show when the wind energy accounts for a big part of the overall system energy mix. Figure 5.22 shows the $ELCC_{LOLE}$ of the RBTS using a HPL-model with a reliability level equal to the base case without the wind farm. The curve describes the ELCC values that are calculated with a wind farm capacity, incrementally increasing from 4 MW to 80 MW.

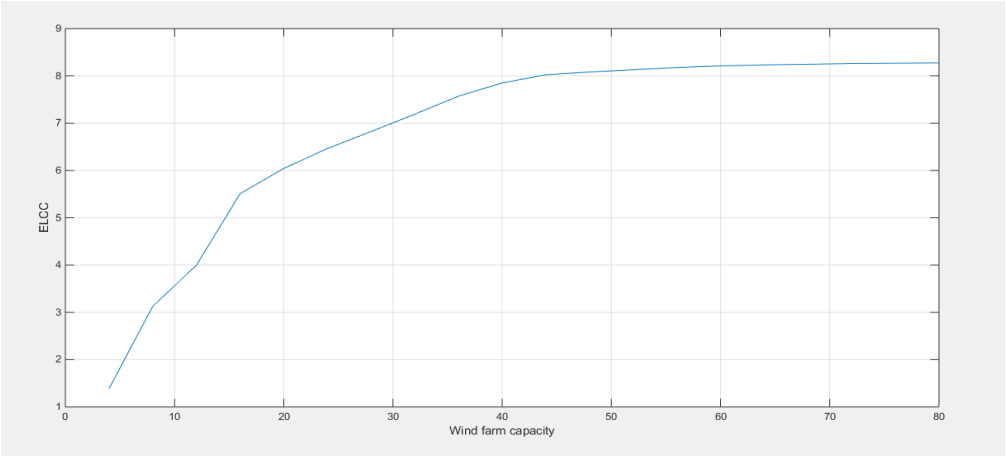

Figure 5.22: The change in ELCC with increasing wind farm capacity

The ELCC saturation point, where adding more generating capacity no longer increases the system reliability appears to be between 60 MW and 70 MW which equals between 25% and 29% of the total system capacity. This observation is in accordance with the findings in [5, 21, 26].

To investigate the effect this saturation has in the ELCC values, a larger wind farm is installed in the RTS. The contribution of the wind farm is chosen such that it makes up the same percentage of the RTS generation capacity as the RBTS system. To make up 7.69% of the system generation, the 20 MW wind farm in RBTS is scaled up to 284 MW for the RTS. The resulting $ELCC_{LOLE}$ for the RTS using a DPL-model is shown in Figure 5.23. An ELCC of 109.87 MW which equals 38.69% of the installed capacity.

5.5.4 ECC for Different Generator FOR Levels

As ECC is a relative value considering that the conventional generator used for comparison can be chosen by the user, a selection of generators with different FORs are applied to evaluate the same system. This is done to demonstrate that the conventional generator's capabilities are crucial for the adequacy assessment performed. The RBTS is used alongside a DPL load model and the ECC_{EENS} metric to perform this task. The generation added to the system is a wind farm with 10 WTGs and an individual generator capacity of 2 MW.

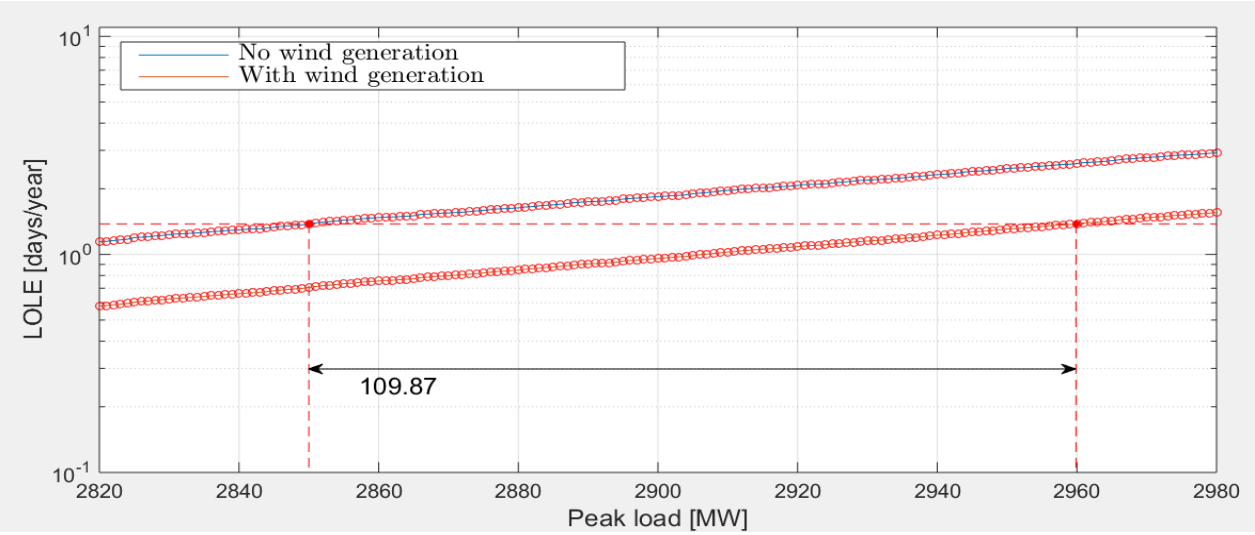

Figure 5.23: $ELCC_{LOLE}$ of a wind farm with a capacity of 284 MW in the IEEE-RTS

Table 5.24a and Figure 5.24b show the resulting values and a plot where the increase in ECC can be observed. Note that the initial FOR value of zero describes an ideal generator and thus is an EFC metric, not an ECC.

(a) ECC calculated values

FOR %	ECC [MW]
0	6.611
1	6.711
2	6.814
3	6.920
4	7.030
5	7.145
10	7.782
15	8.534
20	9.441
25	10.54
30	11.92

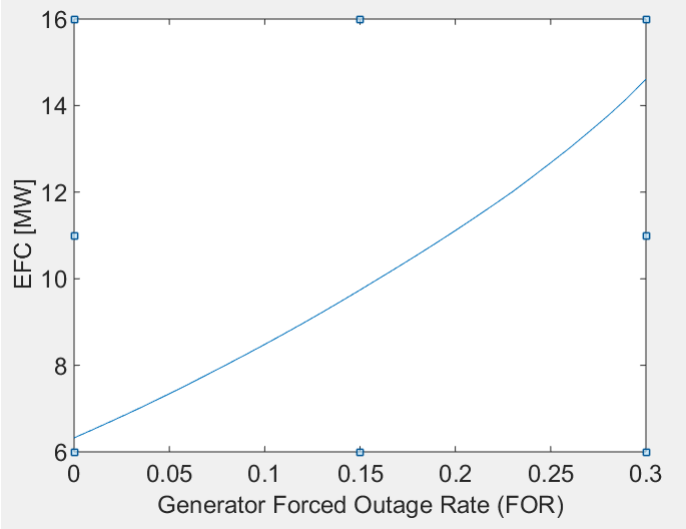

(b) ECC calculated plot

Figure 5.24: ECC calculated using various forced outage ratings for the fictitious generator

Comparing these results from the ECC_{LOLE} with the results for $ELCC_{LOLE}$ from Section 5.5.4 shows that to get a similar result, the conventional generator needs to have a FOR of 11%. The same calculations performed using the HPL-model obtains the intersection point for the $ELCC_{LOLE}$ and ECC_{LOLE} with a FOR of 14% for the conventional generator.

Chapter 6

Conclusions and Future Work

6.1 Summary of Results

Tables 6.1, 6.2 and 6.3 show the capacity credit results for each test system, including the simple system from Chapter 3. CYPL-modelling stands out with highly polarising results for both the example system and RTS for all reliability metrics. Although the values for the RBTS system are reasonable, this can be attributed to the effect from the step-wise increase as discussed in Section 5.5.1. These results provide motivation to avoid CYPL-modelling when performing generation adequacy evaluations.

Table 6.1: Results from the simple example system in MW and percentage of installed capacity

Reliability Metric	Load Model					
	CYPL		DPL		HPL	
	[MW]	[%]	[MW]	[%]	[MW]	[%]
$ELCC_{LOLE}$	0	0	1.04	26.00	1.60	40.00
$ELCC_{EENS}$	0.18	4.50	1.67	41.75	1.87	46.75
ECC_{LOLE}	1.65	41.25	2.02	50.50	1.36	34.00
ECC_{EENS}	0.06	1.50	1.51	37.75	1.65	41.25

Table 6.2: Results from the RBTS in MW and percentage of installed capacity

Reliability Metric	Load Model					
	CYPL		DPL		HPL	
	[MW]	[%]	[MW]	[%]	[MW]	[%]
$ELCC_{LOLE}$	8.88	44.00	7.85	39.25	8.07	40.35
$ELCC_{EENS}$	8.33	41.65	7.57	37.85	7.62	38.10
ECC_{LOLE}	5.53	27.65	6.61	33.05	6.71	33.55
ECC_{EENS}	5.93	29.70	6.92	34.60	6.67	33.35

Table 6.3: Results from the RTS in MW and percentage of installed capacity

Reliability Metric	Load Model					
	CYPL		DPL		HPL	
	[MW]	[%]	[MW]	[%]	[MW]	[%]
$ELCC_{LOLE}$	17.58	87.90	11.14	55.7	10.18	50.90
$ELCC_{EENS}$	9.49	47.45	10.57	52.85	11.09	55.45
ECC_{LOLE}	0.82	4.10	9.00	45.0	10.37	51.85
ECC_{EENS}	10.21	51.05	10.13	50.65	10.10	50.50

Table 6.4 shows the reliability improvement that occurs when installing the 20 MW wind farm in the RBTS and RTS calculated using $LOLE$ and $EENS$.

Table 6.4: System reliability evaluations with and without installed wind farm and the improvement quantified in %. (NOTE: The LOLE values have all been scaled to hours/year for easier comparison)

Test System	Metric	Load Model		
RBTS		CYPL		
		Old	New	[%]
	LOLE [hours/year]	73.382	40.186	33.197
	EENS [MWh/year]	821.184	447.283	45.532
		DPL		
		Old	New	[%]
	LOLE [hours/year]	53.508	26.863	49.796
	EENS [MWh/year]	513.313	251.160	51.070
		HPL		
		Old	New	[%]
	LOLE [hours/year]	1.092	0.533	51.168
	EENS [MWh/year]	9.862	4.774	51.594
RTS		CYPL		
		Old	New	[%]
	LOLE [hours/year]	834.561	757.602	9.222
	EENS [MWh/year]	128364.163	121072.224	5.680
		DPL		
		Old	New	[%]
	LOLE [hours/year]	502.575	471.453	6.193
	EENS [MWh/year]	66153.651	61410.731	7.170
		HPL		
		Old	New	[%]
	LOLE [hours/year]	9.4192	8.8146	6.419
	EENS [MWh/year]	1176.400	1087.200	7.582

6.2 Discussion and Conclusion

The objective of this thesis has been to study and implement the algorithmic approaches to calculate the ELCC and EFC/ECC metrics for power systems with wind-integration. The thesis work has applied several power system reliability concepts in order to evaluate the capacity credits of wind power. The application of probabilistic reliability concepts to evaluate wind power contribution is beneficial due to the inherent random and variable nature of wind energy. Adequacy indices, such as LOLE and ELCC, are used to include the reliability effects of introducing wind energy in the power system. The underlying concepts of reliability indices and capacity credits have been presented in detail to uncover their nuances and their inherent advantages and disadvantages.

Different capacity credits (e.g. ELCC, ECC and EFC) have been applied and the indices used for their calculation (e.g. LOLE and EENS) have been combined to evaluate their relevance for the evaluated system. Most literature apply ELCC in combination with the LOLE metric, but this is not necessarily the optimal metric for every task. The adequacy metric EENS considers the severity of outages, not the mere probability of occurrence as LOLE does. This gives EENS an advantage in scenarios where amount of energy produced by generators vary greatly, as is the case with wind turbines. Also, the ECC and EFC capacity credits are included as they are different in their approach in how to quantify the reliability contribution of wind generation. These concepts and methodologies were included in the development of MATLAB scripts to model a wind farm and evaluate its reliability contribution in different case studies. The case studies provided means to demonstrate the methodologies, the different aspects of the reliability metrics and capacity credits.

The MATLAB scripts were used to calculate ELCC, EFC and ECC. Three different test-systems were evaluated for different configurations of generation system size, load model resolutions and number of derated generator states. The greatest influence on the simulation results came from the load model. CYPL provided highly erratic and polarising results ranging from very optimistic to very pessimistic. This was evident in both the small test system and the RTS. However,

the CC results from the RBTS were reasonable. Figure 5.18 demonstrates how small changes in reliability level can result in very pessimistic or very optimistic CC values for the RBTS. This is due to the very step-wise increase of the LOLE/EENS curve when utilising the CYPL model. The difference between the HPL- and DPL-model results are on average 0.5-3.5%. It can be argued that the DPL provides satisfyingly accurate representation, although not being as close to the real case as the HPL, but requires less computational power. However, as the solution time is of small concern and the test systems are small enough to not require severe amounts of computational power the HPL-model is recommended.

It can also be observed from the plots and results that a larger amount of capacity level possibilities leads to an increase in LOLE and EENS levels, which can decrease the discontinuity of the peak load vs LOLE/EENS lines. Also, the size of the system generation fleet has small influence, as can be observed when comparing Figures 5.5 and 5.12. Both the effect from utilising EENS or a large test system are dwarfed by the influence from the load model resolution, therefore no further investigations were performed on these topics.

The results from Section 5.5.2 show that the number of derated states has a direct influence on the ELCC level. Figure 5.20 gives an intuitive illustration of why more derated states allow for more of the actual wind generation to be included in the generation modelling. It can be observed in Figure 5.21 that the capacity credit values are stabilised around 9-12 derated states. This has led to the inclusion of 10 derated states for this thesis and highlights the importance of applying a suitable number of derated states.

Results obtained using LOLE or EENS metrics produce similar ELCC and ECC values for both the RBTS and the RTS. For the example system the differences between the LOLE and EENS based capacity credits are more evident. This is due to the small amount of generation and low reliability level creating discontinuous plot curves. The small differences in results for the more realistic systems suggests both indices provide equally valid results. Therefore, a prefered method will not be stated. It is viewed as a strength that neither index is dominant and the user can choose the one most suitable for their evaluation. The growing penetration of wind and so-

lar in the power system cause an increase in energy limited scenarios with their variable energy output. Such scenarios would benefit EENS as it encompasses the energy aspect of loss-of-load situations and is therefore a more realistic and preferred reliability index.

From Tables 6.2 and 6.3, it can be observed that both ELCC and ECC give higher results for the RTS than for the smaller RBTS. These results are influenced by the size of the wind farm relative to the total system generation capacity. The wind farm used for both test systems has a capacity of 20 MW. For the RBTS 20 MW of installed wind power equals a wind penetration of 7.69%. For the RTS 20 MW of installed wind power equals a wind penetration of 0.58%. Further investigating this effect in Section 5.5.3 shows that increasing the wind farm capacity to the same percentile ratio for RBTS and RTS returns results of similar value: An $ELCC_{RBTS}$ of 40.35% and $ELCC_{RBTS}$ of 38.69%. Figure 5.22 shows the decrease in reliability contribution with increasing wind penetration. These two examples clearly demonstrate one of the future problems concerning further renewable energy integration in systems where such energy sources are already present.

The capacity credits applied in this thesis have different characteristics, thus influencing their usefulness. One such characteristic is their output unit and what it represents. EFC returns a value in MW where its magnitude describes the capacity of an ideal generator that obtains the same increase in reliability as the evaluated generator. The EFC index is easily comparable with EFCs obtained from other system configurations, but an ideal generator is only a theoretical possibility with little practical or intuitive value. ECC is very similar to EFC as it also returns a value in MW, but its magnitude describes the capacity of the conventional realistic generator that obtains the same increase in reliability as the evaluated generator. The ECC value is based on a realistic generator and gives a practical value that successfully can be used to compare the reliability contribution of a wind farm to that of any desired conventional generation. However, as the capabilities of the conventional generator are chosen for each individual study, the comparative abilities are reduced due to the results being dependent on this choice. ELCC returns a value in MW and is not modelled after a fictitious generator but rather quantifies the extra load that can be added to the system while maintaining the system reliability level. Additional

load is an universal quantity and has the same function across power systems thus making it a comparative value. Also, ELCC is an independent value which does not use any other input than load and generation. Both EFC and ECC have their uses, and in some cases are arguably the best capacity credits, e.g. using ECC when a conventional generator is to be replaced with a wind farm. They have glaring disadvantages: ECC has bad comparative capabilities and EFC does not have a practical unit. The robustness and overarching abilities of the ELCC makes it the preferred CC.

Compared to how power system reliability is ensured today, the methods applied in this thesis allow for a more flexible reserve generation capacity. This flexibility will decrease the need for reserve capacity in instances with low probability of loss-of-load situations, thus allowing more effective power grid operations and reduce operational costs for the TSOs. It will also allow for better simulation of future scenarios with an increase in load and change in generation mix as the probabilistic calculation can handle more variables than deterministic approaches. Capacity from renewable sources can also be weighted on their contribution to system reliability and correlation between load and generation. This will provide a more realistic value for the contribution from aforementioned sources to the power system. As presented in Section 2.2, a new generation adequacy method is under development for the Nordic system that will include many of the concepts applied in this thesis.

6.3 Limitations

Although the wind data is gathered from measured wind speeds over multiple years, these undergo some statistical processing before being applied to the model. Little focus is put on these processes or on how weaknesses in the wind modelling affects the ending results. These limitations could be solved if the existence of a standardised wind data collection could be found, but no such data was discovered during this work. Also, for the wind farm modelling it is assumed that all turbines are 100% correlated. This is not the case in real life due to aerodynamic influence from other turbines as well as surrounding geography.

The general theoretical basis and use of established test systems in this thesis makes it well suited for comparison with values obtained in similar reports and theses. However, the lack of a real-life case study and the inability of comparing the theoretical results with realistic values weakens the foundation for discussion.

Reliability concepts are only applied to the generation adequacy aspect of the power system and do not include market models nor any type of power flow analysis. Wind power is often generated relatively far from the load point which implies that issues regarding transmission congestion and accompanying transmission reliability can arise; this issue has not been addressed.

6.4 Recommendations for Further Work

There are several aspects of this thesis that can form the basis for further research. Some of them are presented in this section.

6.4.1 Monte Carlo Simulations

Utilising MCS for reliability purposes instead of purely analytical methods would be a natural step. It can be applied for wind modelling purposes or to assess LOLE and EENS. MCS is far better at maintaining the correlating effect between load levels and generation compared to analytical methods. This correlation is especially interesting when dealing with energy sources that have semi-regular variability i.e. seasonal changes for wind.

6.4.2 Real Case Study

As the data foundation in this thesis only includes theoretical test systems and no real case study, this would be a natural expansion. A real-life case study would allow for further analysis of the methodological approaches and their accuracy.

6.4.3 Composite Systems

This thesis only focuses on the reliability issues from the perspective of generation adequacy. A natural extension would be the inclusion of a transmission system. Load flow, line outages and transmission congestion could be analysed and their influence on the capacity credits evaluated.

6.4.4 Simulate Wind Speeds Instead of Historical Data

Actual on-site wind measures are crucial when assessing wind capacity reliability contributions, but the simplistic wind data processing in this thesis would benefit from a more sophisticated approach. Many reliability studies involving wind apply the Auto Regressive Moving Average (ARMA) model. This would make the wind modelling, and by extension the wind generator modelling, more robust.

6.4.5 Integrate Wind and Energy Storage

The main issue with intermittent renewable energy sources is that production might occur when there is little or no demand. This can be bypassed by an effective electrical energy storage. Studies integrating wind generation and battery storage could investigate the reliability effect from the complementary configuration. Other means of energy storage like curtailment of hydro power with reservoir in peak generation scenarios could be assessed in a similar way.

6.4.6 Integrate Wind With Complimentary Production

The saturation effect mentioned in this thesis proves to be a big hindrance to reaching a high wind penetration in the power system. Studies integrating wind with other energy sources that can complement wind production and have generation peaks when wind is low would allow for a higher renewable penetration. Solar, tidal or run-of-river hydro could be investigated. Also, the effect of other wind generation with a different wind regime, due to geographical distance or other factors, would be of interest.

6.4.7 Include Seasonal Variations

The analytical approach in this thesis is unable to include the correlation between load and generation. Splitting the load and generation data into seasonal intervals would allow us to account for some of the seasonal variations in load and wind regimes, thus making the models more realistic. This would be especially interesting at locations with big differences between summer and winter for either mean wind speeds, peak loads or both.

Appendix A

Test System Load

Figures A.1, A.2 and A.3 show how the different load solutions are calculated from the yearly peak load. The load variations are the same for RBTS and RTS, but the top load is different.

Table A.1: Weekly peak load data

Week w	WPL [% of YPL]	Week w	WPL [% of YPL]	Week w	WPL [% of YPL]	Week w	WPL [% of YPL]
1	86.2	14	75.0	27	75.5	40	72.4
2	90.0	15	72.1	28	81.6	41	74.3
3	87.8	16	80.0	29	80.1	42	74.4
4	83.4	17	75.4	30	88.0	43	80.0
5	88.0	18	83.7	31	72.2	44	88.1
6	84.1	19	87.0	32	77.6	45	88.5
7	83.2	20	88.0	33	80.0	46	90.9
8	80.6	21	85.6	34	72.9	47	94.0
9	74.0	22	81.1	35	72.6	48	89.0
10	73.7	23	90.0	36	70.5	49	94.2
11	71.5	24	88.7	37	78.0	50	97.0
12	72.7	25	89.6	38	69.5	51	100.0
13	70.4	26	86.1	39	72.4	52	95.2

Table A.2: Daily peak load data

Day d	DPL [% of WPL]
Monday	93
Tuesday	100
Wednesday	98
Thursday	96
Friday	94
Saturday	77
Sunday	75

Table A.3: Hourly load data

	Winter weeks 1-8 & 44-52		Summer weeks 18-30		Spring/Fall weeks 9-17 & 31-43	
Hour h	Weekday [% of DPL]	Weekend [% of DPL]	Weekday [% of DPL]	Weekend [% of DPL]	Weekday [% of DPL]	Weekend [% of DPL]
1	67	78	64	74	63	75
2	63	72	40	70	62	73
3	60	68	58	66	60	69
4	59	66	56	65	58	66
5	59	64	56	64	59	65
6	60	65	58	62	65	65
7	74	66	64	62	72	68
8	86	70	76	66	83	74
9	95	80	87	81	95	83
10	96	88	95	86	99	89
11	96	90	99	91	100	92
12	95	91	100	93	99	94
13	95	90	99	93	93	91
14	95	88	100	92	92	90
15	93	87	100	91	90	90
16	94	87	97	91	88	86
17	99	91	96	92	90	85
18	100	100	96	94	92	88
19	100	99	93	95	96	92
20	96	97	92	95	98	100
21	91	94	92	100	96	97
22	83	92	93	93	90	95
23	73	87	87	88	80	90
24	63	81	72	80	70	85

Appendix B

COPT for the RBTS system

Table B.1 shows the full COPT for the RBTS system including the equivalent wind farm generator.

Table B.1: COPT for the RBTS

State	Capacity Outage [MW]	Cumulative Probability	Individual Probability
1	0	1	0.812859614
2	5	0.187140386	0.016421406
3	10	0.170718979	0.016671908
4	15	0.154047071	0.000335131
5	20	0.153711941	0.070358538
6	25	0.083353403	0.00142135
7	30	0.081932052	0.001443033
8	35	0.080489022	2.90072E-05
9	40	0.080460012	0.069269729
10	45	0.011190284	0.001399385
11	50	0.009790898	0.001420733
12	55	0.008370166	2.85589E-05
13	60	0.008341607	0.005828452
14	65	0.002513155	0.000117744

State	Capacity Outage [MW]	Cumulative Probability	Individual Probability
15	70	0.002395412	0.00011954
16	75	0.002275872	2.40293E-06
17	80	0.002273469	0.002001483
18	85	0.000271986	4.04338E-05
19	90	0.000231552	4.10506E-05
20	95	0.000190502	8.25179E-07
21	100	0.000189676	0.00015945
22	105	3.02E-05	3.22112E-06
23	110	2.70E-05	3.27026E-06
24	115	2.37E-05	6.57372E-08
25	120	2.37E-05	2.12228E-05
26	125	2.45E-06	4.28736E-07
27	130	2.02E-06	4.35276E-07
28	135	1.58E-06	8.74971E-09
29	140	1.57E-06	1.4634E-06
30	145	1.11E-07	2.95628E-08
31	150	8.10E-08	3.00138E-08
32	155	5.10E-08	6.03323E-10
33	160	5.04E-08	4.76162E-08
34	165	2.79E-09	9.61882E-10
35	170	1.83E-09	9.76556E-10
36	175	8.52E-10	1.96303E-11
37	180	8.32E-10	7.92868E-10
38	185	3.95E-11	1.60155E-11
39	190	2.35E-11	1.62598E-11
40	195	7.22E-12	3.26847E-13
41	200	6.90E-12	6.60252E-12
42	205	2.94E-13	1.33351E-13

State	Capacity Outage [MW]	Cumulative Probability	Individual Probability
43	210	1.61E-13	1.35385E-13
44	215	2.55E-14	2.72145E-15
45	220	2.28E-14	2.18951E-14
46	225	9.00E-16	4.42047E-16
47	230	4.58E-16	4.48791E-16
48	235	9.07E-18	9.02138E-18
49	240	4.56E-20	4.55625E-20
26	125	2.45E-06	4.28736E-07
27	130	2.02E-06	4.35276E-07
28	135	1.58E-06	8.74971E-09
29	140	1.57E-06	1.4634E-06
30	145	1.11E-07	2.95628E-08
31	150	8.10E-08	3.00138E-08
32	155	5.10E-08	6.03323E-10
33	160	5.04E-08	4.76162E-08
34	165	2.79E-09	9.61882E-10
35	170	1.83E-09	9.76556E-10
36	175	8.52E-10	1.96303E-11
37	180	8.32E-10	7.92868E-10
38	185	3.95E-11	1.60155E-11
39	190	2.35E-11	1.62598E-11
40	195	7.22E-12	3.26847E-13
41	200	6.90E-12	6.60252E-12
42	205	2.94E-13	1.33351E-13
43	210	1.61E-13	1.35385E-13
44	215	2.55E-14	2.72145E-15
45	220	2.28E-14	2.18951E-14
46	225	9.00E-16	4.42047E-16

State	Capacity Outage [MW]	Cumulative Probability	Individual Probability
47	230	4.58E-16	4.48791E-16
48	235	9.07E-18	9.02138E-18
49	240	4.56E-20	4.55625E-20

Appendix C

Pseudocodes for a Select-few MATLAB Scripts

Algorithm 1 Script to model the output of a wind turbine

Require: Wind data is read from the appropriate data-file together with the wind turbine specifications: Rated effect, $P_{turbine}$, cut-in wind speed, V_{ci}, rated wind speed, V_r and cut-out wind speed, V_{co}. The function implements the power curve calculation from Equation (3.20). Turbine output stores the generation output from one wind turbine.

1: **function** WIND2GEN_MULTI($V, V_{ci}, V_{co}, V_r, P_{turbine}$)

2: $\quad$ A = $\frac{1}{(V_{ci}-V_r)^2}\left\{V_{ci}(V_{ci}+V_r) - 4V_{ci}V_r\left[\frac{V_{ci}+V_r}{2V_r}\right]^3\right\}$

3: $\quad$ B = $\frac{1}{(V_{ci}-V_r)^2}\left\{4(V_{ci}+V_r)\left[\frac{V_{ci}+V_r}{2V_r}\right]^3 - (3V_{ci}+V_r)\right\}$

4: $\quad$ C = $\frac{1}{(V_{ci}-V_r)^2}\left\{2 - 4\left[\frac{V_{ci}+V_r}{2V_r}\right]^3\right\}$

5: $\quad$ **if** V is between V_r and V_{co} **then**

6: $\quad\quad$ Turbine output, $turbine\_output$ is equal to P_r

7: $\quad$ **else if** V is between V_ci and V_r **then**

8: $\quad\quad$ $turbine\_output$ is calculated by: $(A + B \cdot V + C \cdot V^2) \cdot P_{turbine}$

9: $\quad$ **else**V is above V_{co} or below V_ci

10: $\quad\quad$ $turbine\_output$ is equal to zero.

11: $\quad$ **end if**

12: **end function**

Output: The function outputs the $turbine\_output$ value for the correlating wind speed.

Algorithm 2 Script to model a wind farm as a multi-state generator

Require: Wind data is read from the appropriate datafile together with the wind turbine specifications: Rated effect, $P_{turbine}$, cut-in wind speed, V_{ci}, rated wind speed, V_r and cut-out wind speed, V_{co}. The amount of wind turbines, *WTG* and their forced outage rate, *FOR* is obtained from what is defined by the user. The wind farm equivalent generator is created using Equation (3.22).

function WINDFARMMODEL($V, V_{ci}, V_{co}, V_r, P_{turbine}, FOR, WTG, prob, G, outage, states$)
Create the availability table
for the number of WTGs, plus one, if all are in outage **do**
Calculate the probability for all available amounts of WTGs
end for
Returns The mechanical outage table describing available turbines and probabilities
Calculate generation outputs for an individual turbine
for each wind speed level in V **do**
Call *wind2gen_multi* to get the $turbine\_output$
$P\_wind \leftarrow$ wind2gen_multi($V, V_{ci}, V_{co}, V_r, P_{turbine}$)
end for
Finding all generation output levels from the wind turbine and their probabilities
while last wind turbine outage value is not exceeded **do**
while wind turbine outage state is equal to current outage level **do**
Increase counter by one
if last wind turbine outage value is exceeded **then**
Exit while-loop
else
Increase current outage level
end if
end while
$wind\_MW$ = current outage level
$wind\_MW\_prob$ = counter divided by amount of wind speed measures in V
end while
Reduce the number of states for the wind turbine to the amount given by $states$
As mentioned in Section 3.5.3 to optimise calculation time the valid states for the wind farm are pre-calculated.
for each state in the mechanical outage table **do**
for each value from wind_outage **do**
Valid wind farm states are calculated by multiplying all increments of available wind turbines and all increments of wind outage states
end for
end for

Combining the mechanical availability table and wind turbine outage following the same procedure as in Section 3.5.3 using Equation (3.22)

for each valid state **do**
  for each mechanical outage **do**
    for each wind turbine outage **do**
      if the output in the current valid state divided by the counter for turbine outage state, is less than the turbine outage **then**
        Exit for-loop
      else
        The cumulative probability value *cum.prob.* is equal to:
        (curr.)value + ((curr.)wind out.prob.) × ((curr.)mechanical out.prob.)
      end if
    end for
  end for
  The current valid outage state is assigned the *cum.prob.* value
end for

As the probability for each valid wind farm state is given in cumulative probability, this is reformed to the individual probability for each state.

for each valid wind farm output **do**
  The individual probability for output in step i is set to be equal to cum.prob.(i)-cum.prob.($i+1$)
end for
Reduce the number of states for the wind farm to the amount given by $states$
Add the wind farm outages and their corresponding probabilities to $outage$ and $prob$ and update G to include the amount of outage states there is for the wind farm. The new arrays now describing a system with a wind farm are G^{wind}, $outage^{wind}$ and $prob^{wind}$
end function

Output: Returns three single column arrays: one containing the number of the system generator G^{wind}, the second containing the outage states of the wind farm $outage^{wind}$ and the third containing the corresponding individual probabilities $prob^{wind}$.

Algorithm 3 Script to calculate ECC

Require: Generator and load data for the system with wind and the system with a fictitious generation. The reliability level of the system with present wind generation

1: **function** CALCECC($G^{wind}, outage^{wind}, prob^{wind}, G^{fic}, outage^{fic}, prob^{fic}, load$)
2: Create the $COPT^{wind}$ with $G^{wind}, outage^{wind}$ and $prob^{wind}$
3: Calculate $LOLE^{wind}/EENS^{wind}$ for the system with wind generation
4: Decide the capacity interval (from *cap_min* to *cap_max*) for the fictitious generator and the incremental step (*capIncrement*) for calculations.
5: **for** each increment of fictitious generator capacity from *cap_min* to *cap_max* **do**
6: Update $outage^{fic}$ with the current generator capacity
7: Create the $COPT^{fic}$ for the system with the current $G^{fic}, outage^{fic}$ and $prob^{fic}$
8: Calculate the $LOLE^{fic}/EENS^{fic}$ of the current system
9: Add the current capacity and $LOLE^{fic}/EENS^{fic}$ to the arrays *cap_vec* and *rel_level*
10: **end for**
11: Plot capacity vs. $LOLE^{fic}/EENS^{fic}$ on a semi-logaritmic scale along with the line describing the reliability level of the system with present wind. Find the intersection point between the capacity vs. $LOLE^{fic}/EENS^{fic}$ curve and the reliability line. The generator capacity read from the x-axis is the ECC_{LOLE}/ECC_{EENS} value in MW.
12: **end function**

Output: A, ECC_{LOLE}/ECC_{EENS} value and plot of capacity vs. $LOLE^{fic}/EENS^{fic}$ is produced.

Bibliography

[1] International Energy Agency, "*Renewables 2017*," 2017. https://www.iea.org/publications/renewables2017/ [Accessed: 10.1.2018].

[2] H. Ibrahim, M. Ghandour, M. Dimitrova, A. Ilinca, and J. Perron, "Integration of wind energy into electricity systems: technical challenges and actual solutions," *Energy Procedia*, vol. 6, pp. 815–824, 2011.

[3] R. Billinton and R. N. Allan, *Reliability Evaluation of Engineering systems*. Springer, 1992.

[4] United Nations, "*Joint Declaration: The Way Forward On Renewable Energy*," 2002. http://www.un.org/events/wssd/statements/joint-declaration.htm [Accessed: 10.1.2018].

[5] K. Koldingsnes, "Reliability-based derating approach for interconnectors," Master's thesis, NTNU, 2017.

[6] R. N. Allan, R. Billinton, I. Sjarief, L. Goel, and K. So, "A reliability test system for educational purposes-basic distribution system data and results," *IEEE Transactions on Power systems*, vol. 6, no. 2, pp. 813–820, 1991.

[7] C. Grigg *et al.*, "The ieee reliability test system-1996. a report prepared by the reliability test system task force of the application of probability methods subcommittee," *IEEE Transactions on power systems*, vol. 14, no. 3, pp. 1010–1020, 1999.

[8] Global Wind Energy Council, "Global wind report," *GWEC, Ulaanbaatar, Mongolia, Technical Report*, 2017.

[9] The Norwegian Climate- and Environmental Department, "*Law for Climate Goals*," 2018. https://lovdata.no/dokument/NL/lov/2017-06-16-60 [Accessed: 18.1.2018].

[10] Statistics Norway, "*Electricity, 2016*," 2017. https://www.ssb.no/energi-og-industri/statistikker/elektrisitet/aar [Accessed: 16.1.2018].

[11] Vindportalen, "*Vindkraft i Norge*," 2017. http://www.vindportalen.no/Vindportalen/Vindkraft/Vindkraft-i-Norge [Accessed: 11.1.2018].

[12] NVE, "*Ny kraft: Endelige tillatelser og utbygging, 3. kvartal 2017*," 2017. http://webfileservice.nve.no/API/PublishedFiles/Download/201202014/2216283 [Accessed: 14.1.2018].

[13] D. E. Weir, "Vindkraft—produksjon i 2016, annual report," *Norges vassdrags-og energidirektorat, Norway*, 2017.

[14] J. S. Amundsen, G. Bartnes, *et al.*, "Kraftmarkedsanalyse 2017 - 2030, rapport nr 79-2017," *Norges vassdrags- og energidirektorat*, 2017.

[15] Kjeller Wind Technique and NVE, "*Vindkart for Norge*," 2009. https://www.nve.no/media/2470/vindkart_for_norge_oppdragsrapporta10-09.pdf [Accessed: 23.1.2018].

[16] ENTSOE-E, "*ENTSO-E Target Methodology for Adequacy Assessment*," 2015. https://www.entsoe.eu/Documents/SDC%20documents/SOAF/141014_Target_Methodology_for_Adequacy_Assessment_after_Consultation.pdf [Accessed: 15.1.2018].

[17] Statnett, FINGRID, Svenska, Kräftnett, and Energinet, "*Generation Adequacy – market measures to secure it and methodology for assessment*," 2016. http://www.statnett.no/Global/Dokumenter/Nyheter%20-%20vedlegg/Nyheter%202017/Generation_Adequacy_market%20measures%20to%20secure%20it%20and%20methodology%20for%20assessment.pdf [Accessed: 12.1.2018].

[18] M. Liserre, T. Sauter, and J. Y. Hung, "Future energy systems: Integrating renewable energy sources into the smart power grid through industrial electronics," *IEEE Industrial Electronics Magazine*, vol. 4, no. 1, pp. 18–37, 2010.

[19] ENTSOE-E, "*Nordic Balancing Philosophy*," 2016. https://www.entsoe.eu/Documents/Publications/SOC/Nordic/Nordic_Balancing_Philosophy_160616_Final_external.pdf [Accessed: 12.1.2018].

[20] P. Kundur, N. J. Balu, and M. G. Lauby, *Power system stability and control*, vol. 7. McGraw-hill New York, 1994.

[21] M. Mosadeghy, *Reliability impacts of increased wind generation in the Australian national electricity grid*. PhD thesis, The University of Queensland, 2016.

[22] C. D'Annunzio, *Generation adequacy assessment of power systems with significant wind generation: a system planning and operations perspective*. PhD thesis, The University of Texas at Austin, 2009.

[23] R. M. Castro and L. A. Ferreira, "A comparison between chronological and probabilistic methods to estimate wind power capacity credit," *IEEE Transactions on Power Systems*, vol. 16, no. 4, pp. 904–909, 2001.

[24] R. Billinton and R. N. Allan, "Power-system reliability in perspective," *Electronics and Power*, vol. 30, no. 3, pp. 231–236, 1984.

[25] W. K. Hastings, "Monte carlo sampling methods using markov chains and their applications," *Biometrika*, vol. 57, no. 1, pp. 97–109, 1970.

[26] R. Billinton and Y. Gao, "Multistate wind energy conversion system models for adequacy assessment of generating systems incorporating wind energy," *IEEE Transactions on Energy Conversion*, vol. 23, no. 1, pp. 163–170, 2008.

[27] H. G. Stoll and L. J. Garver, *Least-cost Electric Utility Planning*. J. Wiley, 1989.

[28] R. Billinton and R. Karki, "Capacity reserve assessment using system well-being analysis," *IEEE Transactions on Power Systems*, vol. 14, no. 2, pp. 433–438, 1999.

[29] M.Papic, "*Generation Reliability Concepts*," 2014. https://www.wecc.biz/Administrative/20140909_RAWG_Item5A1_Probabilistic_MPapic.pdf [Accessed: 04-12-2017].

[30] International Energy Agency, "*Re-powering Markets*," 2016. https://www.iea.org/publications/freepublications/publication/REPOWERINGMARKETS.pdf [Accessed: 05-12-2017].

[31] L. L. Garver, "Effective load carrying capability of generating units," *IEEE Transactions on Power Apparatus and Systems*, no. 8, pp. 910–919, 1966.

[32] A. Keane, M. Milligan, C. J. Dent, B. Hasche, C. D'Annunzio, K. Dragoon, H. Holttinen, N. Samaan, L. Soder, and M. O'Malley, "Capacity value of wind power," *IEEE Transactions on Power Systems*, vol. 26, no. 2, pp. 564–572, 2011.

[33] R. Billinton, R. Karki, Y. Gao, D. Huang, P. Hu, and W. Wangdee, "Adequacy assessment considerations in wind integrated power systems," *IEEE Transactions on Power Systems*, vol. 27, no. 4, pp. 2297–2305, 2012.

[34] Y. Zhou, P. Mancarella, and J. Mutale, "Framework for capacity credit assessment of electrical energy storage and demand response," *IET Generation, Transmission & Distribution*, vol. 10, no. 9, pp. 2267–2276, 2016.

[35] J. Haslett and M. Diesendorf, "The capacity credit of wind power: A theoretical analysis," *Solar Energy*, vol. 26, no. 5, pp. 391–401, 1981.

[36] M. Amelin, "Comparison of capacity credit calculation methods for conventional power plants and wind power," *IEEE Transactions on Power Systems*, vol. 24, no. 2, pp. 685–691, 2009.

[37] S. Sulaeman, M. Benidris, J. Mitra, and C. Singh, "A wind farm reliability model considering both wind variability and turbine forced outages," *IEEE Transactions on Sustainable Energy*, vol. 8, no. 2, pp. 629–637, 2017.

[38] A. Chowdhury, "Reliability models for large wind farms in generation system planning," in *IEEE Power Engineering Society General Meeting*, pp. 1926–1933, 2005.

[39] J. Slootweg, S. De Haan, H. Polinder, and W. Kling, "General model for representing variable speed wind turbines in power system dynamics simulations," *IEEE Transactions on Power Systems*, vol. 18, no. 1, pp. 144–151, 2003.

[40] M. Lei, L. Shiyan, J. Chuanwen, L. Hongling, and Z. Yan, "A review on the forecasting of wind speed and generated power," *Renewable and Sustainable Energy Reviews*, vol. 13, no. 4, pp. 915–920, 2009.

[41] Vestas Globe Newswire, "*Press release from Vestas Wind Systems A/S, Aarhus, Denmark*," 2017. https://www.vestas.com/en/media/company-news?n=1660416#!grid_0_content_0_Container [Accessed: 03-01-2018].

[42] P. Giorsetto and K. F. Utsurogi, "Development of a new procedure for reliability modeling of wind turbine generators," *IEEE transactions on Power Apparatus and Systems*, no. 1, pp. 134–143, 1983.

[43] Meterologisk Institutt, "*Observations - Hourly Data*," 2017. http://sharki.oslo.dnmi.no/portal/page?_pageid=73,39035,73_39049&_dad=portal&_schema=PORTAL [Accessed: 23.10.2017].

[44] R. Billinton and D. Huang, "Basic concepts in generating capacity adequacy evaluation," in *International Conference on Probabilistic Methods Applied to Power Systems.*, pp. 1–6, IEEE, 2006.